



BRNO UNIVERSITY OF TECHNOLOGY

VYSOKÉ UČENÍ TECHNICKÉ V BRNĚ

FACULTY OF MECHANICAL ENGINEERING

FAKULTA STROJNÍHO INŽENÝRSTVÍ

INSTITUTE OF SOLID MECHANICS, MECHATRONICS AND BIOMECHANICS

ÚSTAV MECHANIKY TĚLES, MECHATRONIKY A BIOMECHANIKY

UNIT FOR SIGNAL ACQUISITION AND PROCESSING IN RAINWATER MANAGEMENT

JEDNOTKA PRO SBĚR A ZPRACOVÁNÍ SIGNÁLŮ V SYSTÉMU DEŠŤOVÉ VODY

MASTER'S THESIS

DIPLOMOVÁ PRÁCE

AUTHOR

AUTOR PRÁCE

Bc. Vojtěch Slabý

SUPERVISOR

VEDOUCÍ PRÁCE

Ing. Radek Tománek

BRNO 2022

Assignment Master's Thesis

Institut: Institute of Solid Mechanics, Mechatronics and Biomechanics
Student: **Bc. Vojtěch Slabý**
Degree programm: Mechatronics
Branch: no specialisation
Supervisor: **Ing. Radek Tománek**
Academic year: 2021/22

As provided for by the Act No. 111/98 Coll. on higher education institutions and the BUT Study and Examination Regulations, the director of the Institute hereby assigns the following topic of Master's Thesis:

Unit for signal acquisition and processing in rainwater management

Brief Description:

The proposed unit will be part of a complex system of rainwater collection, accumulation, and usage. The unit will be placed the switchboard within the main underground tank. It will be necessary to use a microcontroller for signal processing as some quantities will be measured indirectly or using multiple sensors. The resulting data will be sent by the unit via the RS-485 to a superior central unit, which is not part of the actual unit. The unit will also include an isolated power supply (transformer-based DC/DC converter) and an RS-485 bus driver.

Master's Thesis goals:

1. Get acquainted with the used measurement methods and the technical parameters of the sensors used in the system.
2. Study the STM32 series microcontrollers, especially timer blocks, A/D converters, UART interface, and DMA.
3. Design the HW part concept of the evaluation unit.
4. Design the unit circuit diagram.
5. Design, manufacture and populate PCB.
6. Design the software concept.
7. Create firmware and document it.
8. Prototype the evaluation unit and verify functionality by measuring in the laboratory.

Recommended bibliography:

ĎAĎO, Stanislav a Marcel KREIDL, 1996. Senzory a měřicí obvody. Praha: Vydavatelství ČVUT. ISBN 80-010-1500-9.

PATOČKA, Miroslav, 2011. Magnetické jevy a obvody ve výkonové elektronice, měřicí technice a silnoproudé elektrotechnice. V Brně: VUTIUM. ISBN 978-80-214-4003-6.

HOROWITZ, Paul a Winfield HILL, 2015. The art of electronics. Third edition. New York: Cambridge University Press. ISBN 978-0-521-80926-9.

VRBA, Kamil a Pavel HANÁK, 2021. Konstrukce elektronických zařízení [online]. VUTIUM, 298 s. [cit. 2021-10-21]. ISBN 978-80-214-5957-1. Dostupné z:
doi:10.13164/book.construction.electronic.devices

Dokumentace k vybraným součástkám

Deadline for submission Master's Thesis is given by the Schedule of the Academic year 2021/22

In Brno,

L. S.

prof. Ing. Jindřich Petruška, CSc.
Director of the Institute

doc. Ing. Jaroslav Katolický, Ph.D.
FME dean

Abstrakt

Diplomová práce se zabývá návrhem desky pro zpracování signálu a dat v systému dešťové vody, návrhem vlastního napájecího zdroje a firmwaru. Hlavní deska obsahuje třináct vstupů senzorů a signálu, dále zdroj se čtřmi výstupy a spojení s ultrazvukovým modulem. Samotná jednotka spotřebuje 6 W. Práce popisuje návrh dílkých bloků a popis zapojení celého zařízení včetně programovací části.

Summary

The thesis describes the unit's design for signal acquisition in the rainwater recollection system, designing a power supply and a firmware. The mainboard contains thirteen inputs from sensors and signals, a power supply with four outputs and a connection to the ultrasound module. The board consumption is 6 W. The thesis also describes the design of every part of the control board and a programming approach.

Klíčová slova

blokující měnič, sběr dat, RS485, In-application programming, aktualizace softwaru, signálové přizpůsobení

Keywords

flyback converter, data acquisition, RS485, In-application programming, firmware update, signal conditioning

Bibliographic citation

SLABY, V. *Unit for signal acquisition and processing in rainwater management*. Brno: Brno University of Technology, Faculty of Mechanical Engineering, 2022. 100 pages, Master's thesis supervisor: Ing. Radek Tománek.

I declare that the thesis with the title "Unit for signal acquisition and processing in rainwater management" was performed independently with the guidance of the thesis supervisor and with the help of technical literature and other information sources. They are all cited in the thesis bibliography at the end.

As an author of this thesis, I declare that there was no disobeying of third-party rights. Moreover, the creation of this work complies with regulation S 11 and the copyright law n. 121/2000 col..

Vojtech Slaby

Brno

I thank the thesis supervisor Ing. Radek Tománek, for the professional guidance, many consultation hours, helpful suggestions and advice, and the help with reviving the device.

Vojtech Slaby

Contents

List of Tables	9
List of Figures	10
1 Introduction	12
1.1 Rainwater retention system	13
1.2 Measurement unit requirements	14
2 Research	16
2.1 Sensors and Measuring methodology	16
2.2 Measuring system	16
2.2.1 Sensed physical quantities	17
2.2.2 Temperature sensors	20
2.2.3 Water level sensors	21
2.2.4 Flow metres	24
2.2.5 Monitoring filter clogging	26
2.3 Electronic circuit research	27
2.3.1 PSU conditions	27
2.3.2 Control circuitry	27
2.3.3 Flyback converter	28
2.3.4 Signal conditioning circuits	33
2.3.5 Bus driver of TIA/RS-232 and TIA/RS-485	37
2.3.6 Voltage sensing circuit	38
2.3.7 Input current sensing circuit	39
2.4 Software design	40
2.4.1 STM32 microcontrollers and its peripherals	41
2.4.2 Software updates	43
3 Electronic design	48
3.1 Flyback converter design	48
3.1.1 Flyback parameters	48
3.1.2 Design of the winding	48
3.1.3 PSU - complementary circuits	50
3.2 Bus driver circuit	55
3.3 Microcontroller and ICSP	55
3.4 Signal Conditioning circuits	56

4 Software design	59
4.1 Bootloader	59
4.2 Memory partition	60
4.3 Firmware concept description	60
4.4 Sensor connection	62
5 Electronic implementation and testing	64
5.1 A prototype board	64
5.2 Main board	66
5.2.1 Main board parameters	66
6 Software implementation and testing	71
6.1 IAP implementation and testing	71
6.2 RS485 communication	71
6.3 Sensor input testing	74
7 Conclusion	76
List of Abbreviations	77
Bibliography	78
Appendices	80
A Electronic schema	80
B PCB mask and board	85
C Parts	91
D List of capacitors	91
E List of diodes	94
F List of LEDs	95
G List of Integrated circuits	95
H List of transistors	96
I List of connectors and optocouplers	96
J List of resistors	97
K List of parts for ultrasound module	100

List of Tables

2.1	DS18B20[6].	21
2.2	Water level sensor characteristics.	22
2.3	Water level switch.	24
2.4	Diferential pressure sensor characteristics	25
2.5	FS400A parameters.	26
2.6	AJ-SR04m parameters [9]	27
2.7	Topology specification	28
3.1	LJ E 2507 dimensions	48
3.2	LJ T 1606 dimensions[24]	57
5.1	Final board specifications	66
7.1	List of capacitors - part 1	91
7.2	List of capacitors - part 2	92
7.3	List of capacitors - part 3	93
7.4	List of capacitors - part 4	93
7.5	List of diodes	94
7.6	List of LEDs	95
7.7	List of ICs	95
7.8	List of transistors	96
7.9	List of optocouplers	96
7.10	List of connectors	96
7.11	List of resistor parts - 1	97
7.12	List of resistor parts - 2	98
7.13	List of resistor parts - 3	99
7.14	List of resistor parts - 4	99
7.15	Ultrasound sensor module parts list	100

List of Figures

1.1	Basic concept for the signal acquisition board	12
1.2	Rainwater retention system diagram	14
1.3	More detailed board description	15
2.1	An output current graph.	20
2.2	An output current graph.	22
2.3	Physical principle of a piezoresistive sensor.	23
2.4	Operation block diagram.	23
2.5	XGZP6899A[7]	25
2.6	FS400A[8]	26
2.7	AJ-SR04m[9]	26
2.8	Flyback's principle for $s < s_m$. The figure shows a schematic representation of the flyback converter.[3]	30
2.9	Flyback's principle for $s < s_m$. Current and voltages graphs[3]	31
2.10	RC-step for damping the overhang[3]	32
2.11	Regulation scheme of the flyback PSU[3]	33
2.12	Differential amplifier with noninverting stage[4]	34
2.13	Differential amplifier with noninverting stage[4]	35
2.14	Hex Schmitt trigger for suitable levels of the MCU[4]	36
2.15	A circuit for controlling the compressor and the static pressure[4]	36
2.16	TTL logic input with voltage divider[4]	37
2.17	Schmitt trigger for pulse acquisition[4]	37
2.18	General input for analogue signal[4]	37
2.19	UART waveforms for RX and TX[4]	38
2.20	Voltage sensing circuit	39
2.21	Theoretical model of the current transformer [3]	40
2.22	Current sensing circuit[3]	41
2.23	Basic architecture of the STM32 MCU based on ARM architecture[19]	42
2.24	Bootloader flow chart[17]	44
2.25	IAP with UART flow chart[17]	46
2.26	Idea for IAP with RS485 and DMA[17]	47
3.1	Core drawing [20]	49
3.2	Schematic representation of the RCD circuit + RC snubber circuit	52
3.3	The chart A) shows the flyback converter U_{DS} voltage without RC and RCD stage and the chart B) show behaviour of the voltage with RCD and RC stages	53
3.4	Voltage regulator with TL431	54
3.5	Core drawing and image [24]	58

LIST OF FIGURES

4.1	Memory partition of STM32F446 [5]	61
4.2	Memory partition of STM32F446 for the SW	61
4.3	Connectors layout with respect to the board	62
4.4	Software's flow chart representation	63
5.1	Top side of the prototype PSU board	65
5.2	Top side of the prototype PSu board	65
5.3	Chart of the U_{DS} voltage and a voltage across the shunt resistors and a current through the primary side	66
5.4	Blue: U_{DS} across the MSOFET and Pink: U_{CS} across the shunt resistors .	67
5.5	Blue: U_{DS} across the MSOFET and Pink: U_2 on the 6V secondary winding .	67
5.6	Bottom side of final main board	68
5.7	Top side of final main board	69
5.8	Bottom side of the ultrasound module	70
5.9	Top side of the ultrasound module	70
6.1	Example of the flashing environment	72
6.2	Data received in the terminal through the RS485-USB adapter	72
6.3	Testing the Bootloader + IAP + updating new software while the old application is running and jumping to the new application	73
6.4	Sensor input image - 1	74
6.5	Sensor input image - 2	75

LIST OF FIGURES

1 Introduction

This thesis goes through the design process of the signal acquisition unit that will be part of a more extensive system. It should be able to communicate via RS485 with the master unit and work with different signals that serve diagnostics and possibly a feedback control system for the rainwater collection system. Different quantities might serve as information about the system and, with that knowledge, control the rainwater management around the house and in the house. The scope of the thesis is not only the electronic design of the board but also the design of the system updater and essential communication with the sensors and signals.

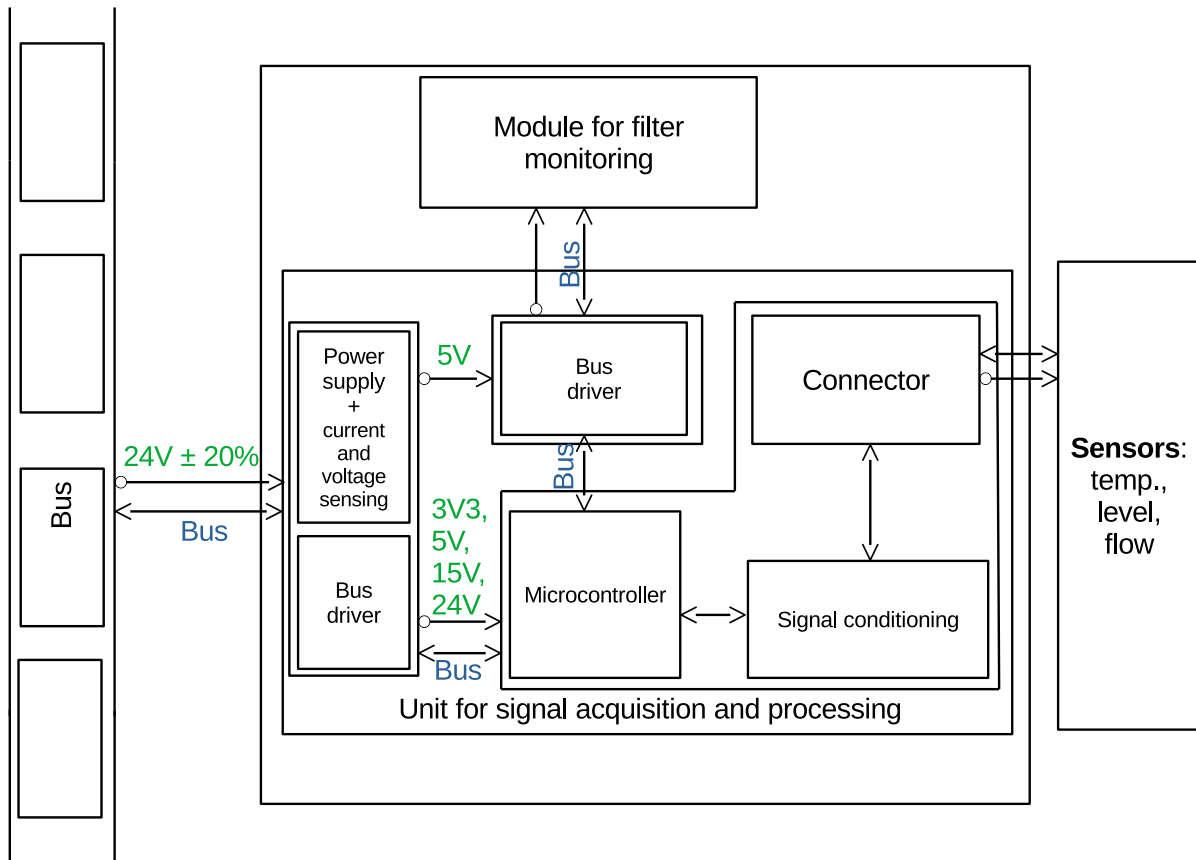


Figure 1.1: Basic concept for the signal acquisition board

The introduction briefly describes the system network and unit requirements. Figure 1.1 shows the situation in the network. The board itself acts as a slave device and has various functionalities. The system's heart is a microcontroller from the company STMicroelectronics that provides all the necessary features for the signal acquisition, storing the software in its memory and communication with sensors and the server.

1.1 Rainwater retention system

This thesis involves building and designing a PCB that implements diagnostics and monitoring of a rainwater retention tank and subsidiary distribution systems. The PCB is part of a more extensive system communicating based on a half-duplex peer to peer TIA/RS-485 serial communication.

The entire system has at least five units.

1. First is in an attic.
2. Second in a garage
3. Third in a corridor
4. Fourth in a basement
5. Fifth in the underground tank

A water retention tank in the attic uses a gravity flow to supply water. The measurement and control unit in the attic controls a valve with servomechanism and adjacent sensors to help with the distribution and water management.

The second unit is in the garage for automatic irrigation with a servo mechanism, water monitoring and water consumption control.

The third unit is in the corridor. This unit is an interface with a DB server. Its job is to communicate with a server and with trigger commands. The unit also facilitates packet management and clock synchronization, basically communication between all units and the server.

The fourth unit takes place in the rack in the basement, and it is a central unit of an entire system. The rack has multiple cards that handle different tasks. Examples are a UPS, HW protection card, IO card with network detectors, a card with power electronics, a card with the control circuit, a bus driver circuit, and a memory slot.

The fifth and last unit is the unit for the underground filter and water tank diagnostics and monitoring. This thesis focuses on this fifth unit, and its descriptions are in the next section.

A system diagram is in the figure 1.2. The diagram shows where the units are and the water accumulation placement. The communication with the server is via serial TIA/RS-485 communication, and the communication between an underground filter and an underground tank is via TIA/RS-232 serial communication.

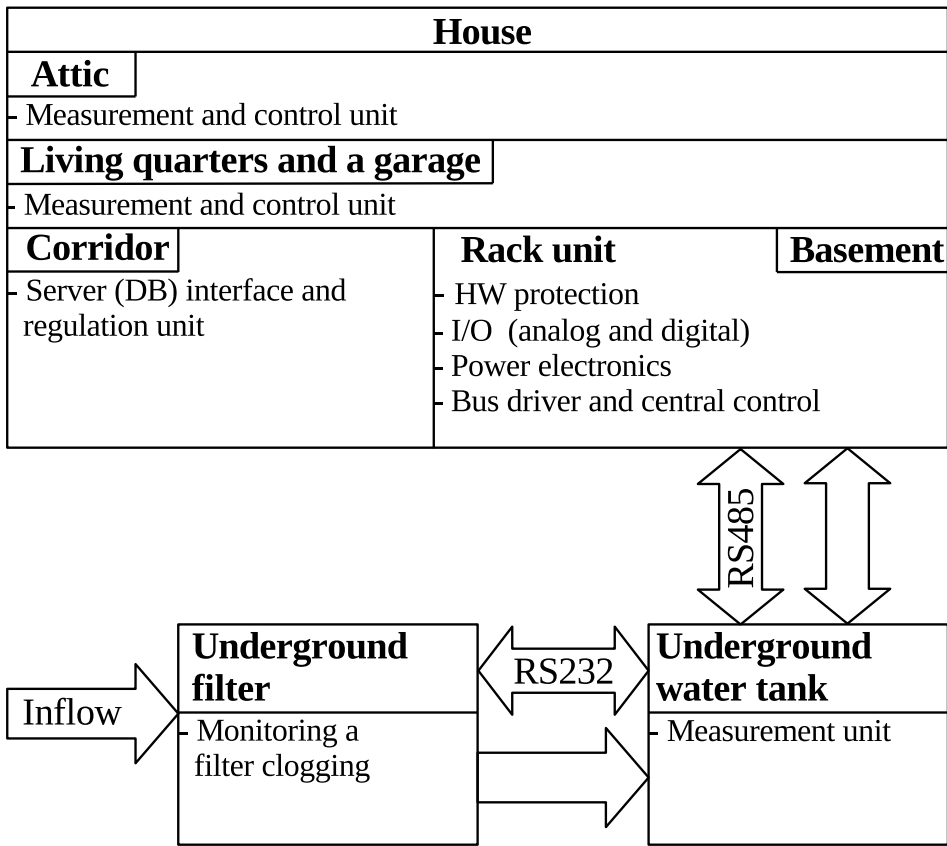


Figure 1.2: Rainwater retention system diagram

1.2 Measurement unit requirements

The measurement requirements are the possibility of communicating with a server via RS485, providing the necessary protection from environmental situations such as lightning strokes, avoiding leaky currents, and keeping minimal distances between the wires on the board. Another requirement is the power supply for different areas, circuits and communication between galvanically isolated ultrasound filter clogging sensors. The basic concept of such a board with more detail is in the figure 1.3. The board blocks are discussed in the research and design and presented in the implementation and testing chapter.

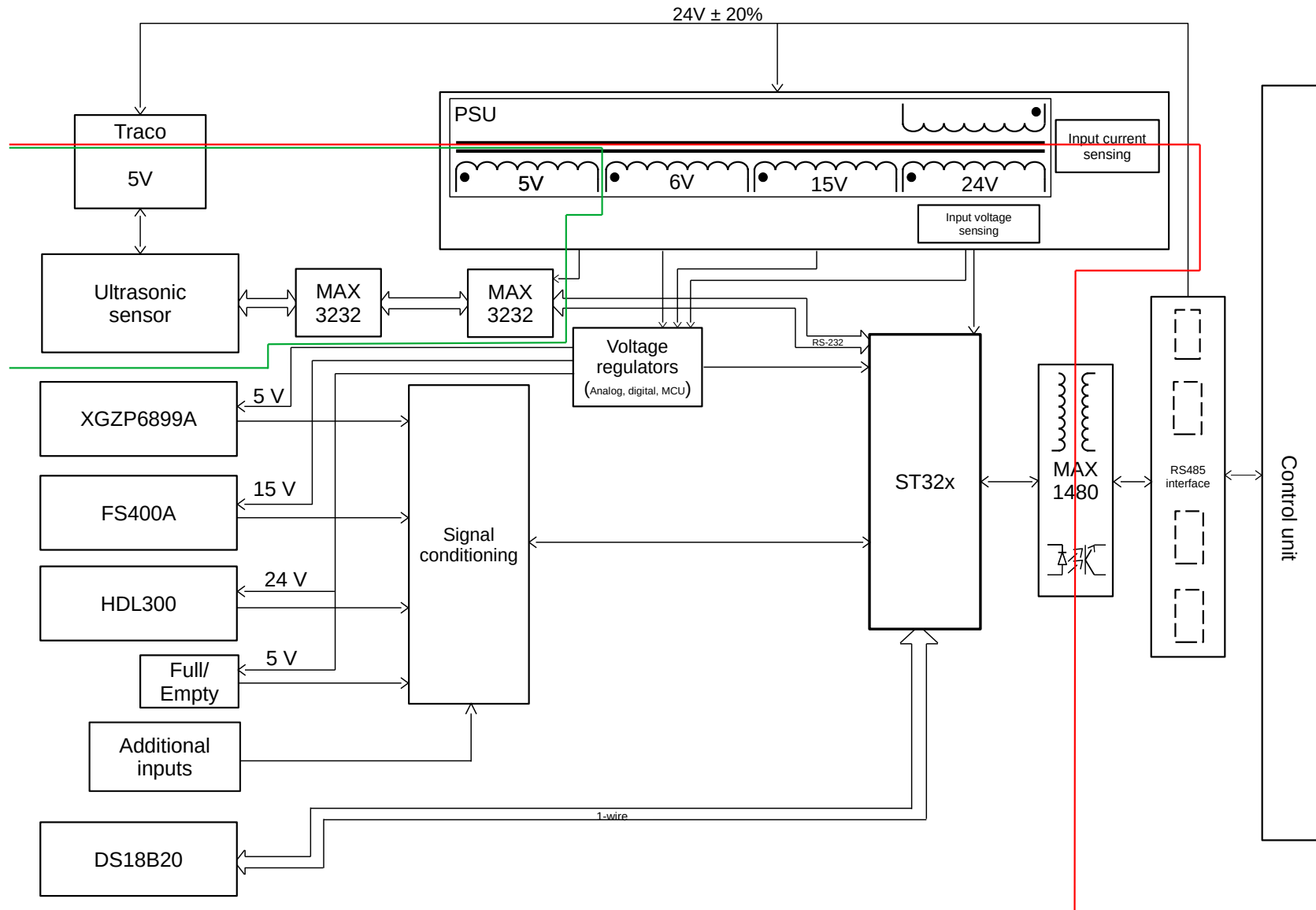


Figure 1.3: More detailed board description

2 Research

The research contains a brief description of the measured quantities, measurement methods, and sensors division into groups. Then a description of the used sensors in the system and their characteristics and operation. Then suitable circuits are selected and described. A principle of the flyback converter and its design is described. Then STM32 peripherals are described in the context of this thesis. Software research describes the system update approach and signal acquisition of each sensor.

2.1 Sensors and Measuring methodology

The measurement methodology shows how to measure physical quantities. The method strongly depends on the amount of data measured, the precision of the method, the precision of the equipment, and the demand for the accuracy of the measurement.

Methods are in different groups.

- **Direct:** One quantity for one measurement device.
- **Indirect:** A quantity depends on other different quantities.

Or:

- **Absolute method:** gives a value of a quantity in its SI unit.
- **Relative method:** compares the measured quantity with an etalon, a norm, or a precise reference quantity.

There are other possibilities to divide the methods, but these are the basic ones.

2.2 Measuring system

The measuring unit processes signals and data from different sensors that measure different states of the rainwater retention system. The retention system has a sensor system that composes of following sensors.

Sensed phenomena

- Water level sensors
 - A continuous type sensor - piezoresistive type
 - Water level switch - based on Hall effect
- Flow meters

- Turbine flow metre
- open channel flow metre - type of pressure
- Temperature sensing
 - Submersible sealed SMART sensor with 1-wire bus
- Voltage and current detection
 - Voltage sensor - input of PSU
 - Current sensor - input of PSU

A sensor, transducer, or detector serves as a primary source of information on the physical, chemical, or biological value measured. The sensor transforms a particular phenomenon into a measurable quantity, mainly electrical. Some sensors can directly give a digital signal as an output.

For signal conditioning and signal acquisition, it is necessary to summarise helpful information about the sensors for further use. These pieces of information are crucial for choosing the appropriate circuitry, and the appropriate acquisition of signals by a microcontroller unit (from now on called an MCU) [1].

2.2.1 Sensed physical quantities

Sensed physical quantities to be measured with a microcontroller are:

Temperature

The temperature is a thermodynamic state quantity based on the efficiency of a reversed Carnot cycle. Based on the idea of an ideal heat engine and constant volume, the formula describing this process is:

$$p = T \frac{p_o}{T_o} \quad (2.1)$$

Where p is a pressure [Pa], T is a temperature in [K], p_o is an atmospheric pressure and T_o is a temperature of the triple point of water [Pa].

The definition of the temperature scale is the triple point of water. The equilibrium of ice, water, and saturated vapour. $T = 273.16\text{ K}$. The basic unit is *kelvin* [K]. The Celsius unit is defined as:

$$\vartheta = T - T_o \quad (2.2)$$

where ϑ is the temperature in Celsius and T in kelvin.

Every thermometer is subject to the international temperature standard ITS-90. Measurement of temperature uses dependence on physical quantities to its advantage. The choice of the physical phenomenon is founded on the minimal deviation of the mathematical description of temperature dependence. Gas thermometry is the most precise form of obtaining the temperature. Because this approach is complicated, an international

temperature scale, ITS-90, was created. This scale is an empirical scale stated from 17 precise temperature points settled at equilibrium points between phases of different materials with the help of interpolation equations and interpolation instruments [1].

Pressure

$$p = \frac{dF}{dS} \quad (2.3)$$

Ambient pressure p is defined as the ratio of an element of the force dF that affects an unit area dS . A unit of pressure is a pascal [Pa]. Pressure of 1 N that affects an area of $1\ m^2$ ($1\ Pa = 1\ N.m^{-2}$). The pressure of the atmosphere of the Earth has 1 bar = $10^5\ N.m^{-2}$. A zero-pressure belongs to the vacuum, a space without a mass. Absolute pressure is calculated from zero pressure. For environments with flow-like conditions, pressure is divided into static, dynamic, and absolute pressure. An equation for a dynamic pressure is as follows:

$$\vec{p}_d = \frac{\vec{v}^2}{2} \rho_v \quad (2.4)$$

where ρ_v is the density of the liquid and \vec{v} is the speed of flow of the liquids.

A material with reasonable force transducer properties is chosen to measure pressure (except for vacuum). Transduction is related to the conversion properties of the material (deformation ε). Deformation is translated directly into a charge (piezoelectric), magnetic properties (induction), optical quantities, and electric resistance or through an elastic object. Hook's law uses bending, stretching, torsion, or shear. A deformation is calculated according to the mechanical stress, or position [1].

Water level height

To determine the height of the water level, specialised position sensors or sensors that detect physical phenomena affected by height change can provide such information. Sensors determining the height divide into continuous and discontinuous types. Continuous types are mass, force, pressure, electromechanical, and others. The discontinuous types are floating, vibrational, ultrasound, radiation, Etc.

The signal acquisition board will use a continuous type measurement (piezoresistive element) that is submerged under the level and is subject to the following relation:

$$h_x = \frac{p_2 - p_1}{\rho g} \quad (2.5)$$

where p_2 is the hydrostatic pressure in [Pa], p_1 is the atmospheric pressure in [Pa], ρ is the density of the liquid, g is the gravity constant [$m s^{-2}$] and h_x is the height [m]. And for filter clogging, an ultrasound sensor is used.

For discontinuous monitoring of water level, end-stop switches are used.

Flow

Sensors that monitor a flow of liquids sorts out in two quantitative groups *Volumetric* Q_v and *Mass* Q_m of liquid flown in a specified cross-section for a unit of time. Calculation of a volumetric flow and a mass flow needs a known cross-section S [m^2] and a bulk velocity v [m/s^{-1}].

$$Q_v = \frac{\Delta V}{\Delta t} = \vec{v} \cdot S \text{ [m}^3 \cdot s^{-1}\text{]}; Q_m = \frac{\Delta m}{\Delta t} = \rho \cdot \vec{v} \cdot S \text{ [kg} \cdot s^{-1}\text{]} \quad (2.6)$$

Indirect acquisition of Q_m and Q_v works with knowledge and stability of a liquid density ρ , and in both approaches, a bulk velocity is present.

Direct acquisition of a liquid flow is possible with dispenser-type sensors that quantify the liquid in a specific container and move it in the flow direction.

The signal acquisition board acquires a signal from a differential pressure sensor for open channel measurements and from the turbine flow metre, which monitors the flow in the pipes [1].

Voltage and current sensing

Voltage and current detection are necessary to monitor the board's power consumption. There are different possibilities to detect such quantities for sensing the voltage level and current on the board's input. Such a sensor aims to sense and modify the suitable signal for microcontroller levels.

- **Voltage sensing**

Voltage sensors work in a way that modulates the detected voltage on measurable scales for further acquisition. There are different approaches to acquiring these signals. The method depends on the situation. Very popular are voltage sensing transformers with a cascaded transformation ratio and small secondary current. The transformer approach has flaws because it is only suitable for alternating voltages. The frequency bandwidth limits the lower side with time constant $\tau = \frac{L_1}{R_i}$, where L_1 is an induction of the primary side and the inner resistance R_i of the source.

Another possibility is using a voltage divider with a capacitor C as a low-pass filter with a parallel combination of the voltage divider. It has a frequency bandwidth higher than that of detection transformers with the flaw of galvanic isolation [1].

- **Current sensing**

The most popular method for sensing the current is using a series shunt resistor in the current path. The resistor is chosen to be small for lowering the voltage drop across it. It is necessary to minimise parasitic inductance and capacitance or/and modify the voltage on the shunt resistor if necessary.

Another method is the use of a current-sensing impulse transformer. The primary site of this transformer has one turn, and the secondary side has a significantly more significant number of turns to transform the current. Then it is detected across the shunt resistor. It is advised to use a peak detector for the one polarity impulses, and for

microcontroller acquisition, a large capacitor is placed on maintaining the voltage during the demagnetisation cycle [3].

There is another approach to using Hall's effect for high currents, but this is not the situation of this board [1], [3].

Sensors are divided into five groups.

- **According to the physical quantity:** temperature, pressure, flow, radiation sensors, mechanical value sensors (translation, rotation, velocity), analysis of substances, liquids, gases, electrical values, and others.
- **Physical principle:** Resistive, inductive, capacitive, magnetic, piezoelectric, pyroelectric, optoelectric, and others.
- **According to the contact with measured environment:** in contact and without contact.
- **According to signal transformation:** Active and passive sensors.
- **Manufacturing technology:** Electromechanical, mechanical, pneumatic, electric, electronic, electrochemical, semiconductor, microelectronic, and others.

Sensors that act as a source of electrical energy (thermoelectric effect) due to the influence of their surroundings are **active sensors**.

Sensors that require the transformation of an electrical quantity into an analog voltage or current signal are **passive sensors**. The output is a frequency, amplitude, or phase. These sensors require an external power supply to operate [1].

2.2.2 Temperature sensors



Figure 2.1: An output current graph.

Measurement of a board temperature, MCU and water is possible with the use of widely used integrated circuit (from now on as IC) temperature sensors DS18B20 and onboard IC temperature sensor in the MCU.

MCU temperature sensor

The MCU temperature sensor works on the temperature dependence of the base-emitter voltages of PNP bipolar junction transistors (from now on as BJT) and their current densities. Because the temperature sensor cannot be precisely manufactured and its offset varies from chip to chip, temperature sensing is suitable for detecting temperature changes instead of absolute temperatures. For accurate temperature detection, an external temperature sensor part should be used. The STM32F446 temperature sensor is linearly dependent on temperature. The conversion range is between 1.7V and 3.6V. The onboard sensor has its sampling characteristics and acquisition methods. More detailed description is in the MCUs datasheet.[5].

External DS18B20 sensor

The DS18B20 ensures direct-to-digital temperature conversion. The benefit of this sensor is its programmability, low-power operation, and use of several parallel sensors on one wire. The power supply to the device is achieved directly through the power supply or indirectly with parasitic power from the data line. The sensor needs additional pull-up circuitry to work correctly [6].

Model No.	DS18B20
Accuracy	$\pm 0.5^\circ$ from -10°C to $+85^\circ\text{C}$
Package	IO-92
Rated power supply	4.9-5.1 VDC
Powered with	0 – 5.5 V
Rated output signal	digital 1-wire bus
Additional features	Identifies, user-definable nonvolatile alarm settings

Table 2.1: DS18B20[6].

2.2.3 Water level sensors

A water level measurement in the reservoir has two sensors. First, a continuous measurement-type sensor is a submerged piezoresistive device that monitors the water level. Moreover, we have a water level switch that reacts to the state of the water level full/empty.

Sensor characteristics

The given water level sensors are:

- HDL300-5M-V1-B1-G1-I - for continuous measurement
- MH1SS1 - contactless magnetic switch

Continuous type sensor - HDL300

The following paragraph describes the characteristics of a sensor and the measurement approach.

Model No.	HDL300
Accuracy	$\pm 0.5 \%FS$
Response Time	5 ms
Sealing class	IP68
Rated power supply	9-35 VDC
Powered with	24 VDC
Rated output signal	4-20 mA
Output signal	4-10.4 mA
Rated measuring range	0-5 m
Measuring range	0-2 m
Housing	Stainless steel probe

Table 2.2: Water level sensor characteristics.

Table 2.2 shows that the sensor has enough response time to measure the water level within the reservoir continuously. The sensor needs 24 V of DC voltage. The output signal is in the form of a current. The sensor translates the height into a current signal form, where $4 - 20mA \rightarrow 0 - 5m$. The chosen water level sensor for this system is HDL300-5M-V1-B1-G1-I. The sensor operates in the range of 0-2m instead of 0-5m, so the current operating range is 4-10.4 mA.

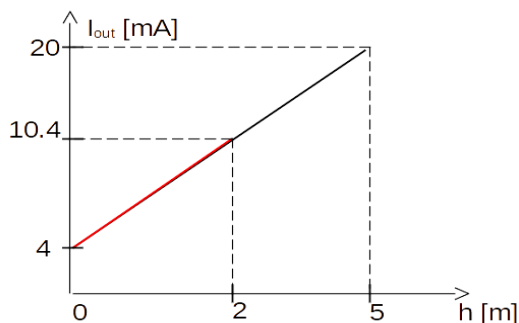


Figure 2.2: An output current graph.

Water level measurement principle

The sensor measures atmospheric pressure above a water level and a water column pressure above the sensor. This pressure difference represents the height in the form of a current signal. Sensor characteristics are given in table 2.2. Figure 2.2 demonstrates a physical principle. The sensor acts as a current source, operating in a current loop with the power source and the acquisition unit. Increasing the water column above the sensor translates the pressure difference between the stainless steel and piezo-ceramic membrane through the oil filament.

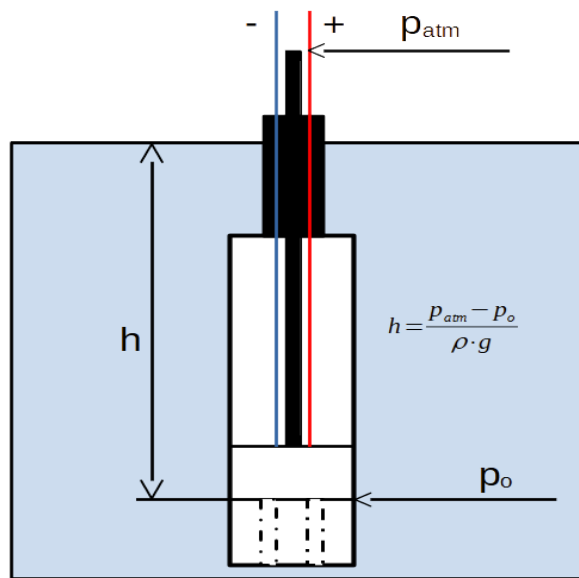


Figure 2.3: Physical principle of a piezoresistive sensor.

Water level signal conditioning

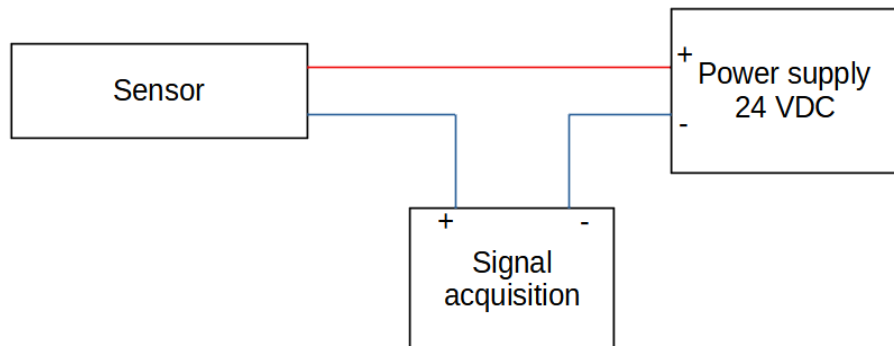


Figure 2.4: Operation block diagram.

HDL300 outputs a 4-20 mA signal, depending on the height of the water column above the sensor. Current-voltage conversion is through a differential amplifier that converts 4-10.4mA to 0-3.3V representing height. This signal leads to an analogue input of the microcontroller with an AD converter.

Switch type indication - MH1SS1

Model No.	MH1SS1
Response Time	$t_{up} \leq 0.5 \mu s, t_{down} \leq 10 \mu s$
Rated power supply	4.9-5.1 VDC
Powered with	5 VDC
Rated output signal	$U_L \leq 0.25V, U_H \geq 3.15V$
Input current	$I_{in} \leq 15mA$

Table 2.3: Water level switch.

Contactless water level switch principle

The sensor works on the Hall principle. If the conductor is floating close to the wall, where is the end switch, and crosses the sensor, a magnetic field is induced, and the sensor changes state on the output pin as an indication of reaching the end. certain level.

2.2.4 Flow metres

The flow metres used in the system are of two types. Differential pressure sensor for open channel measurement and turbine flow metre for pipe measurement.

Differential pressure sensor for flow rate measurement

The differential pressure sensor measures the pressure in the piping system and compares the pressure in the pipe created from the flow rate of the liquid. The difference in pressure between the atmospheric pressure and the pressure given by the flow gives a characteristic dependence of the pressure and the water flow. With experimentally measured dependence, it is possible to interpolate the desired flow with known pressure.

The equation for Atkinson's law depends on the knowledge of the spillway geometry, particularly the cross-section. The equations that serve to determine the rate of flow are

$$\Delta p = f(Q) \quad (2.7)$$

where Δp is the difference in pressure between the atmospheric pressure and the pressure in the liquid flow of the pipe [Pa]. The pressure is a function of the flow rate..

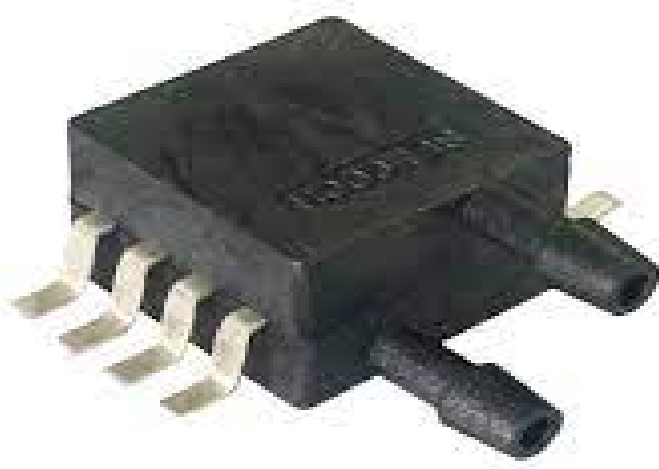


Figure 2.5: XGZP6899A[7]

Model No.	XGZP6899A
Rated power supply	5 VDC
Powered with	5 VDC
Rated output signal	$U_L = 0.5V, U_H \geq 4.5V$ mA
Pressure range	-0.5 - 0.5 kPa

Table 2.4: Differential pressure sensor characteristics

Turbine flow meter

For flow measurement, a turbine flow meter FS400A was chosen. A table 2.5 indicates the parameters necessary for the design of the electronic circuit.

A wide range of linear dependence is achieved if the motor's friction is minimised. The difference between the angular velocity ω [rad/s] of the motor and the flow speed v [m/s] is caused by the friction. Angular velocity is detected with a position sensor and the number of blades. Revolutions and induction sensing give pulse voltage. The disadvantage is the low voltage level at low speeds. Impulses are measured with the counter in the MCU. The characteristic has the following formula

$$f = KQ_v, \quad (2.8)$$

where f is the pulse frequency [Hz], K is the constant of the turbine sensor, and Q_v is the liquid flow [m^3/s]. The sensor has a Hall sensor and magnets on the blades [1],[8].



Figure 2.6: FS400A[8]

Model No.	FS400A
Accuracy	3% 5%
Rated power supply	4.5-18 VDC
Powered with	15 VDC
Operating temperature	-25°C to +80°C
Flow ratet	160 l/min
K constant	5

Table 2.5: FS400A parameters.

2.2.5 Monitoring filter clogging

The filter clogging sensor also acts as the water level measurement sensor. An ultrasound sensor monitors the filter filling that gives status information about the filter clogging.

The sensor is configurable with a resistor that switches between a few modes. If the resistor is not soldered, a trigger mode is set. With a $300\text{k}\Omega$ resistor, a low-power mode is set with a $120\text{k}\Omega$ resistor, an automatic serial port mode. With a $47\text{k}\Omega$ resistor, a low-power serial port mode is set. With a $0\text{k}\Omega$ resistor, the sensor enters computer printing mode. Serial mode is intended to be used with the RS-232 bus.



Figure 2.7: AJ-SR04m[9]

Model No.	AJ-SR04m
Resolution	0.5cm
Rated power supply	5 VDC
Farthest distance	4.5m
Operating temperature	-10°C to +70°C
Total current work	30 mA

Table 2.6: AJ-SR04m parameters [9]

2.3 Electronic circuit research

The board situates in an underground reservoir with different temperature conditions, supposedly lower than the ambient above ground and higher humidity. The tank is located a few dozens of metres from the house, so there is no reliable protection from lightning and other effects. Consequently, the board needs to have some protection against lightning bolts and other effects of electrical overload.

2.3.1 PSU conditions

The board needs a galvanically isolated power supply (from now on as a PSU) and another isolation to monitor filter clogging. The control circuitry also needs different voltage levels.

- **Input voltage from stabilised PSU:** 24V ±20%
- **Output voltage** 5V/0.03A, 6V/0.6A, 15V/0.02A, 24V/0.03A

2.3.2 Control circuitry

For signal acquisition from the sensors, signal conditioning circuits are necessary. Signal conditioning circuits for different sensors are

1. One signal conditioning circuit for the input of the water level sensor HDL300,
2. One signal conditioning circuit for the input of the differential pressure sensor for flow rate,
3. One signal conditioning circuit for the input of turbine flow meter,
4. One signal conditioning circuit for the input of DS18B20 sensors,
5. One output circuitry for Pulse Width Modulation (from now on as PWM) to the static pressure compressor,
6. Voltage sensing circuit,
7. Current sensing transformer.

Aside from signal conditioning circuits for given sensors, several different IOs with their circuits need an implementation. The list of required IOs to suit the requirements of the board are

1. Second input for another turbine flow meter,

2. Two inputs for different pulse-like sensors to be connected to MCUs counter,
3. Two inputs of an analog signal,
4. Two TTL signal inputs.

Bus drivers were chosen to communicate with the ultrasound sensor to prevent filter clogging and communication with the server.

1. MAX1480 - for TIA/RS-485 communication with the server and MCU
2. MAX232 - for TIA/RS-232 communication with the filter monitoring device that is galvanically isolated from the rest of the control circuitry

2.3.3 Flyback converter

For the PSU, there are several possibilities to supply the board. The power supply area that can provide different outputs with one input and galvanic isolation is the switching power supplies with transformers (from now on, SMPS). For SMPS, there are three main topologies to choose from

1. One-switch forward converter,
2. Two-switch forward converter,
3. Flyback converter.

These are the basic ones. There are many more topologies within these three. The equation for comparing the volume of the transformers used by each topology follows. The comparison tells the difference of each topology for the same power delivery.

$$V_{topol.} = V_{Fe} + V_{wind.} = K(S_0 S_{Fe})^{\frac{3}{4}} \rightarrow \frac{V_{two}}{V_{one}} = x \text{ or } \frac{V_{two}}{V_{FB}} = x \quad (2.9)$$

$$\frac{V_{two}}{V_{FB}} = \frac{K(\frac{P}{k\sigma f B_m \sqrt{s}})^{\frac{3}{4}}}{K(4\sqrt{\frac{s}{3}} \frac{P}{k\sigma f B_m})^{\frac{3}{4}}} = \left(\frac{1}{4\sqrt{\frac{0.5}{3}}}\right)^{\frac{3}{4}} = 0.898 \quad (2.10)$$

Topology	One-switch forward	Two-switch forward	Flyback
Transformer size ratio	0.4585	x	0.898
Transistors	1-2	4	1
Control circuit placement	Secondary side	Secondary side	Primary side

Table 2.7: Topology specification

The control circuit can be on both sides for every topology, but these are recommended by the literature [3]. Another control approach is not forbidden. Choosing the best topology for the board's specific size is essential, and the power consumption must be

calculated. The following output voltages and currents are used to pick the correct topology. Aside from the power output, complexity and cost are also important. According to the PSU conditions, the power of the required PSU must have an efficiency of $\eta = 80\%$,

$$P_{out} = U_2 I_2 + U_3 I_3 + U_4 I_4 + U_5 I_5 = 24 \cdot 0.03 + 15 \cdot 0.02 + 6 \cdot 0.6 + 5 \cdot 0.03 = 5W \quad (2.11)$$

$$P_{in} = \frac{P_{out}}{\eta} = \frac{5}{0.8} = 6.25W \quad (2.12)$$

For low-power areas of as much as 200W or less, a flyback converter with the control circuit on the primary side is well suited. Another advantage is that the flyback converter uses less circuitry and only one transistor in comparison to the forward converters[3], but for the power below 50 W advantage between the one-switch forward converter and flyback converter disappears.

Principle of the flyback converter

Flyback converter works in two modes, first $s < s_m$ and second $s = s_{max}$. The basic schematic of the flyback converter is in figure 2.8. The dots mark the beginning of the winding and are orientated against each other. The rectifier of the secondary winding then follows the conventional orientation as with the positive pole. Inductance L_σ is the parasitic stray inductance of the transformer and is not the physical part of the transformer. This inductance is not wanted because it creates a parasitic voltage overshoot on the transistor when it is turning off. The overshoot increases as the current increases, and consequently, the power output grows. Power growth is the biggest flaw of the flyback SMPS.

In time t_{on} , the transistor is turned on, and the magnetisation of the transformer carries out with the current i_1 on the primary side. When magnetisation occurs, the diode is closed, and the charged capacitor feeds the load. At t_d , the transistor turns off, and the transformer demagnetises on the secondary side. Also, the diode is open, and the capacitor is charging from the demagnetisation current i_2 of the triangle form. At that time, the secondary winding is connected through the diode to the constant voltage of the capacitor U_z and demagnetises through it. This is shown in the figure 2.9.

The magnetisation current i_1 grows linearly because it is the integral of $+U_d$ and i_2 from $-U_z$.

The steepness of the primary and secondary currents is given by equations 2.13 and 2.14. The current grows and drops according to the derivations of primary and secondary currents.

$$\frac{di_1}{dt} = \frac{I_{\mu 1}}{t_{on}} = \frac{U_d}{L_1} \quad (2.13)$$

$$\frac{di_2}{dt} = \frac{I_{\mu 2}}{t_d} = \frac{U_z}{L_2} \quad (2.14)$$

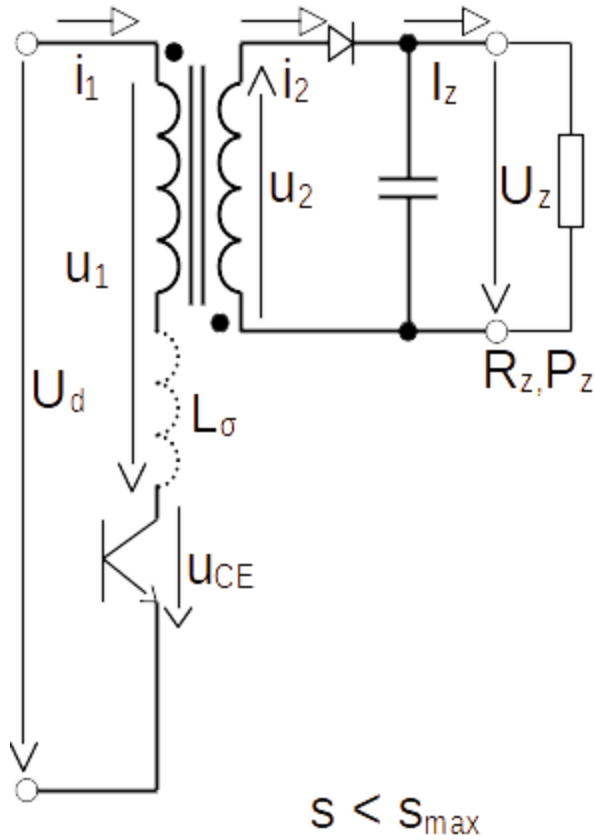


Figure 2.8: Flyback's principle for $s < s_m$. The figure shows a schematic representation of the flyback converter.[3]

Calculating the maximum ratio for the transistor to be turned on is done with a formula 2.15. Because it is necessary to maintain the safe operation of the transistor, condition 2.16 must be met, or the transistor cannot operate. Usually, a double the value of the supply voltage is chosen $U_{CEmax} = 2U_d$. Equation 2.17 serves to calculate the optimal number of turns.

$$s_{max} = 1 - \frac{U_d}{U_{CEmax}} \quad (2.15)$$

$$U_{CEmax} > U_d \quad (2.16)$$

$$N_2 = N_1 \frac{U_z}{U_{CEmax} - U_d} \quad (2.17)$$

For the design of the transformer, it is necessary to calculate the inductance of the primary side turns. Then it is necessary to calculate the maximum magnetisation current, primary turns, and the gap length to let the magnetic field accumulate in that gap.

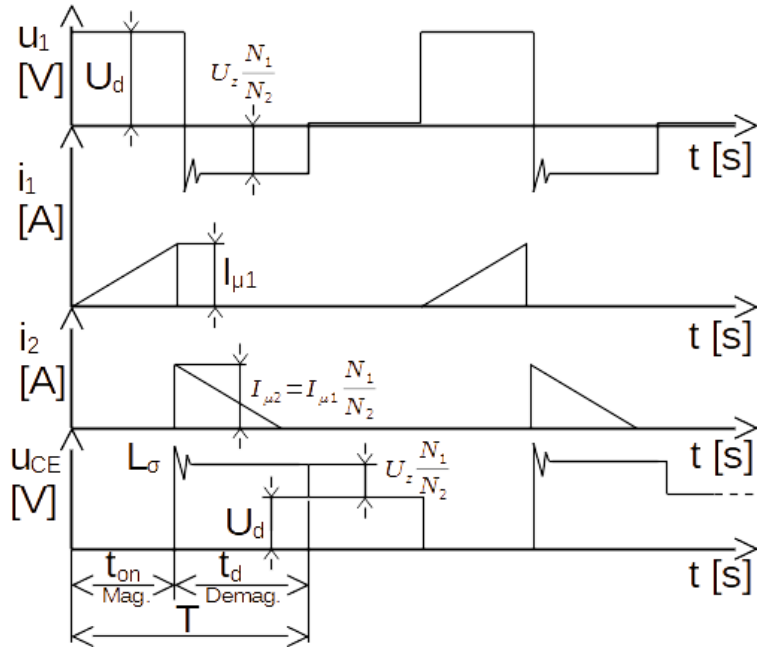


Figure 2.9: Flyback's principle for $s < s_m$. Current and voltages graphs[3]

$$L_1 = \frac{U_d^2 s_{max}^2}{2f P_{zmax}} \quad (2.18)$$

$$I_{\mu 1max} = \frac{2P_{zmax}}{U_d s_{max}} \quad (2.19)$$

$$N_1 = \frac{L_1 I_{\mu 1max}}{B_{max} S_{Fe}} \quad (2.20)$$

$$l_v = \frac{N_1 \mu_0 I_{\mu 1max}}{B_{max}} - \frac{l_{Fe}}{\mu_{rFe}} \quad (2.21)$$

An RCD element converts the overhang energy into heat for protection. The overhang is the result of parasitic inductance. The inductance grows with the length of the current path. It is preferred to minimise the current loop as much as possible. The RC element deals with the energy accumulated in the stray parasitic inductance when the transistor turns off, as in equation 2.22. RC values are chosen according to the power consumption of the resistor, which dissipates power according to the equation 2.23. The circuit example is shown in the figure 2.10 [3].

$$W_{\sigma max} = \frac{1}{2} L_\sigma I_{\mu 1max}^2 \quad (2.22)$$

$$P_R = f \cdot 2W_C = fCU_d^2 \quad (2.23)$$

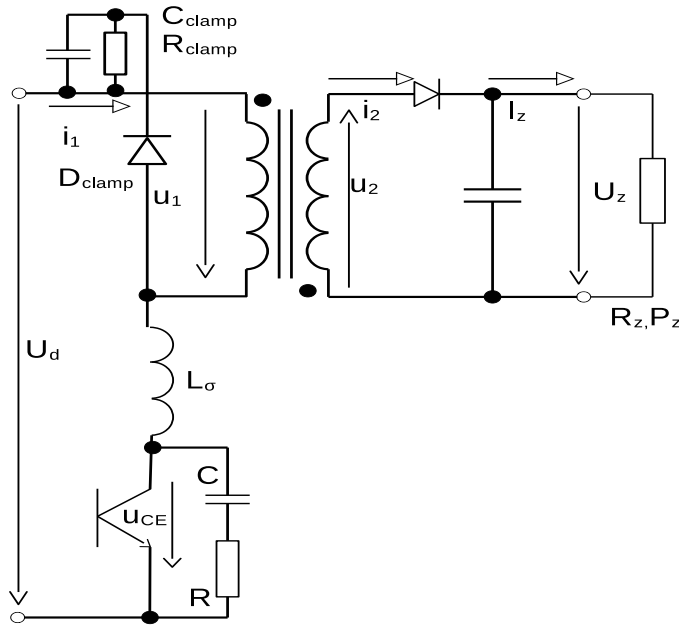


Figure 2.10: RC-step for damping the overhang[3]

Control circuit of the flyback PSU

A current loop and its superior voltage loop control the output voltage regulation. The control circuit is on the primary side. The current loop controls the steady current on the primary side, and the voltage feedback loop maintains the output voltage at the desired level. Suppose the load current of the output increases above the limit set on the primary side. In that case, the voltage regulation \$U_{FB}\$ stops and the current regulation loop \$I_{CS}\$ takes control by limiting the primary current.

The current control loop goes to the limit linearly and then shuts off accordingly. The voltage loop is connected right after the LC filter to lower the regulation loop by one order and precisely control the output. The PI controller regulates the feedback signal. The output voltage is set with the TL431 IC and is redirected through the optocoupler to the controller circuit on the primary side [3], [4].

Except for the 24V voltage output, the other outputs have linear voltage regulators or stabilisation circuits with TL431. On the main 6V output, four voltage regulations will take place. Six voltage regulation units are needed. The specifications are in the following list.

1. **6V:** 3V3 for MCU, 3V3 for AD, 5V for MAX1480 and 5V for differential pressure

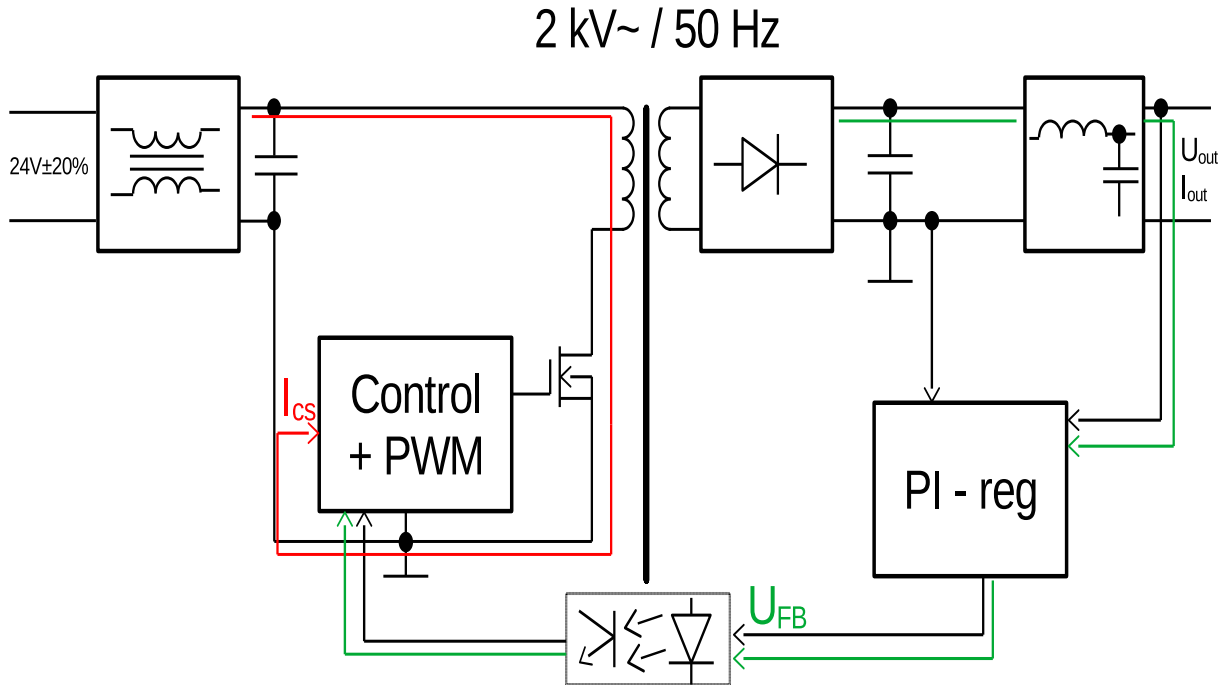


Figure 2.11: Regulation scheme of the flyback PSU[3]

sensor

2. **15V:** 15V voltage regulator for operational amplifiers, hex Schmitt trigger and for powering the sensors
3. **24V:** 24V output has no regulator, just safety Zener diode on the output to not cross allowed voltage.
4. **5V:** 5V voltage regulator isolated from 6V, 15V, 24V and primary side

2.3.4 Signal conditioning circuits

Different circuits were chosen to adjust the signals from the sensors to the measurable voltage levels of the MCU.

HDL300 - Differential amplifier with noninverting stage

According to subsubsection 2.2.3 the HDL output signal will give 0-10.4mA, representing a height of 0-2m. A differential amplifier circuit with a shunt resistor converts a current signal into a 0-3V3 signal suited for MCUs ADC. A proportional noninverting circuit is used for precise offset control of the differential amplifier. The circuit used is shown in the figure 2.12.

For a noninverting operational amplifier, a proportional gain is chosen. The circuit serves to trim the offset needed using an MCU digitally. The noninverting circuit has almost infinite input impedance, so it looks as if there is no load on the DAC output. And the zero difference in the input of the amplifier results in 0 deviations of the output voltage. The equations needed to calculate the output voltage are 2.24. The gain of the amplifier is calculated with the equation 2.25.

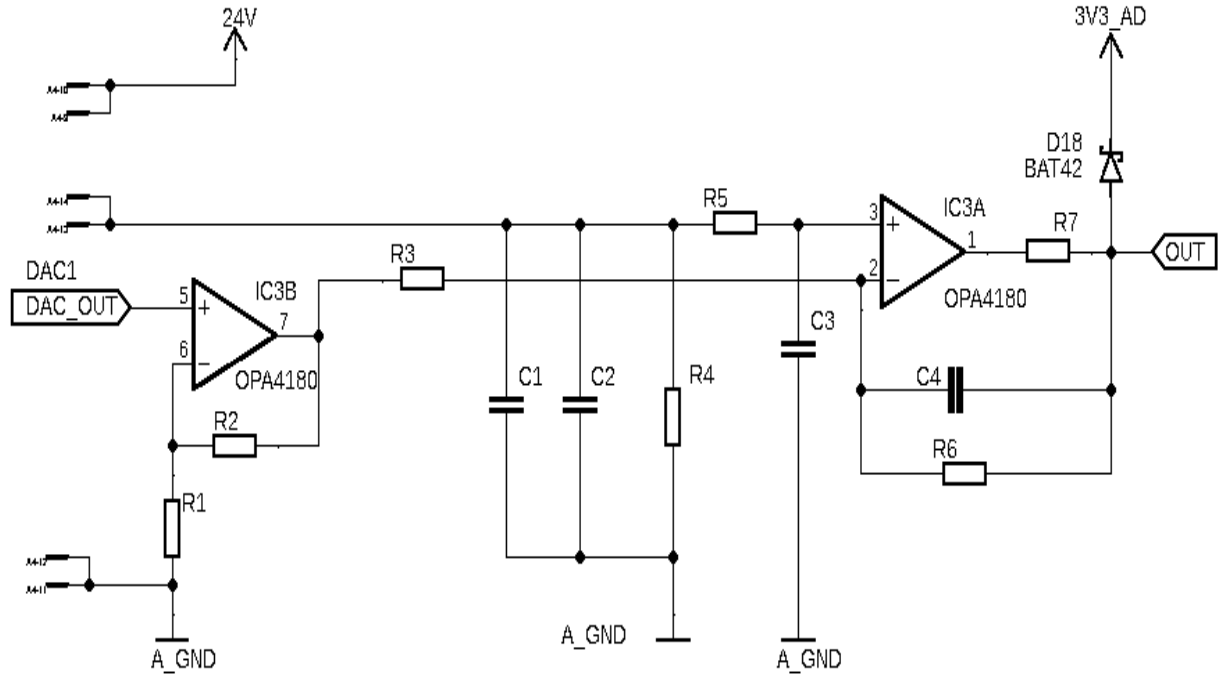


Figure 2.12: Differential amplifier with noninverting stage[4]

$$u_{non}(t) = \left(1 + \frac{R_2}{R_1}\right) u_1(t) \quad (2.24)$$

$$K = \frac{U_{non}}{U_1} = \left(1 + \frac{R_2}{R_1}\right) \quad (2.25)$$

The differential amplifier amplifies the voltage signal to a specific voltage level in the range of the ADC input. The equations for inverting and for non-inverting inputs are 2.26, 2.27 and 2.28. According to the equations and solving the equations for u_o . The necessary RC low-pass stages are placed for filtering purposes. The voltage of the sensor's current loop is $U_{HDL300} = R_4 * I_{HDL}$ [4].

$$U_- = U_{non} \cdot \frac{Z_{c_3}}{Z_{c_3} + R_5} \quad (2.26)$$

$$U_+ = U_{HDL300} \cdot \frac{R_6 || Z_{C_4}}{R_6 || Z_{C_4} + R_3} + U_{out} \cdot \frac{R_3}{R_6 || Z_{C_4} + R_3} \quad (2.27)$$

$$\Delta U = 0 \rightarrow U_+ = U_- \quad (2.28)$$

Flow meters

There are three circuits for two flow meters. The first is the flow meter acquisition circuit and the differential pressure sensor signal the flow rate measurement. The other two circuits serve to invert the pulses for the MCU counters and the PWM step-down converter circuit to control the compressor that gives static pressure in the pipes system.

1. Differential pressure sensor circuit: The circuit follows the same equations as 2.26,

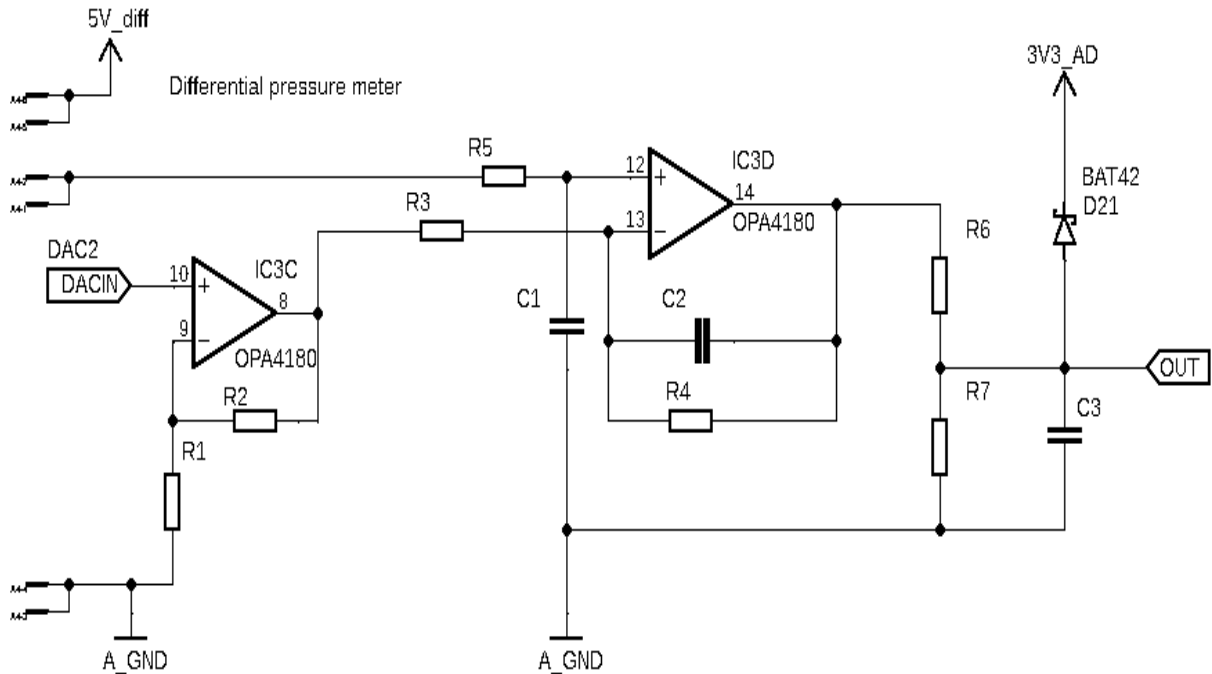


Figure 2.13: Differential amplifier with noninverting stage[4]

2.27 and 2.28. These equations apply to the design of the amplifier. The output signal changes to the MCUs level with the voltage divider.

2. Turbine flow meter signal conditioning circuit: The pulse levels are between 0 and 15V of the power supply. The input pulses might be noisy, so two stages of RC filter with similar time constants but different resistor values are necessary to not load the input signal. The output signal is divided with a voltage divider to level 0-3V3 of the MCU.
3. PWM step-down converter for the compresor. The compressor gives the parameters for calculating resistor and collector current. These calculations will be performed in the design section.

Additional circuits

Additional circuits are a TTL logic input, an end switch signal inverter, and a general analog input circuits.

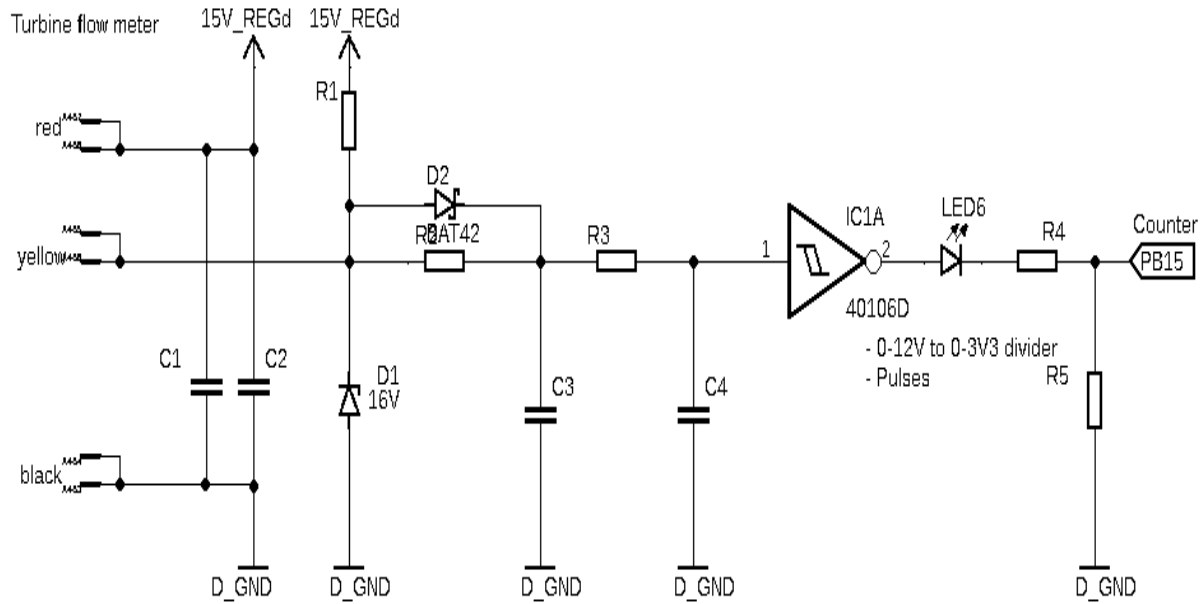


Figure 2.14: Hex Schmitt trigger for suitable levels of the MCU[4]

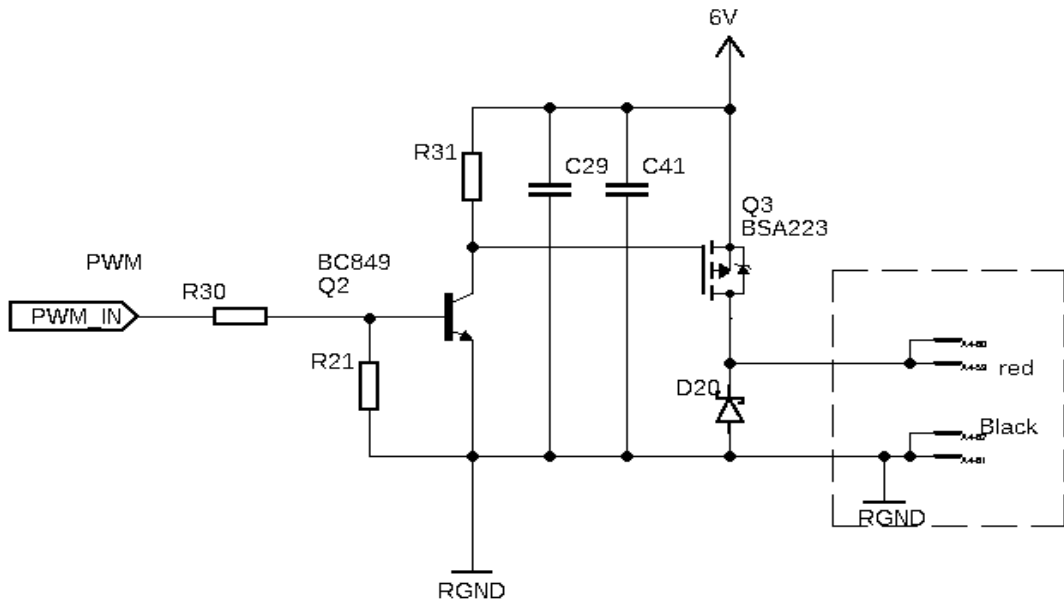


Figure 2.15: A circuit for controlling the compressor and the static pressure[4]

The 5V TTL signal will be reduced and divided with a voltage divider to a suitable 0-3V to work with the MCU TTL input.

The circuit 2.17 filters the input pulse signal and, with a hex Schmitt trigger and a voltage divider, adapts to the MCU voltage levels.

The general analog input circuit with the RC filter for filtering purposes goes to the signal of the microcontroller's general input.

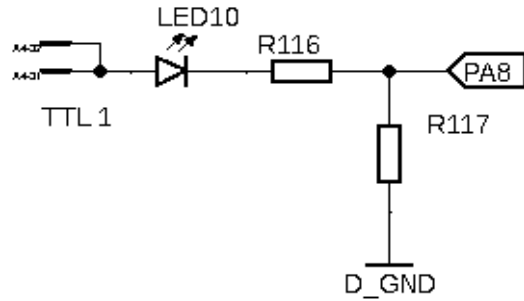


Figure 2.16: TTL logic input with voltage divider[4]

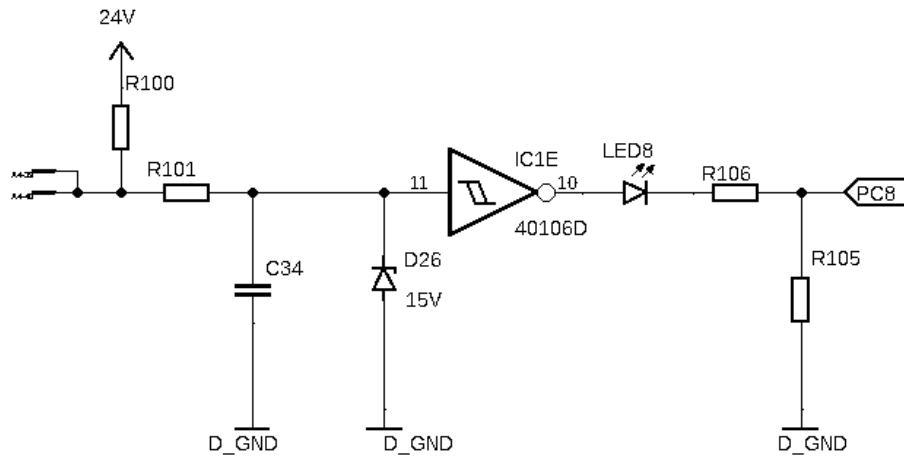


Figure 2.17: Schmitt trigger for pulse acquisition[4]

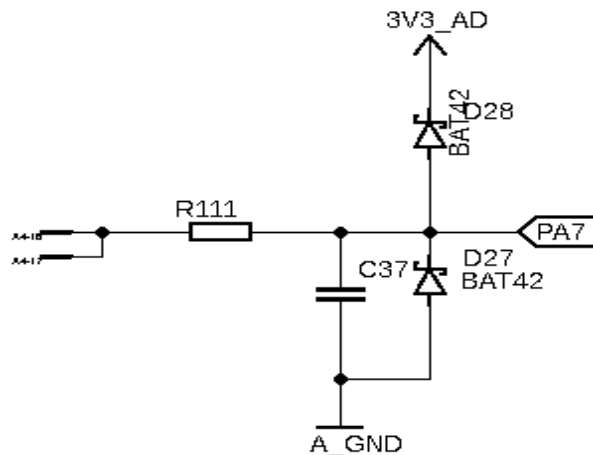


Figure 2.18: General input for analogue signal[4]

2.3.5 Bus driver of TIA/RS-232 and TIA/RS-485

TIA/RS-232 and TIA/RS-485 belong to the group of asynchronous serial bus interfaces and are widely popular in specific situations. TIA/RS-232 is used as a single device-to-device communication and cannot be used for long distances or more than one device. TIA/RS-485, on the other hand, has the possibility of connecting 32x receivers and 32x

transmitters, and with different protocols such as Profibus DP, CAN, and others, it can facilitate more communication between more devices. The general composition of the signal waveforms is shown in figure 2.19. The RS-485 bus can control master-slave communication. The RS-232/485 is the hardware layer for serial communication. The maximum transmission speed is a quarter of the clock of the microcontroller.

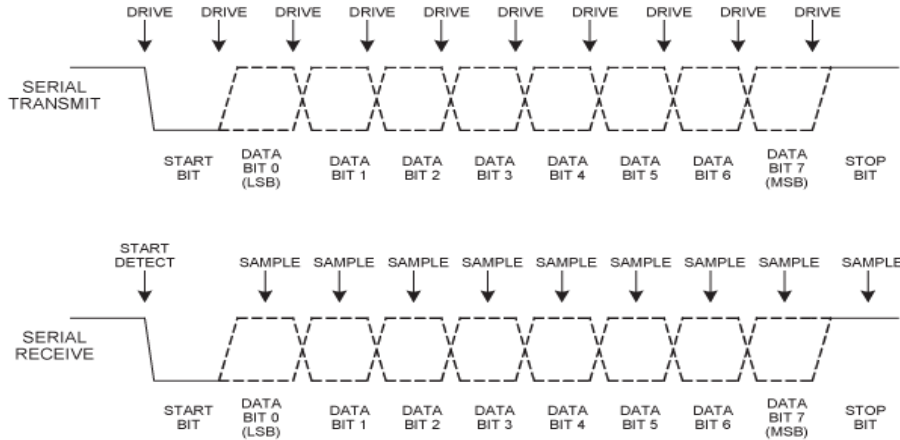


Figure 2.19: UART waveforms for RX and TX[4]

- **TIA/RS-232:** Is an asynchronous full-duplex two-way bus and allows a connection between two devices. For communication via RS-232, an IC needs to be chosen. For this board, a MAX3232 is chosen. This device serves as a transceiver for communication between the MCU and the galvanically isolated ultrasound sensor. A 5V regulated power supply powers the IC. Transmission and reception are in CMOS logic[14].
- **TIA/RS-485:** Is an asynchronous full/half-duplex two-way bus. The transfer speed is 10Mb/s or more for PROFIBUS. The half-duplex communication: all devices listen, and the signal control signal switches to transmission mode and back. Communication speeds can be changed. The MAX1480 has a built-in isolation barrier suitable for isolated MCU from the PSU on the secondary side of the board. The device is self-powered on the connector's side and 5V power on the secondary side. Communication between the MCU and the MAX1480 has 3.3V levels. The device pin FS is the selection between high and low switching frequencies for the isolated power driver. Low frequencies are around 535kHz and HIGH frequencies 725kHz when the FS pin is HIGH. The SD pin serves as a shutdown pin. The DE pin enables and disables the input and output data pins. [15]

2.3.6 Voltage sensing circuit

A voltage divider with a filtration capacitor is chosen to sense the output voltage circuit. Figure 2.20 shows the schematic representations. The final circuit has only resistor combination R55 and R54, diodes D9 and D19 and a filtration capacitor C25. R38 and D7 are omitted. The circuit works in a narrow bandwidth as it cannot stretch the output for the full resolution of the ADC. So, choosing the resistor's value of the voltage divider is to

maximise the output resolution of such a sensing circuit. In the SW, it will be converted with the turns ratio to the input supply voltage of the flyback convertor.

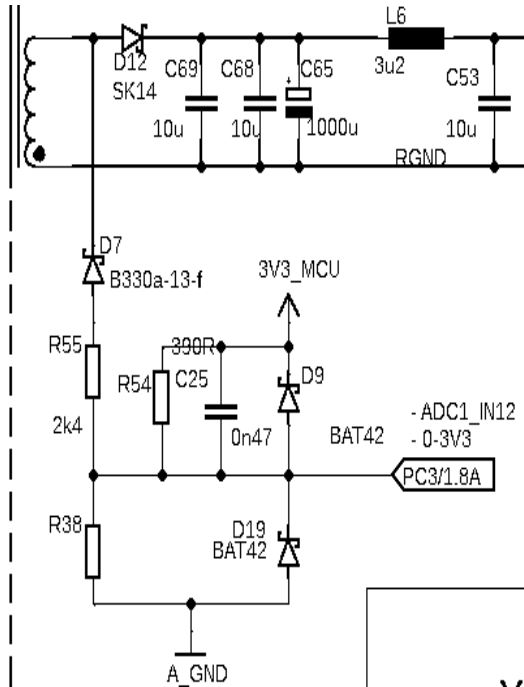


Figure 2.20: Voltage sensing circuit

2.3.7 Input current sensing circuit

Different circuits exist for isolated current sensings, such as Rogowski coil, LEM senor, Etc. An impulse current sensing transformer circuit is chosen to target the primary impulse current. The idea of the transformer lies in an ideal primary side current source with infinite theoretical impedance. Therefore, the supply does not strongly force the supply voltage of the flyback converter. The primary voltage of the current transformer arises as a side product of the secondary voltage. The magnetisation of the core is calculated with the use of secondary voltage.

According to the model 2.21 if the primary winding is connected to the current source with a current $i_1(t)$ a secondary winding seems to be a source of the current $i'_1(t)$ with a parallel secondary inductance L_2 . With a non-zero load resistor connected to the secondary side a non-zero secondary voltage $u_2(t)$ rises across the inductance L_2 . This induced voltage appears on the primary side as a transformed voltage with respect to the turns ratio of the transformer. With the secondary voltage rises the magnetisation current of the secondary inductance $I_{\mu 2} = I_0 + \frac{1}{L_2} \int u_2(t) dt$. Because of this current a magnetic flux density $B(t)$ in the core develops (2.29).

$$B(t) = \frac{L_2 i_{\mu 2}}{S_{Fe} N_2} \quad (2.29)$$

The current flowing to the sensing resistor has a formula $i_2 = i'_1 - i_{\mu 2}$. With this

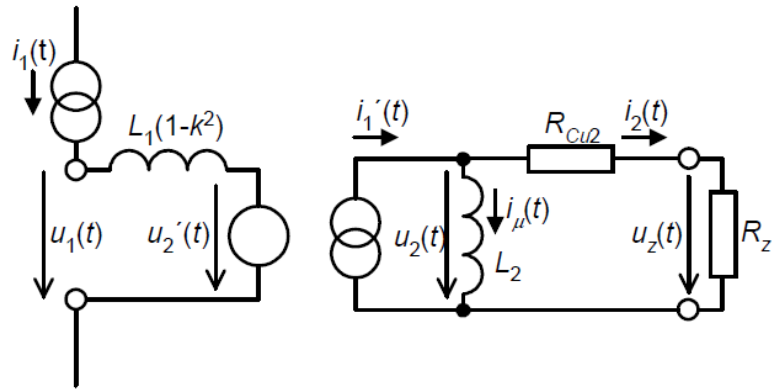


Figure 2.21: Theoretical model of the current transformer [3]

formula, a Current sensing resistor is calculated concerning the maximum allowed voltage of the MCU analog-to-digital converter.

The circuit schema for the impulse transformer is in the figure 2.16. The above formulas and the impulse transformer model show that the transformer cannot work with DC. However, it can give current impulses with a non-zero mean value. The diode D8 ensures that the resistor is disconnected from the secondary winding when the primary MOSFET is off and will not affect the demagnetisation of the secondary winding. The demagnetisation closes through the Zener diode D3 and the diode D4. This pair ensures constant negative voltage on the secondary winding and facilitates a linear decrease of the magnetisation current. Behind the current sensing stage, a peak detector is placed. The capacitor charges to the voltage of the shunt resistor R1, and with R41, it creates an RC filter. The capacitor keeps a constant output for the signal acquisition [3].

Further circuit connection is in the implementation part.

2.4 Software design

The scope of the software design ties to the goal of updating software via server interface without the need to go down to the water tank and flash it manually with the classical In-Circuit System Programming (from now on as ICSP) method. The software design comprises three main parts: Firmware: bootloader + file - transfer + application. The basic scheme for ICSP or solely bootloader programming is direct flash writing to memory and booting up directly to the application. The bootloader adds a decision step to jump to the written application in memory. File transfer mainly serves to upload binary files from an application to the MCU buffers. A file transfer protocol serves to send a larger application binary file. The most basic protocols with simple UART are Xmodem/Ymodem and Zmodem. These protocols are in various terminal applications, so there is no need to program an additional PC application in addition to the MCU protocol [16], [17], [18].

Aside from software design, a study on STM32 and its specific peripherals are in the following sections. STM32 provides a wide variety of peripherals and features used in software development. The requirements for the STM32 MCUs are:

STM32F446 - chosen [5]

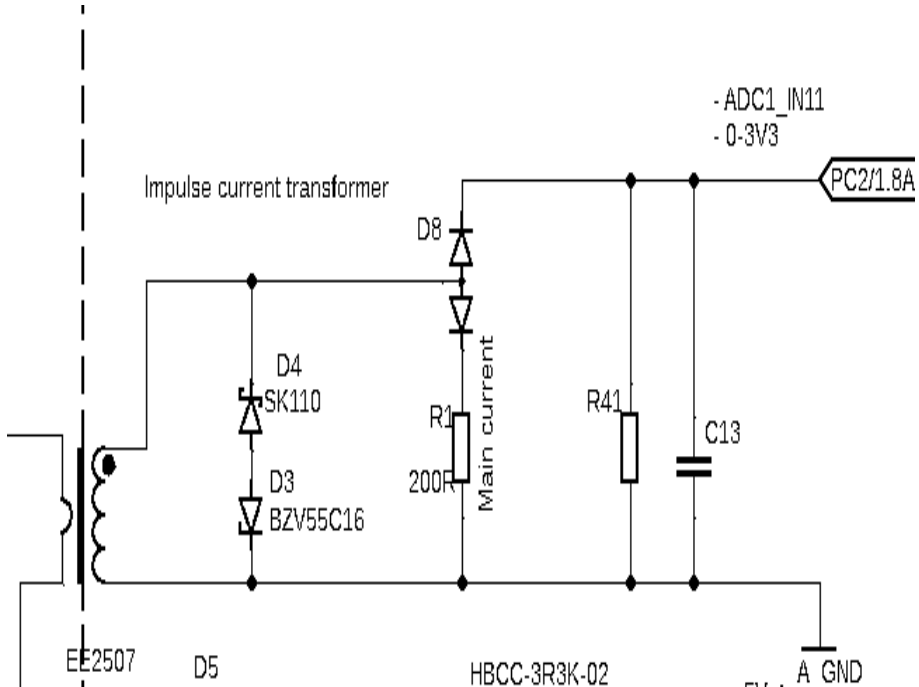


Figure 2.22: Current sensing circuit[3]

- **Memory aspect:** Large memory: FLASH 512 kB and SRAM 128 kB for Buffers
- for updates, future RTOS and 2 application at the same time
- **Timers:** Up to 17 timers for all the needs of sensors connected to the chip
- **Analog to digital converters (from now on as ADC):** 3x12-bit ADC with 24 channels
- **Digital to analog converters (from now on as DAC):** 2x12-bit DAC with 24 channels
- **Interfaces:** up to 4 USARTs, up to 4 I²C and others.

These are the most critical parameters for choosing the correct MCU. In the following sections, a brief discussion of FLASH memory, ADC, DAC, UART, and DMA is needed.

2.4.1 STM32 microcontrollers and its peripherals

The STM32 line-up has many peripherals and a different architecture version. Its family uses an ARM platform. A further description gives an overview of the different peripherals of the chosen MCU.

Architecture of the STM32 MCUs

The chosen chip is the arm based architecture of line Cortex class M4 with a floating-point unit. The processor has a 32-bit floating-point unit with a RISC processor for efficiency and low power characteristics. It gives an advantage of high-performance operation [19], [5].

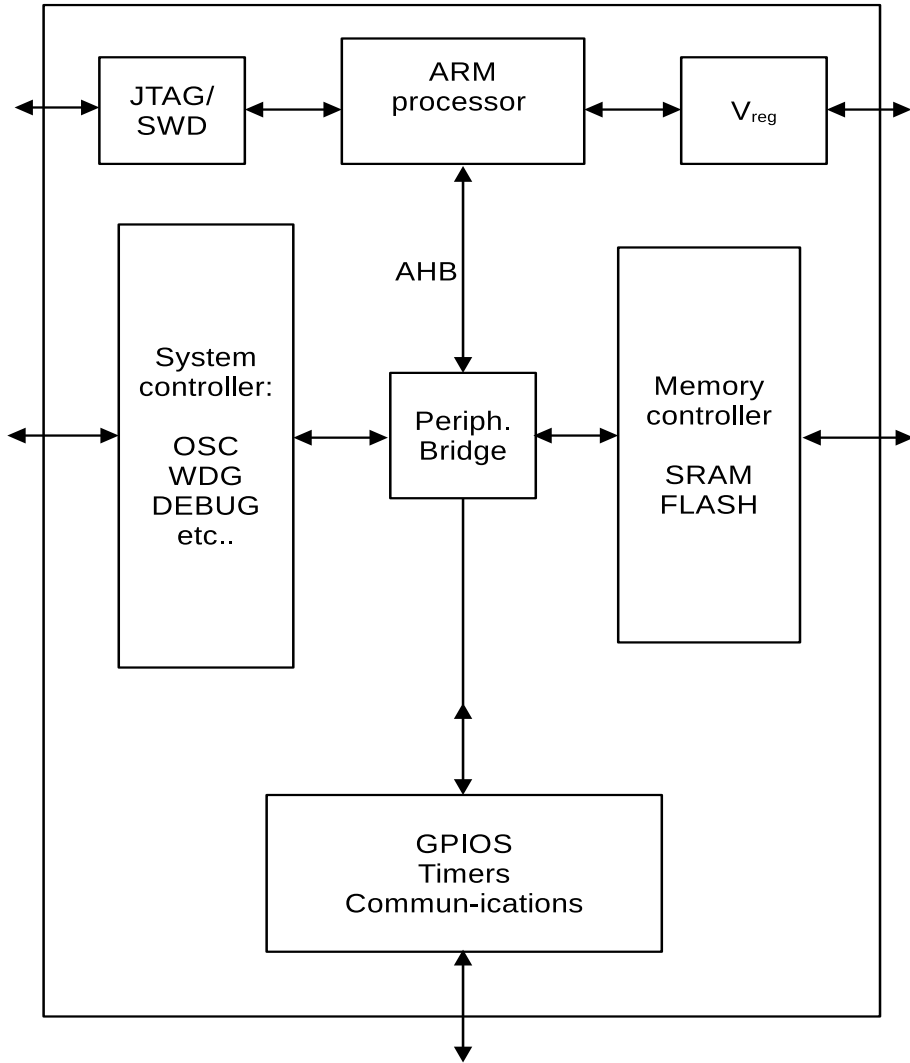


Figure 2.23: Basic architecture of the STM32 MCU based on ARM architecture[19]

- **Timers:** The stm32f446 has two advanced timers (TIM1, TIM8) that provide three-phase PWM with Input Capture, Output Compare, PWM generation, One-pulse mode output and independent DMA requests and a few channels. The timers are 16-bit. That can synchronise with other timers. Then there are ten general-purpose timers. Four of them have counters, pre-scalers, multiple channels, the possibility to generate PWM output, and DMA request capability. The four timers have 32-bit up-counter and 16-bit Prescaler, and the remaining six timers have 16-bit up-counter and 16-bit Prescaler. The last are two basic timers for DAC trigger and have DMA request capability.
- **FLASH memory:** The flash memory block on the stm32f446 has a capacity of 512kBytes. Data read/written in a byte, half-word, word, and double-word blocks. The chip can erase a block or entire memory. The memory comprises four 16 kBytes sectors, one 64 kByte sector, three 128 kBytes sectors, a system memory block of 30 kBytes, and an OTP area of 528 Bytes and Option bytes of 16. The OTP bytes are configured for reading/writing protection, BOR level, watchdog, and SW/HW

reset. The module also has a low power mode. The read/erase and write need to go one after another, they cannot overlap, or they will stall.

- **ADC and DAC:**

- *ADC*: has an architecture of a successive approximation register. The ADC needs to establish a direct connection between the measurement voltage source and the embedded sampling capacitor of the ADC. The sampling time can be adjusted for each channel. There is a limitation on the minimum sampling time to charge the capacitor. ADC can multiplex up to 19 channels and measure about 16 external sources, two internal sources, and the V_{BAT} channel. Conversion has properties for single, continuous, scan, or discontinuous modes. The result of the conversion is the right/left alignment of 16-bit data registers. The ADC also has the possibility of DMA, Interrupts, Configurable resolution Etc.
- *DAC*: There are two DACs with two channels each. The DAC configuration has an 8 to 12-bit resolution. The DAC can use a DMA controller, and the 12-bit configuration might be aligned right/left. Dual-channel conversion might be done independently or simultaneously if they are synchronised. Other properties are Noise wave generation, triangular wave generation, DMA underrun detection, and external trigger conversion.

- **USART**: Allows a full-duplex data exchange with external devices and meets the industry standard NRZ asynchronous serial data format. The fractional baud rate generator gives a wide range of baud rates. There is the possibility of DMA control. USART has many functions, but these are crucial: Programmable data word length (8 or 9). Configurable stop bits, Configurable multibuffer communication using DMA, transfer detection flags, Interrupt sources,

- **DMA**: The DMA facilitates high-speed Peripheral to memory, memory to peripheral and memory to memory transfer. Data can be redirected and transferred without CPU interaction. DMA uses a dual AHB master bus and independent First in First out (from now on as FIFO) to optimise the system's bandwidth on the complex bus matrix architecture. There are two DMA controllers with eight streams each to work with one to eight peripherals. DMA requests can have a set of priorities programmatically.

2.4.2 Software updates

There are two main approaches for updating the software and giving the programmer the option to rewrite the flash memory with an updated version. The characteristics of each approach are listed below. The basic function must be present in some way in any updated approach. The following is a schematic description of these approaches and a design idea for the following. this board [19], [17] and [5].

Bootloader

The bootloader is an essential part of software updates. When the board with a bootloader is powered on, a decision tree decides if it is possible to jump to the application on

specific memory address, or wait for the application to be uploaded. Figure 2.24 shows the schematic representation of a bootloader in the SW. [19], [17] and [5].

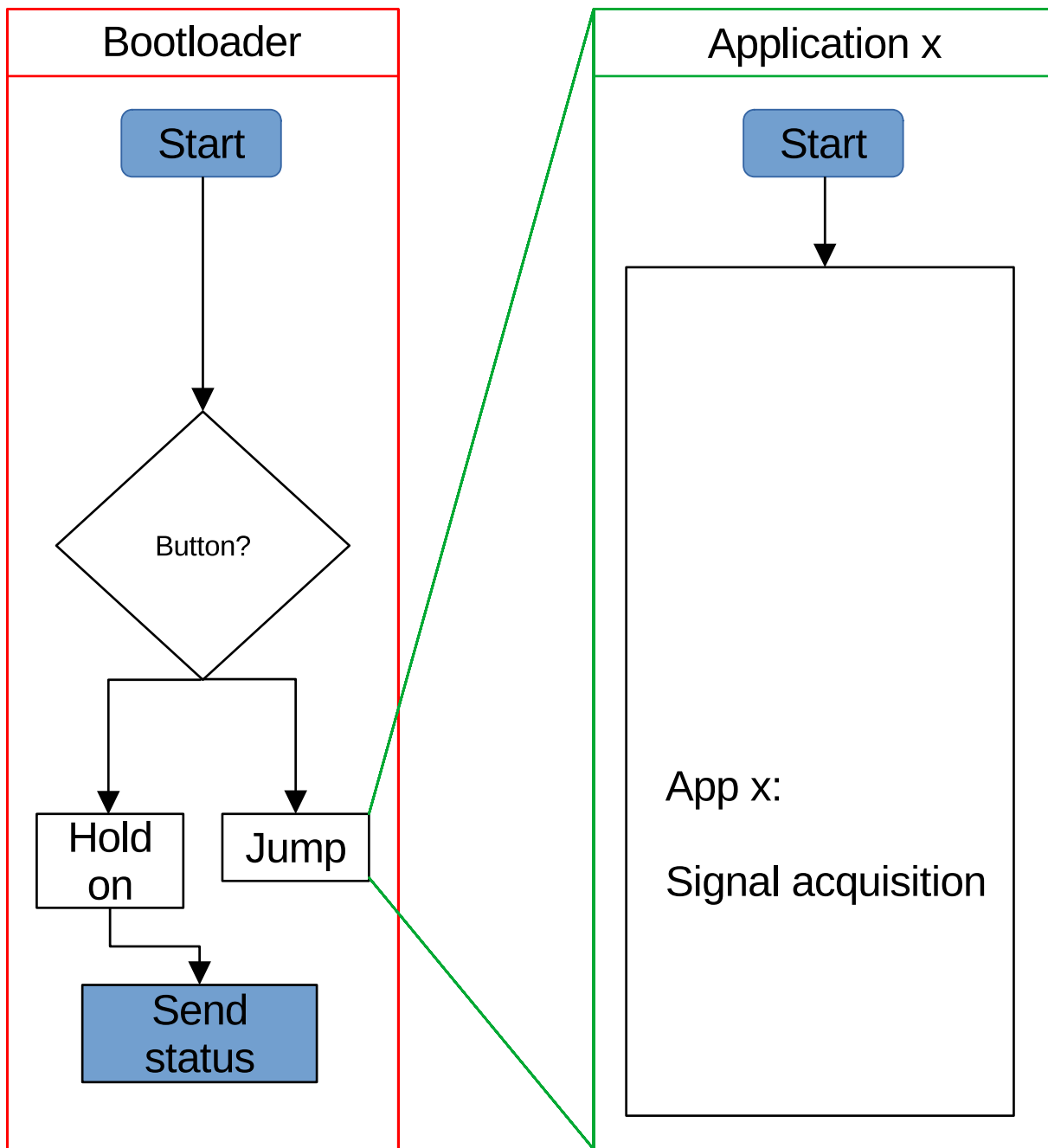


Figure 2.24: Bootloader flow chart[17]

The ICSP programming does not have a bootloader in SW. It uses a built-in protocol for flashing the software. The peripherals for the JTAG or SWD protocols are present, and by setting one or the other and connecting particular pins and the programming device, it is possible to reprogram the device via a wire connection.

In application programming

1. **ICSP:** The In-circuit programming uses different build-in protocols such as JTAG, SWD or bootloader to erase an entire application and upload a new one. The ICSP has the advantage of fast and zero-effort updates for programming the MCU. Programming is tied to a specific use of pins and has one single means of use.
2. **IAP:** The In-application programming is in contrast to ICSP. To update the flash memory, it can use different communication interfaces included in the MCU (I^2C , I/Os, USB, CAN, UART, SPI, Etc.) to update the flash memory. The IAP lets one update the SW while the programming is running, but it needs first to upload the bootloader with ICSP. In the figure 2.25 is the usual IAP configuration. When the MCU powers on, the condition "Is button pressed?" is raised, and the decision follows. If the button is not pressed, a file transfer protocol is waiting for an application to be uploaded. If the file transfer with Xmodem protocol or another receives the binary file, it processes the data, flashes the memory with a new application, and resets the MCU when entering the bootloader. By pressing the button, the MCU enters the application.

The idea for the design of the software update through a server is in the figure 2.26. Reaching for the button is not possible in the tank, and it is not possible to follow the standard IAP procedure. A persistent structure is in a flash and contains information about application addresses, errors and commands to update or jump to the new application. Firstly, the bootloader reads the structure and then enters a condition that determines the state of applications, errors and updates. Secondly, if there is a working application, the bootloader jumps to that address. If it has no application, it is required to flash it with the ICSP approach. If it has an application, it jumps to that location in memory and runs it. Every application needs to include an IAP with a custom protocol on the DMA peripheral to update the software from a server. After the update is complete, the IAPstructure is changed, a software reset is called, and the bootloader acts accordingly.

46

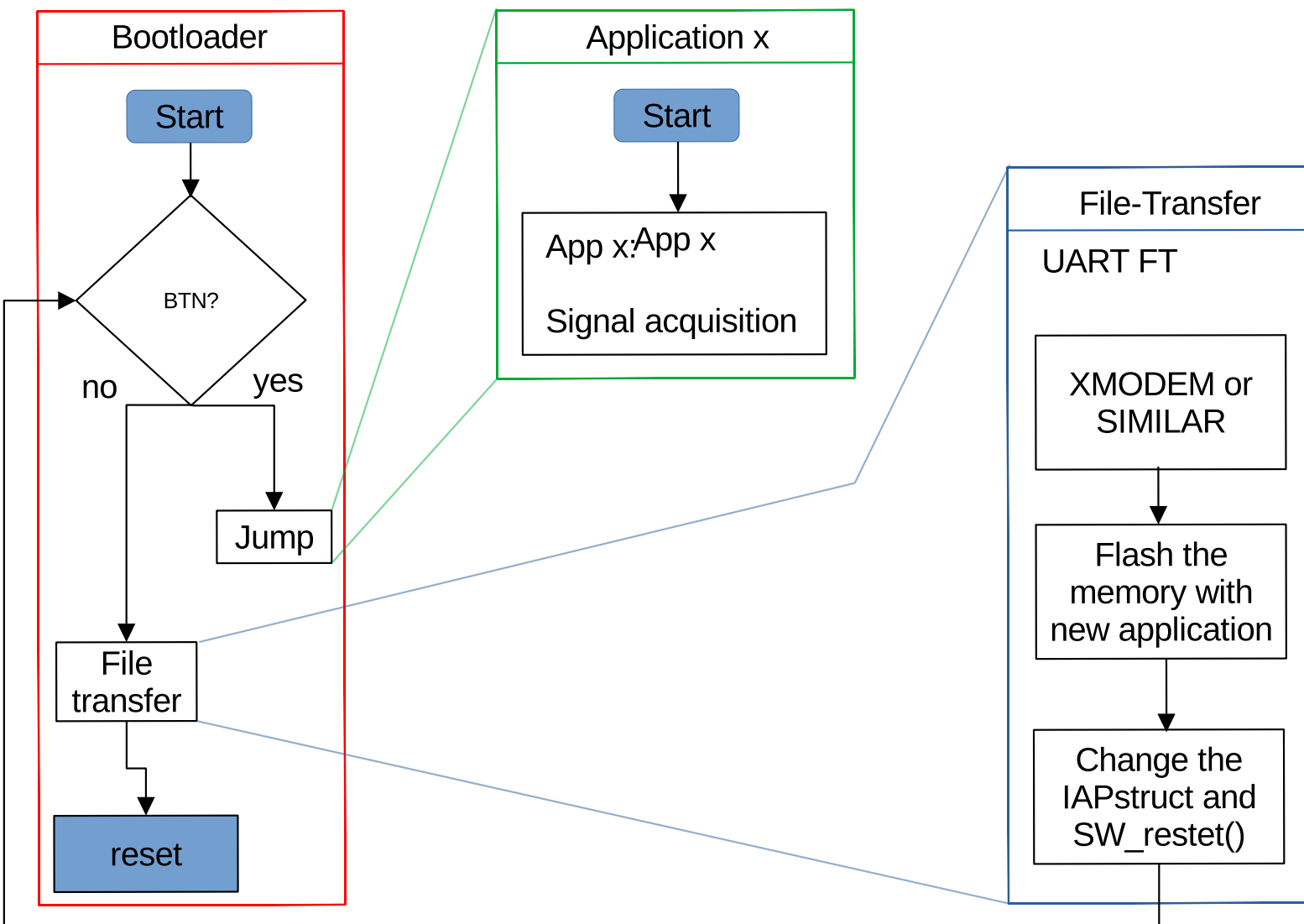


Figure 2.25: IAP with UART flow chart[17]

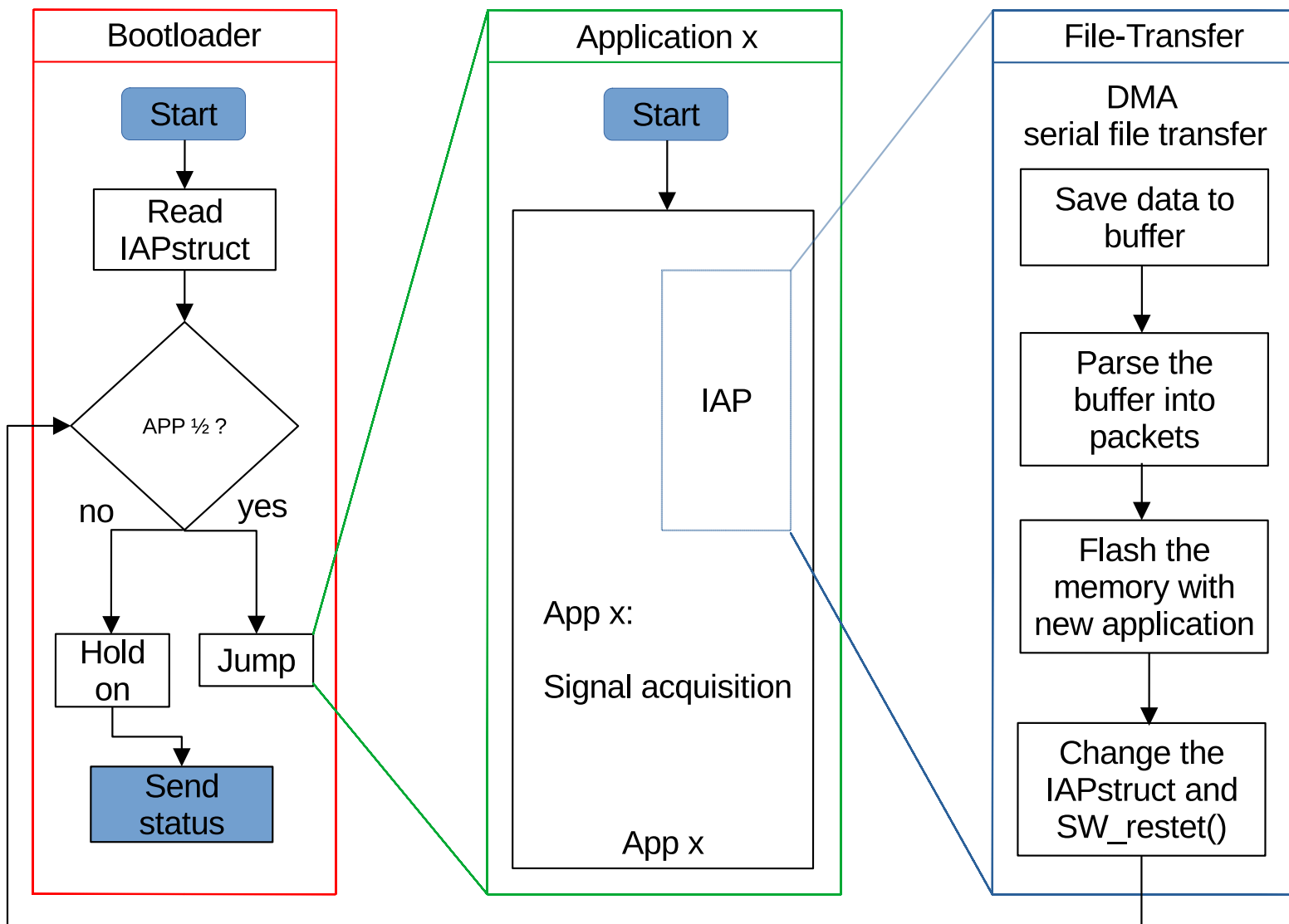


Figure 2.26: Idea for IAP with RS485 and DMA[17]

3 Electronic design

This chapter describes the design of the electronic circuits. Such as transformer design, signal acquisition circuit design, and the board's design as such.

3.1 Flyback converter design

This section goes step-by-step in the design of the flyback PSU.

3.1.1 Flyback parameters

- Output power: $P_{out} = 5 \text{ W}$
- Output voltage: $U_2 = 6 \text{ V}, U_3 = 15 \text{ V}, U_4 = 24 \text{ V}, U_5 = 5 \text{ V}$
- Output current: $I_2 = 600 \text{ mA}, I_3 = 20 \text{ mA}, I_4 = 30 \text{ mA}, I_5 = 20 \text{ mA}$
- Switching frequency $f_s = 80 \text{ kHz}$
- Input voltage: $V_{in} = 24 \text{ V} \pm 20\%$

3.1.2 Design of the winding

The core choice is an Lj E 2507. For this core, winding dimensions were calculated.

LJ E 2507	
Material CF 139	
Effective volume	$V_e = 3020 \text{ mm}^3$
Effective length	$l_e = 57.5 \text{ mm}^3$
Effective area:	$S_{Fe} = 51.5 \text{ mm}^2$

Table 3.1: LJ E 2507 dimensions

Calculation of input power with an efficiency of $\mu = 80\%$ has the relation is $P_o = \frac{P_{out}}{\mu} = \frac{U \cdot I}{\mu}$. Further more, a mark to space ratio of the transistor is chosen with condition 2.15. Where $U_{dmax} = 28.8 \text{ V}$ and $U_{CEmax} = 2 \cdot U_d = 2 \cdot 28.8 \text{ V} = 57.6 \text{ V}$. And the $s_{max} = 1 - \frac{U_{dmax}}{U_{CEmax}} = 1 - \frac{28.8}{57.6} = 0.5$, because the flyback converter will operate in discontinuous magnetic flux a smaller mark to space ratio is chosen as $s_{max} = 0.45$.

$$P_o = \frac{6 \cdot 0.6 + 15 \cdot 0.02 + 24 \cdot 0.03 + 5 \cdot 0.02}{0.8} \doteq 6 \text{ W} \quad (3.1)$$

For the design of the winding dimension a maximal magnetic field strength is chosen $B_{max} = 0.3 \text{ T}$, Space factor $k_{cu} = 0.3$, the current density $sigma = 3 \cdot 10^6 \text{ A/m}^2$ and

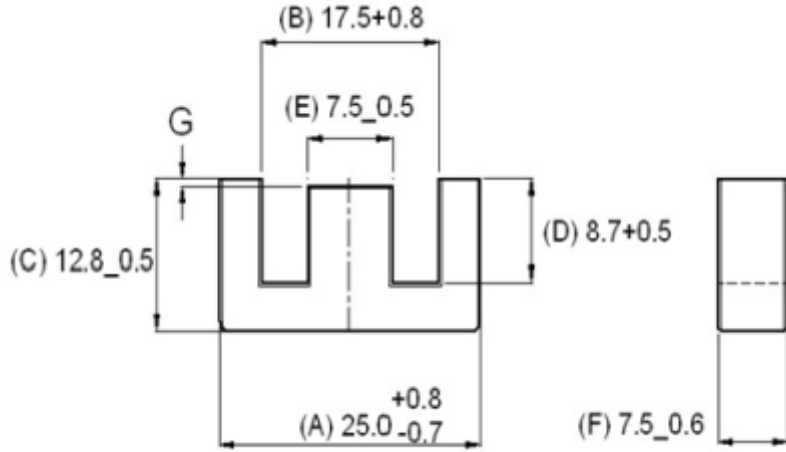


Figure 3.1: Core drawing [20]

material permeability $\mu_0 = 2100 \text{ H/m}$. With use of the equation 2.18 an inductance of primary winding is:

$$L_1 = \frac{19.2^2 0.45^2}{2 \cdot 80 \cdot 10^3 \cdot 6} = 77 \mu\text{H}. \quad (3.2)$$

A maximum peak current in a primary winding with 2.19 is:

$$I_{1max} = \frac{2 \cdot 6}{19.2 \cdot 0.45} \doteq 1.4A \quad (3.3)$$

Calculation of primary turns with 2.20:

$$N_1 = \frac{77 \cdot 10^{-6} \cdot 1.4}{0.3 \cdot 52.5 \cdot 10^{-6}} = 6.8 \doteq 7t. \quad (3.4)$$

Because most of the energy for the flyback converter is concentrated in the air gap an air gap length with 2.20 and permeability of vacuum $\mu_0 = 4\pi 10^{-7} \text{ H/m}$ is:

$$l_v = \frac{7 \cdot 4\pi 10^{-7} \cdot 1.4}{0.3} - \frac{57.5 \cdot 10^{-3}}{2100} \doteq 14 \mu\text{m} \quad (3.5)$$

It is necessary to calculate the turns of each secondary winding and each current to use it in the calculation of the wire cross-section.

$$N_2 = N_1 \cdot \frac{(U_2 + U_d)}{U_{dmin}} = 7 \cdot \frac{(6 + 0.5)}{19.2} = 2.3t. \quad (3.6)$$

$$I_{2ef} = 2 \cdot \frac{I_2}{\sqrt{(3 \cdot s_{max})}} = 2 \cdot \frac{0.6}{\sqrt{3 \cdot 0.45}} = 1.03 A \quad (3.7)$$

$$S_{Cu2} = \frac{I_{2ef}}{\sigma} = \frac{1.03}{3 \cdot 10^6} = 0.34mm^2 \quad (3.8)$$

$$d_2 = 2 \cdot \sqrt{\frac{S_{Cu2}}{\pi}} = 2 \cdot \sqrt{\frac{34 \cdot 10^{-7}}{\pi}} = 0.66mm \quad (3.9)$$

- 19.2 V: $N_1 = 7t$, $I_{1ef} = 0.57 A$, $S_{Cu1} = 0.19 mm^2$, $d_1 = 0.49 mm$
- 6 V: $N_2 = 2.3t$, $I_{1ef} = 1.03 A$, $S_{Cu2} = 0.34 mm^2$, $d_2 = 0.66 mm$
- 15 V: $N_3 = 5.6t$, $I_{3ef} = 0.034 A$, $S_{Cu3} = 0.011 mm^2$, $d_3 = 0.12 mm$
- 24 V: $N_4 = 8.8t$, $I_{4ef} = 0.052 A$, $S_{Cu4} = 0.017 mm^2$, $d_4 = 0.15 mm$
- 5 V: $N_5 = 2t$, $I_{5ef} = 0.052 A$, $S_{Cu5} = 0.017 mm^2$, $d_5 = 0.15 mm$

Selection of the transistor depends on maximum voltage overhang on the primary side $U_{ds} = 94 V$ and a maximum peak current $I_{1max} = 1.4 A$. For this condition it is an IRFR224 with maximum $U_{ds} = 250 V$ and $I_{max} = 3.8 A$ [21]. When winding the transformer it is necessary to follow the beginning of the winding according the dots indication in the figure 2.8.

3.1.3 PSU - complementary circuits

For power supply to work, it is necessary to design different PSU control system building blocks. Choosing a control circuit with PWM output and adjacent circuitry is necessary to switch the transistor and regulate the output voltage.

Input and output capacitors

The essential part is a selection of an input and output capacitor and a startup resistor. The input capacitors are connected in parallel to get a large enough capacitance to minimise input peak current. The choice compromises the physical dimensions and lowering the stress on the MOSFET switch, the transformer, and the output capacitors. The input capacitor has to have at least $40 \mu F$. The larger capacitor is a better choice, but it compromises the SMD package and maximum acceptable capacitance.

Each output of the transformer has a rectification diode and an output capacitor. The UCC28C44 datasheet provides a formula for calculating minimum output capacitance. The rectifier is chosen to maintain at least the maximum current of the output. The relation for the output capacitor and output capacitor list is below.

$$C_{2out} \geq \frac{I_2 \cdot \frac{N_1 \cdot U_2}{U_{dmin} + N_1 \cdot U_2}}{0.001 \cdot f_s \cdot U_2} = 935.9 \mu F \quad (3.10)$$

- $C_{2out} \geq 1000 \mu F$
- $C_{3out} \geq 15 \mu F$

- $C_{4out} \geq 15 \mu\text{F}$
- $C_{5out} \geq 1000 \mu\text{F}$

The startup resistor choice is a compromise between start-up time $\tau_{start} = R_{start} \cdot C_{in}$ and the power loss of the resistor. The formula is $R_{start} = \frac{U_d - U_z}{I_{start}} = \frac{19.2 - 16}{18mA} = 177.8 \Omega \doteq 180 \Omega$ [22].

Integrated circuit for the PWM output and output control

Chosen IC for the PSU control and PWM generation is UCC28C44. Choosing the correct complementary circuit sets the PWM and voltage and current loop control of the power supply. The oscillator and current sensing input need a calculation of components to trim the current limit and PWM output frequency. The oscillator of the PWM generator is adjusted with an RC divider must be calculated. The schematic A is a resistor R68 and capacitor C54. Because the UCC28C44 has $f_{osc} = 2 \cdot f_s = 2 \cdot 80 \cdot 10^3 = 160 \text{ kHz}$. The calculation serves as an equation from datasheet [22]. The equation is from the datasheet of UC3842 because it works for UCC28C44 as well.

$$f_{osc} = \frac{1.72}{R_{R68} \cdot C_{54}} = \frac{1.72}{4700 \cdot 2.2 \cdot 10^{-9}} = 166 \text{ kHz} \quad (3.11)$$

Shunt resistors R78-R80 have 500 mV across, and they have a maximum peak current of $I_{1max} = 1.72 \text{ A}$. It is $R = \frac{0.5}{1.72} = 0.29 \Omega$. Figure A show how the voltage feedback with the PI regulator and TL431 is connected. The output voltage is trimmed with a potentiometer to a point where the output voltage is precisely six volts. The equation for TL431 and the resistors is:

$$U_{out} = U_{ref} \cdot \left(1 + \frac{R59 + R57}{R63}\right). \quad (3.12)$$

For limiting the current, a series resistor has a value of $R59 = 3300\Omega$. A resistor R65 sets the current of the optocoupler to turn it on/off with the change of load on the regulated output. If the 6 V output load rises above nominal values, the LED switches off and the transistor on the primary side also. The control circuit then enters the current control loop. A transistor BC848 serves as a slope compensation for improving current loop stability. It injects portions of oscillator waveforms to minimise loading on the oscillator. A resistor R66 sets the maximum power input. It calibrates by trimming the voltage across R78-R80 to the nominal value.

A dissipative RCD circuit is used to clamp the overhang voltage when the transistor turns off, and an $R_1 - C_1$ snubber circuit serves to damp the ringing after the demagnetisation period. Another secondary $R_2 - C_2$ snubber circuit minimises the ringing amplitude when the transistor turns on by placing a secondary $R_2 - C_2$ circuit over the rectifier diode. This ringing with a large amplitude can partially open the MOSFET and induce unwanted effects on the circuit. The RC snubber circuit 1 and 2 values have similar values concerning the power dissipation allowed. The values were chosen experimentally with a microfarad capacitor and several kilo-ohm resistor in series. The power dissipated is given

by the maximum allowed voltage on the MOSFET. The power dissipated in the snubber circuit by the power given by the parasitic inductance (3.13) of the circuit L_σ , switching frequency f_s and maximum peak current I_{1max} . The C_{clamp} value is assumed to be large enough (with the parasitic capacitances around to charge up) to store all parasitic energy given by one entire switching cycle from the parasitic inductance. The power dissipated on the resistor of the RCD circuit during one cycle is given by the formula 3.14. Figure 3.3A show a schematic waveform of the circuit without an RCD and RC snubber circuit. The peak is associated with the RCD network and the ringing with the RC snubber circuit. The higher the clamp voltage, the lower the dissipation. The MOSFET specification gives the magnitude of the clamp voltage. Usually the $U_{dpeak} - U_d$ is chosen to be around half of the input voltage [23].

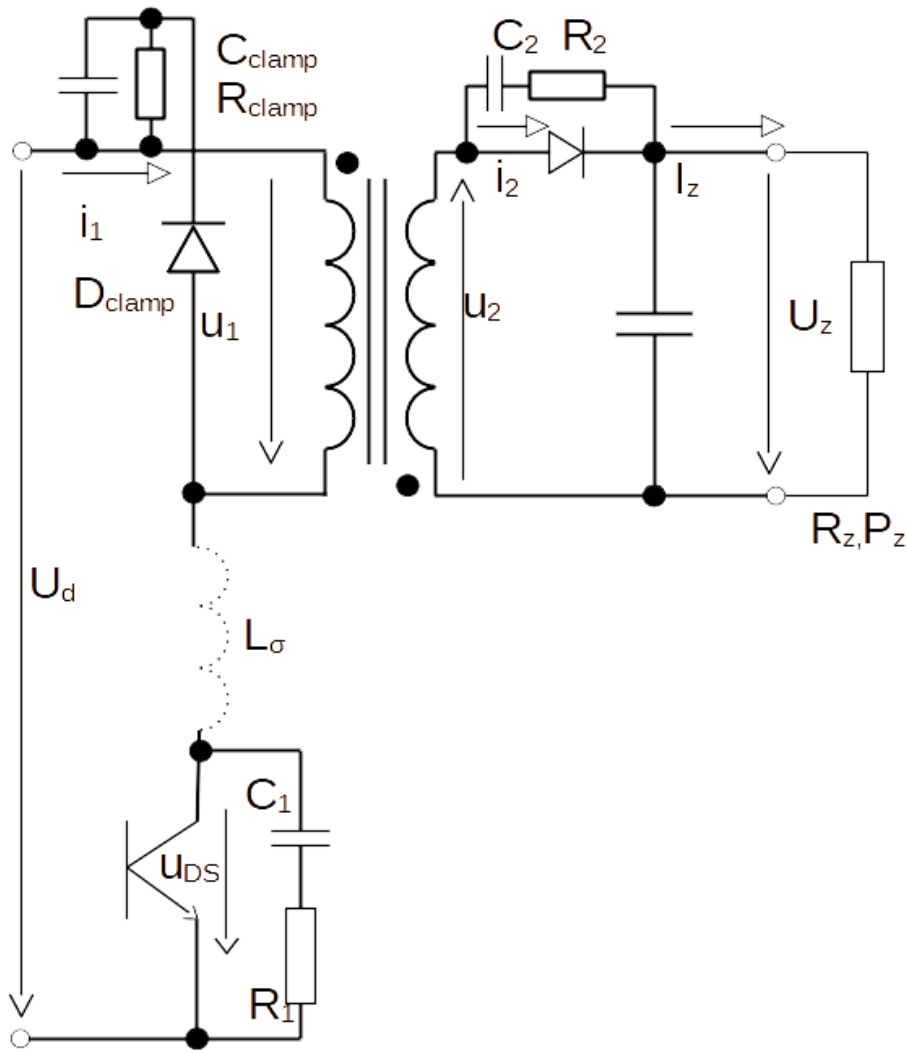


Figure 3.2: Schematic representation of the RCD circuit + RC snubber circuit

$$P_{L_\sigma} = \frac{1}{2} L_\sigma I_{1\max}^2 f_s \quad (3.13)$$

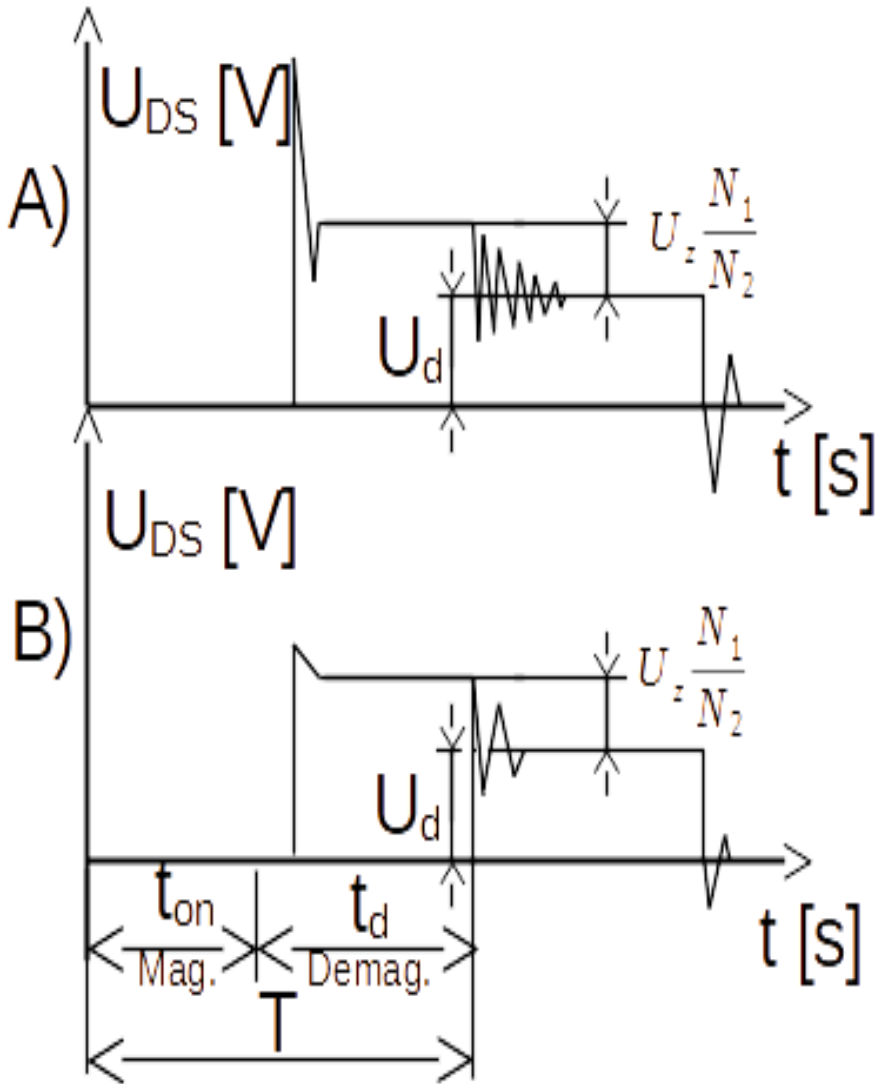


Figure 3.3: The chart A) shows the flyback converter U_{DS} voltage without RC and RCD stage and the chart B) show behaviour of the voltage with RCD and RC stages

$$P_{max}^{sn} = P_{L\sigma} \cdot \left(\frac{U_d}{U_{dpeak} - U_d} \right) \quad (3.14)$$

To minimize instability of the voltage regulator an LC stage is placed after the rectifier diode and an output capacitor [3]. The voltage feedback loop connects after the LC stage to lower the order of the system by one. The LC stage is calculated to filter out higher frequencies on the output. A capacitor and an inductor of $C_{LC} = 10\mu F$ and $L_{LC} = 3.3\mu H$ is chosen with a resonant frequency $f_0 = \frac{1}{2\pi\sqrt{L_{LC}C_{LC}}} = 27.7$ kHz.

For voltage regulation on all outputs, linear voltage regulators are chosen. Only the 24 V output has a Zener diode that clamps the voltage to 24 V. Then there are four commercial linear voltage regulators, MC33269 - 3.3V and BA05 - 5V. For 15V, there is an adjustable voltage regulator AP2204-adj. Two are for 5V: MAX232 isolated for filter clogging sensor and 5V for MAX1480. One for 15V with analog and digital parts. One is

for a 3.3 V microcontroller. After that there are two linear voltage regulators, 5V for the differential pressure sensor and 3.3 V for the ADC of the microcontroller. An example calculation of 3V3_{AD} from 6V is below. Choose R₈₈ = 10kΩ. There is also a low pass filter R₈₆ and C₂₁.

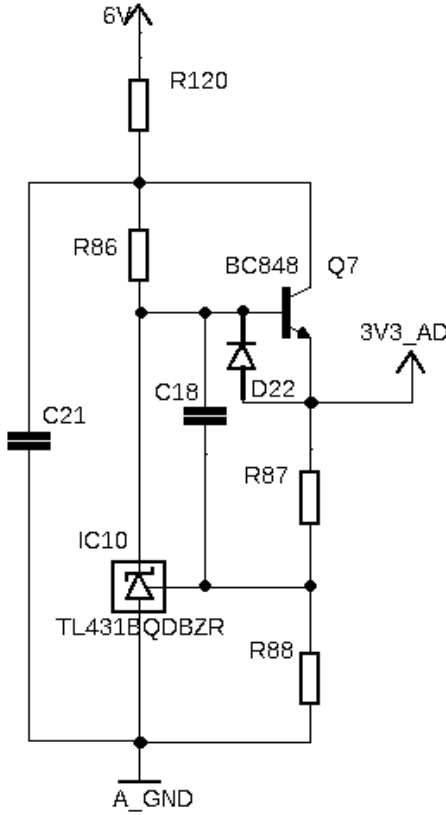


Figure 3.4: Voltage regulator with TL431

$$K_U = \frac{U_{R88}}{U_{out}} = \frac{R_{88}}{R_{88} + R_{87}} \quad (3.15)$$

$$R_{87} = \frac{R_{88}}{K_U} - R_{88} = \frac{10 \cdot 10^3}{\frac{2.5}{3.3}} - 10 \cdot 10^4 = 3.2k\Omega \quad (3.16)$$

$$I_{R87} = \frac{U_{R88}}{R_{88}} = \frac{2.5}{10000} = 2.5mA, I_B = \frac{I_{2max} + I_{R87}}{h_{21E}} = 0.286mA \quad (3.17)$$

$$R_1 = \frac{U_{in} - U_{out} - U_{BE} - U_{R120}}{I_{TL} + I_B} = \frac{6 - 3.3 - 0.6 - 1}{0.002 + 0.286 \cdot 10^{-3}} = 481\Omega \quad (3.18)$$

3.2 Bus driver circuit

An RS485 bus driver must be chosen and define additional circuits to facilitate communication with the server network. There is then an RS232 bus driver for communication with the ultrasound sensor in serial mode. The IC for RS485 is an IC MAX1480 with an integrated isolation barrier, and for the RS232, a MAX232 with two optocouplers for galvanic isolation.

RS485 - MAX1480

The circuit was given with the specifications from the supervisor. There is a supply voltage on the side of the microcontroller. The primary side is only connected to the connector. A 120 Ohm resistor is mounted on the connector between the A and B lines for interference. The resistor is also on the adapter side. The circuit gives the possibility to control the status of receiving or transmitting state of the MCU and a pin for shutting the bus driver off for restrictive power situations. DE pin controls the direction of the data flow, and the SD pin controls the power on/off state. The default is the ON state for the SD pin and receives the state for the DE pin. The user then decides in the application situations in which these states change. The schematic is shown in figure A. The MCU side also has a CMOS inverter for inverting the receiving line as written in the datasheet [15]. The signal debugging connectors of the TX, RX, DE, and SD pinheads are mounted.

RS232 - MAX232

The ultrasound sensor is permanently set to the data transmission state with a resistor value of $47k\Omega$ and 9600 baud / s and a data format of $0xFF + DH + DL + SUM$, where $0xFF$ is the header, HL is the high byte and the DL is the low byte and the SUM is the sum of the previous bytes. Because the sensor is outside the water tank, galvanic isolation from the MCU side and primary side, communication is isolated with two optocouplers for reception and transmission line. The sensor's side is the MAX232, and the five volts regulator supplies the MAX. The connector connects to the ultrasound sensor module with a TRACO isolated PSU for the module with another MAX232 IC. MAX on the module is the first stage of communication between the IC and the sensor. Then comes the communication between two MAX devices. Figure A shows the main PCB part and figure A shows the ultrasound sensor module. To debug the communication or check if the data is on the way a pinhead is placed.

3.3 Microcontroller and ICSP

The microcontroller has four pairs of capacitors connected to the VDD pins and one pair of a capacitor connected to the ADC voltage supply. Each pair has one micro farad and ten nano farad capacitors. The placement on the board needs to be situated the closest to the MCU. ADC pins have closely placed RC low-pass filters with a resonant frequency of around 5Hz to filter out noise. To directly program the MCU, a SW connector is mounted. The schema is shown in Figure A

3.4 Signal Conditioning circuits

Water level conditioning circuit

Because the HDL300 sensor operates in a current loop, a sensing resistor of 300 Ohms is placed in parallel with the sensor. Then there is an non-inverting operational amplifier in a proportional configuration. With the output of the MCUs DAC, an offset can be adjusted for the inverting pin of the differential amplifier. The output of the differential amplifier goes on the ADC input of the MCU. The schema is in the A2 section of the figure A.

Differential pressure sensor circuit

The differential pressure sensor outputs a voltage in a range of 0-5V according to the pressure in the sensor installation in the piping system. The circuit has a proportional non-inverting amplifier for adjusting the Differential amplifier circuit as for HDL300. On the output of the amplifier is a voltage divider dividing 5V to a 0-3.3V level. The schema is in the B2 section of the figure A.

Turbine flow conditioning circuit

The turbine flow meter outputs a pulse voltage signal as the turbine rotates. The amplitude of pulses is around 15 V. The signal is filtered with a two-stage low pass filter with a similar resonant frequency of 34 Hz. For the invention of the signal, a hex Schmitt inverter is used. On its output, a Light-emitting diode is put to signal the pulses, and to divide the voltage to 0-3.3V levels, a voltage divider takes place. The schema is in the D1 section of the figure A.

End stop switches circuit

The circuit has a low pass filter on the input filtering out noise. The hex trigger inverts the signal and the divider divides the voltage to 0-3.3V. The schema is in the D5-6 section of the figure A.

General purpose analog input

For general purpose, two circuits were dedicated to 0-3.3V analog input. The circuit has a low pass filter and two safety diodes. The resistor divider will be omitted. The schema is in the A5-C5 section of the figure A.

Transistor-transistor logic input circuit

The circuit has a diode in series with the input signal to signal the state and a voltage divider to divide the input voltage to measurable values. The schema is in the C6 section of the figure A.

Temperature sensor circuit

A DS18B20 circuit needs a pull-up resistor of $4.7 \text{ k}\Omega$. There is the possibility to connect more sensors in parallel. One sensor is placed directly on the board. The schema is in the C8 section of the figure A.

Step-down converter for the compressor

There is a circuit for a step-down converter for PWM control of a 3 V compressor. The compressor circuit is not part of this thesis, but it can be mounted when necessary. The schema is in the A7 section of the figure A.

Voltage sensing circuit

The voltage divider with a filtering capacitor senses the voltage on the output of the 6 V secondary before the rectification diode. The voltage interval is $U_{out} \in < -25, 9 > \text{V}$. For this circuit, a voltage divider of $2.4 \text{ k}\Omega$ and 300Ω . The output range is about 2 V. The schema is in the C7 section of the figure A.

Impulse current sensing transformer

A cross section of the secondary wire needs to be calculated by designing the transformer and the secondary turns. Then, a shunt resistor value and a peak detector with RC filter with a time constant of $\tau = 1ms$. The toroid core is LJ T 1606 CF195. Parameters of the toroid and design parameters. Below are the parameters and a calculation of the wire cross-section area and the minimal diameter of the secondary wire. The schema is in the A7 section of the figure A [24], [3].

Magnetic flux densitye	$B_{sat} = 0.2 \text{ T}$
Maximum primary current	$I_{1max} = 1.6 \text{ A}$
Mark-to-space ratio	$s_{max} = 0.45$
Effective primary current	$I_{1ef} = 0.6 \text{ A}$
Permeability:	$\mu_{Fe} = 5000 \pm 20 \%$
Core cross section	$S_{Fe} = 19.73 \text{ mm}^2$
Core inductione	$A_L = 11\text{nH}$
Primary and secondary turns	$N_1 = 1t, N_2 = 100t$
Switching frequency	$f_s = 80 \text{ kHz}$
Current density	$J = 3 \cdot 10^6 \text{ A/m}^2$
Maximum magnetization time	$t_{max} = s_{max}/f_s = 5.62\mu\text{s}$
Output voltage	$U_{2max} = 3.7 \text{ V}$

Table 3.2: LJ T 1606 dimensions[24]

$$I_{2max} = I_{1max} \frac{N_1}{N_2} = 1.6 \frac{1}{100} = 16mA \quad (3.19)$$

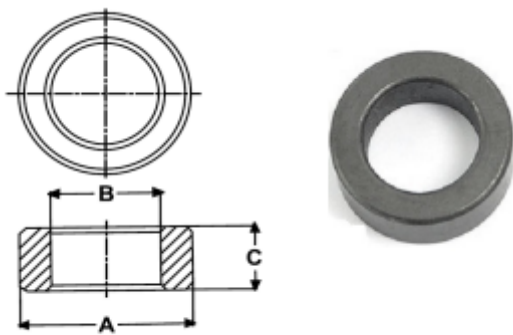


Figure 3.5: Core drawing and image [24]

$$R_s = \frac{U_{2max}}{I_{2max}} = \frac{3.7 - 0.4}{0.016} = 185\Omega \quad (3.20)$$

$$I_{\mu 2} = (U_{2max} + U_{fD}) \frac{t_{1max}}{T - t_{1max}} = (3.7 - 0.6) \frac{5.62 \cdot 10^{-6}}{100^2 11 \cdot 10^{-9}} = 0.22mA \quad (3.21)$$

$$I_{2ef} = I_{1max} \frac{N_1}{N_2} \sqrt{s_{max}} = 1.6 \frac{1}{100} \sqrt{0.45} = 10.7mA \quad (3.22)$$

$$S_{cu2} = \frac{I_{2ef}}{J} = \frac{0.0107}{3 \cdot 10^6} = 3.6 \cdot 10^{-9} m^2 \quad (3.23)$$

$$d_{cu2} = \sqrt{4 \cdot \frac{S_{cu2}}{\pi}} \cdot 1 \cdot 10^3 = \sqrt{4 \cdot \frac{3.6 \cdot 10^{-9}}{\pi}} \cdot 1 \cdot 10^3 = 67.5\mu m \quad (3.24)$$

4 Software design

This chapter describes a bootloader design with an example pseudocode, memory partition for this board, firmware concept description with an IAP, file transfer. A communication between ultrasound sensor, addressing the DAC for the offset of signal conditioning circuits, and RS485 communication .

4.1 Bootloader

The main part of the firmware update is a working bootloader that decides the next steps in the application to load. It serves to decide whether the bootloader can jump to an application or remain in an infinite loop to be programmed directly first. Most bootloader examples use a physical GPIO input by pressing a button to enter the BOOT mode after the startup. This thesis approach deals with a remote bootloader that reads the permanent structure from flash memory and reads the information of the next processes. The structure is the same for all applications that are updated to the system memory. Every application writes new status information to the flash memory for other bootloader processing. When a new application is uploaded with IAP functionality. Before restarting, a new status is written to the structure. After restart, a bootloader decides where to jump. The bootloader algorithm is described below. Flash memory read/write/erase function must be part of every application or bootloader for successful flash memory management. Also, a flashJump application needs to be implemented as well [25].

Data: IAPstruc, initBL
Result: Jumping to the application

```
Initialization;  
flashRead(initBL);  
if not initBL then  
    initializeIAP(IAPstruct);  
    flashWrite(IAPstruct);  
    flashWrite(initBL);  
else  
    flashRead(IAPstruct);  
    print(status);  
    if IAPapp then  
        print(APPaddress);  
        flashAppJump(APPaddress);  
    else  
    end  
end
```

Algorithm 1: Bootloader pseudocode

4.2 Memory partition

Firmware design composes of different sections. The bootloader sits first in memory. Then there is a section with permanent IAP structure and bootloader init variable. Then there are two sections for the applications of the same size. When uploading the first application directly, a memory offset and the desired protected memory area needs to be changed. If the application starts on address 0x8000 and has 2kB length it needs to be set in the linker for flash memory: *FLASH (RX) : ORIGIN = 0x08008000, LENGTH = 2K*. Then an offset for the startup vector table follows. STM microcontrollers have a .c file named *system_stm32Xnxx.c* file, where X is the lineup code: F, L, G ETC. and n for the chip number → *system_stm32f4xx.c*. This file contains the peripheral access layer of the MCU. It is necessary to find and uncomment `/* #define USER_VECT_TAB_ADDRESS */` then an offset of the application needs to change: `#define VECT_TAB_OFFSET 0x00008000U`. After flashing this application to the system memory. It uploads the application to the position in the memory given by the above address. When the controller starts, the offset specification gives information about the application placement. After the startup, it jumps directly to the offset in memory. (Because the MCU starts on 0x0000 0000 address that is the same as 0x0800 0000 of the flash memory)

The flash memory of various STM microcontrollers differ in organization, division, and the possibility of writing/reading and erasing such memory. For example, a chip STM32F303RE has memory divided into 256 pages of 2kByte memory blocks. The microcontroller can erase the memory page by page. On the other hand, a chosen microcontroller (due to limited access to better controllers), a STM32F446RET6, was chosen. This chip has similar capabilities. But worse specs for some peripherals. For example, flash memory is divided into only eight sectors. Four sectors are in 16kB blocks. One sector is in 64 kB blocks and three in 128 kB blocks. This limits the erase and programming capabilities and requires additional commands to handle such limitations. Usually, if it is necessary to change just one byte stored in the memory, it is obligatory to erase the entire sector of 16-128 blocks. So it is necessary first to read the value to the SRAM variable or entire set of variables of the sector. The erasing of the memory sector changes the value and writing the sector back. Read options for the memory are not limited. Also, different memory organisation of another chip is available. It can be divided into Banks - somewhat between sectors and pages approach.

Because the STM32F446 has limited memory erase options, a division for the firmware is in the figure 4.2. Information about the memory organization is saved in the IAP structure, along with additional information about the memory status of those addresses. The SW update erases one of the APP x/y memory sectors and starts writing the new program there.

4.3 Firmware concept description

The bootloader described above is shown in figure 4.4 as a red rectangle. After the MCU is powered on, a decision algorithm takes place. The first iteration initializes the IAP structure and the initBL variable. After the reset, it reads the structure and jumps to the application that is written to the jump variable of the IAP structure. The application typically works with a defined functions. IAP algorithm works with serial communication and the DMA peripheral. In the callback function, a packet handling and flash write

Block	Name	Block base addresses	Size
Main memory	Sector 0	0x0800 0000 - 0x0800 3FFF	16 Kbytes
	Sector 1	0x0800 4000 - 0x0800 7FFF	16 Kbytes
	Sector 2	0x0800 8000 - 0x0800 BFFF	16 Kbytes
	Sector 3	0x0800 C000 - 0x0800 FFFF	16 Kbytes
	Sector 4	0x0801 0000 - 0x0801 FFFF	64 Kbytes
	Sector 5	0x0802 0000 - 0x0803 FFFF	128 Kbytes
	Sector 6	0x0804 0000 - 0x0805 FFFF	128 Kbytes
	Sector 7	0x0806 0000 - 0x0807 FFFF	128 Kbytes
System memory		0x1FFF 0000 - 0x1FFF 77FF	30 Kbytes
OTP area		0x1FFF 7800 - 0x1FFF 7A0F	528 bytes
Option bytes		0x1FFF C000 - 0x1FFF C00F	16 bytes

Figure 4.1: Memory partition of STM32F446 [5]

Start	0x0800 0000	Bootloader 16kB
	Sector 0	
	0x0800 4000	Structures 16kB
	Sector 1	
	0x0800 8000	
	Sector 2-3	
	0x0801 0000	App 1 192 kB
	Sector 4-5	
End	0x0804 0000	App 2 256 kB
	Sector 6-7	

Figure 4.2: Memory partition of STM32F446 for the SW

process occurs. After the software is reset, a bootloader reads the structure and acts accordingly. [11]

4.4 Sensor connection

The sensors' signal conditioning circuits are connected to the FRB Tesla Jihlava TY5176211 and the output voltages and grounds as well. The RS485 and the input supply goes through D-SUB nine-pin connectors. There are two in parallel, male and female. There is a third connector for the ultrasound module. The ultrasound module has a connector to connect to the main PCB.

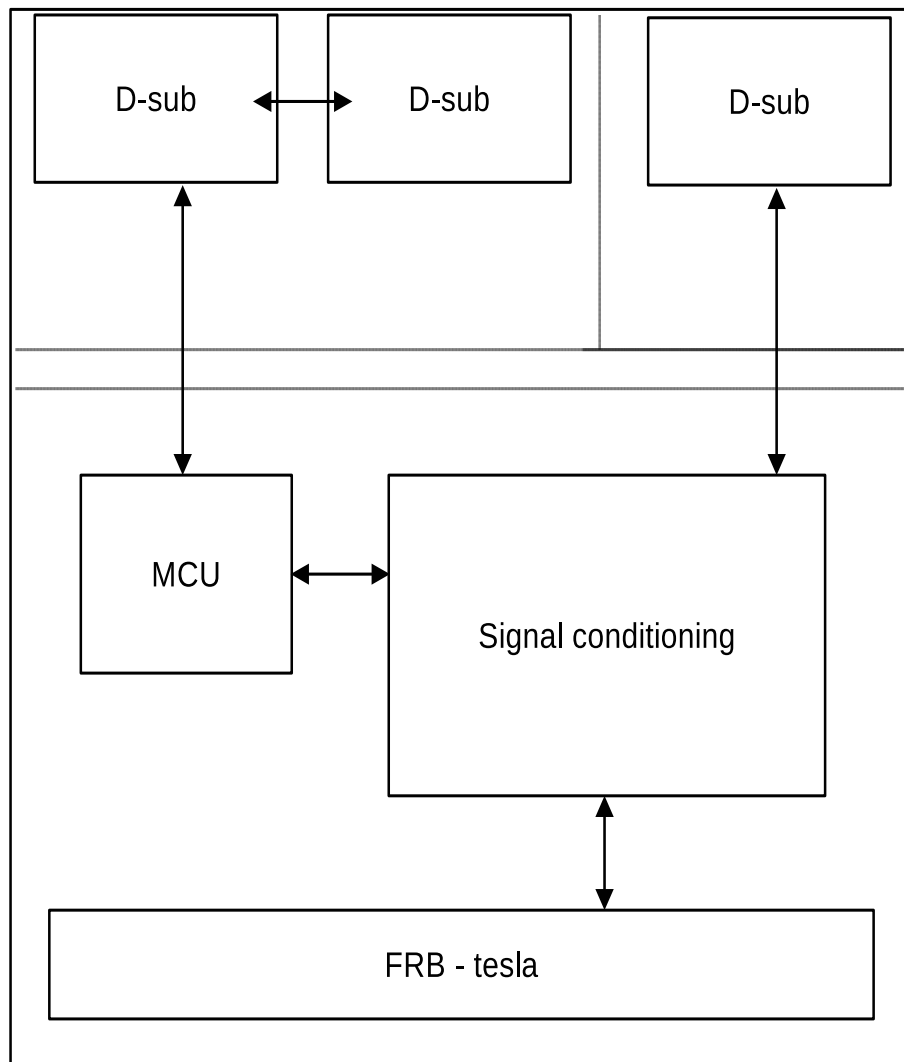


Figure 4.3: Connectors layout with respect to the board

63

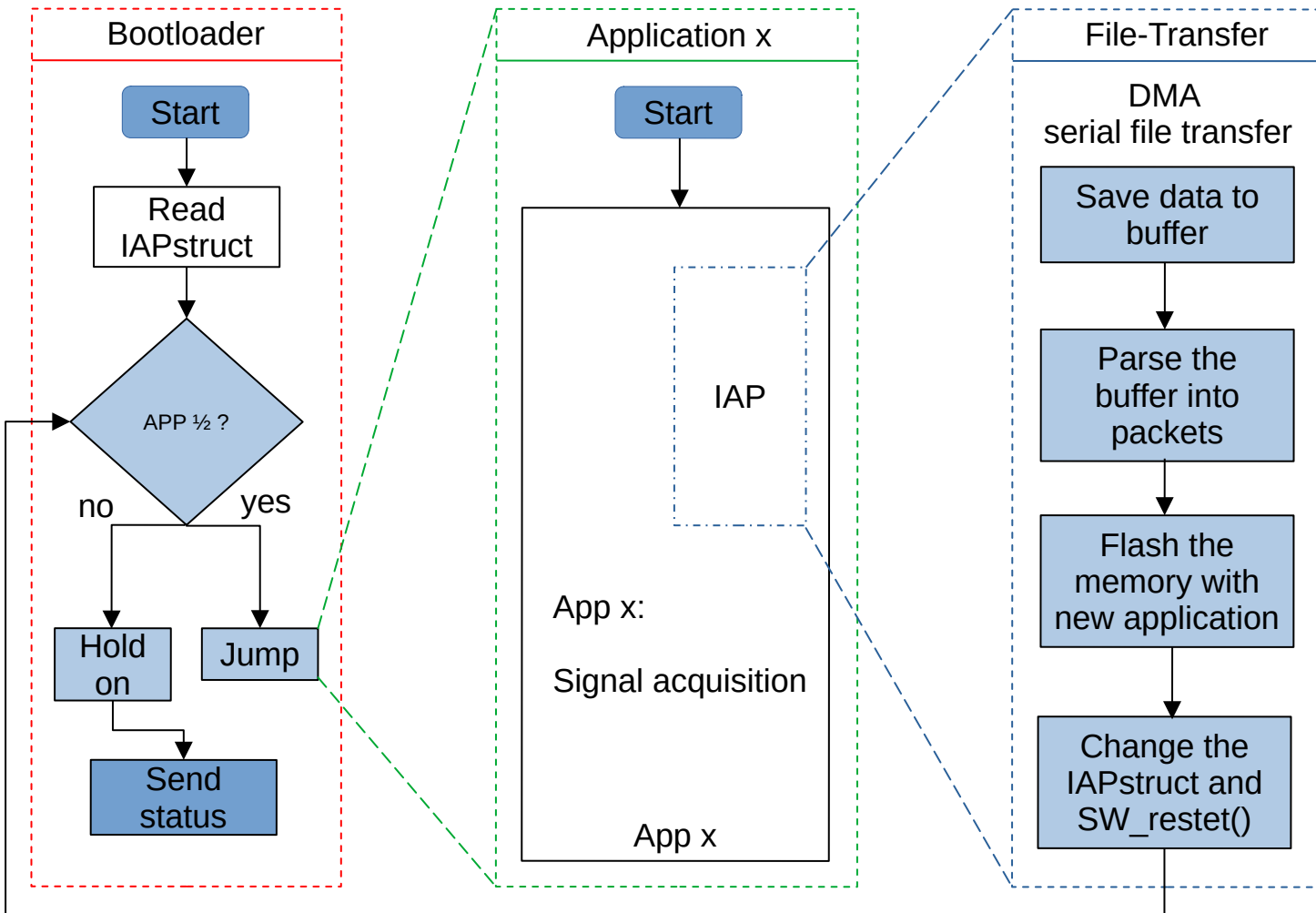


Figure 4.4: Software's flow chart representation

5 Electronic implementation and testing

This chapter describes a fabrication of the PSU prototype and a first version of the main PCB and the ultrasound module. Firstly a PSU board was fabricated and tested for designed parameters to adjust the values of certain components and to observe the behaviour of the PSU. Secondly a main board with a PSU and the remaining components was made. A PSU on the main board was tested and the function of the signal conditioning circuits were tested with software.

5.1 A prototype board

The main part of the entire board is a flyback converter with multiple outputs for low power of 6 W. The efficiency for calculations was 80 percent. The board was tested under load and the final parameters were noted. The prototype board served as a tool for finding the right combination of the voltage feedback loop and for finding if the turns of the secodaries are enough and adjusting it for the final board.

- N1: 7t, for primary side
- N2: 3t for 6V secondary winding
- N3: 6t for 15V secondary winding
- N4: 9t for 24V secondary winding
- N5: 2t for 5V secondary winding

The initial turns configuration and a core with a gap of about $l_{air} = 26\mu m$ and an induction of $L_1 = 40\mu H$ was made. That turned out to be not very good for accepting nominal loads. The adjusted transformer turn ratio follows. The induction of the primary winding for the final transformer is $L_1 = 49\mu m$. And this works perfectly.

- N1: 7t, for primary side
- N2: 3t for 6V secondary winding
- N3: 7t for 15V secondary winding
- N4: 11t for 24V secondary winding
- N5: 3t for 5V secondary winding

5 ELECTRONIC IMPLEMENTATION AND TESTING 5.1 A PROTOTYPE BOARD

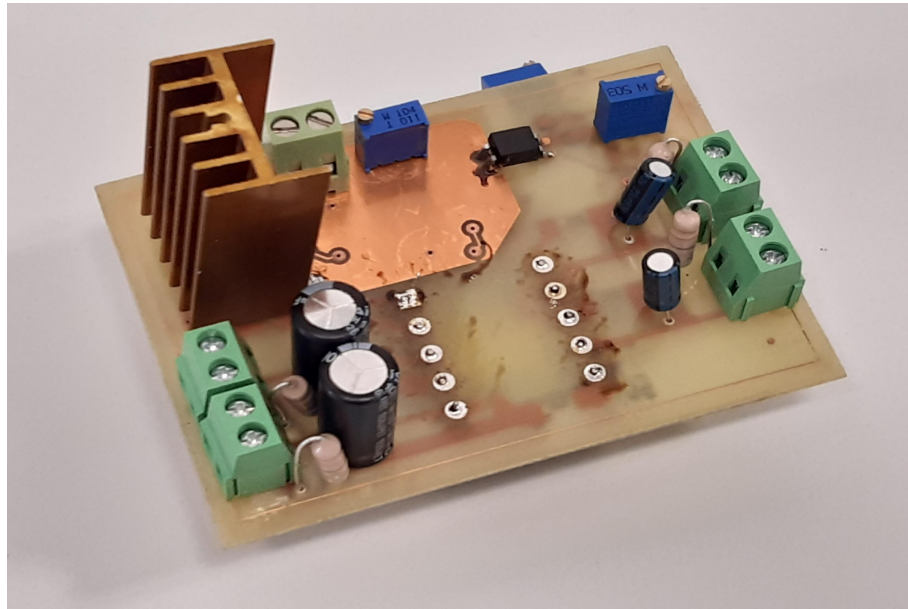


Figure 5.1: Top side of the prototype PSU board

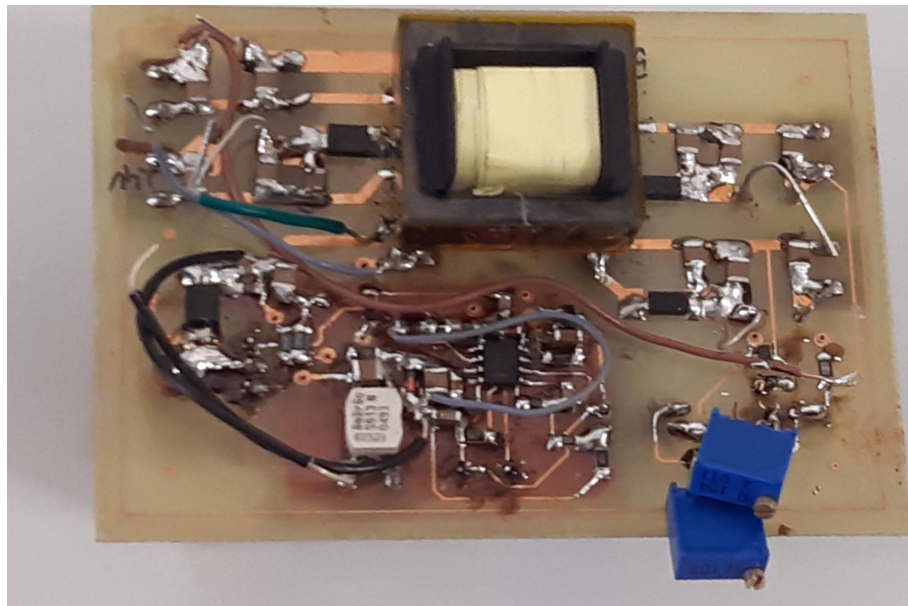


Figure 5.2: Top side of the prototype PSu board

The trimmers on the prototype board help adjust the mark-to-space ratio of the voltage, maximum primary peak current and the output voltage.

The chart shown in the figure 5.3represents the voltage and current in the flyback PSU with no load. There is a ringing on the current when the transistor is turned off. This ringing can be caused by not placing the RC stage on the secondary side. The RC snubber is placed across the transistor. Noise can be attributed to incorrect measurement. But with the corrected probing method the noise was still present with fewer oscillations. This noise propagates to the ground on the secondary side with peaks up to 300mV. This was resolved on the final board.

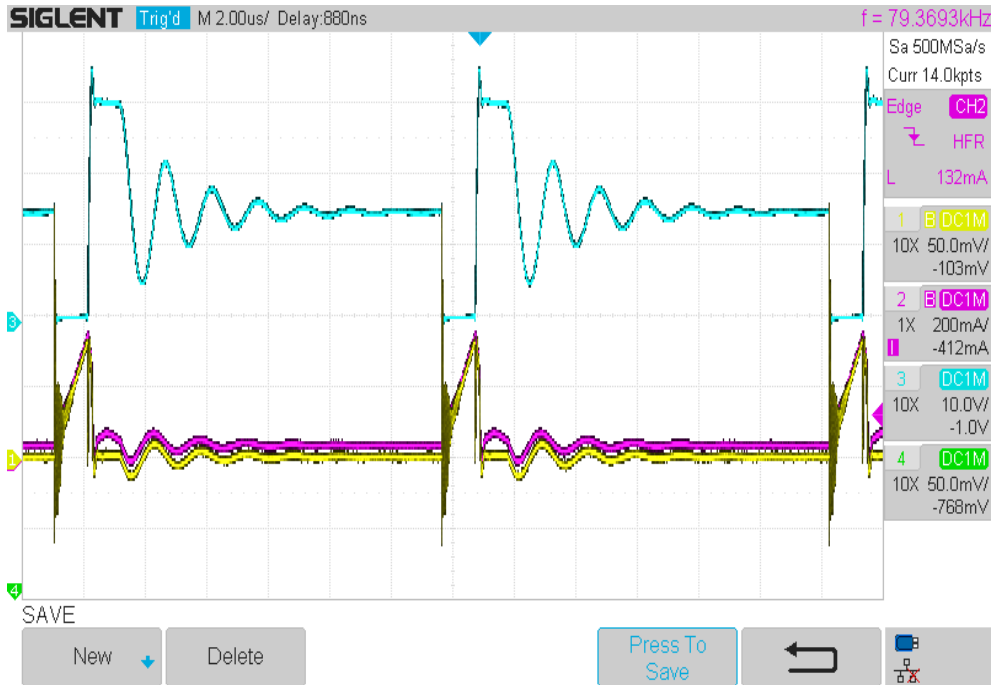


Figure 5.3: Chart of the U_{DS} voltage and a voltage across the shunt resistors and a current through the primary side

5.2 Main board

After the final configuration of the PSU prototype, a main board was designed and fabricated. The final main board is shown in the figures 5.6 and 5.7.

5.2.1 Main board parameters

Input supply	19.2 V / 186 mA \pm 40%
Input power	6 W
Output power	5.32 W
Efficinecy	88.7 %
Pulse input with 15V amplitude	2
End switch input with 24V supply	2
Current loop water lavel input	1
Differential pressure input	1
General analog input	2
TTL input	2
Step down converter	1
Temperature sensor input	1
Filter clogging sensor	1

Table 5.1: Final board specifications

The table shows the parameters of the main board. The desired features of the board were successfully completed in the figure 5.6 which is the voltage across the U_{DS} and the current representation across the shunt resistors. The figure 5.7 shows the output voltage

in the regulated secondary main winding. The output voltage has a snubber circuit across the rectifier diode to suppress the high-frequency noise.

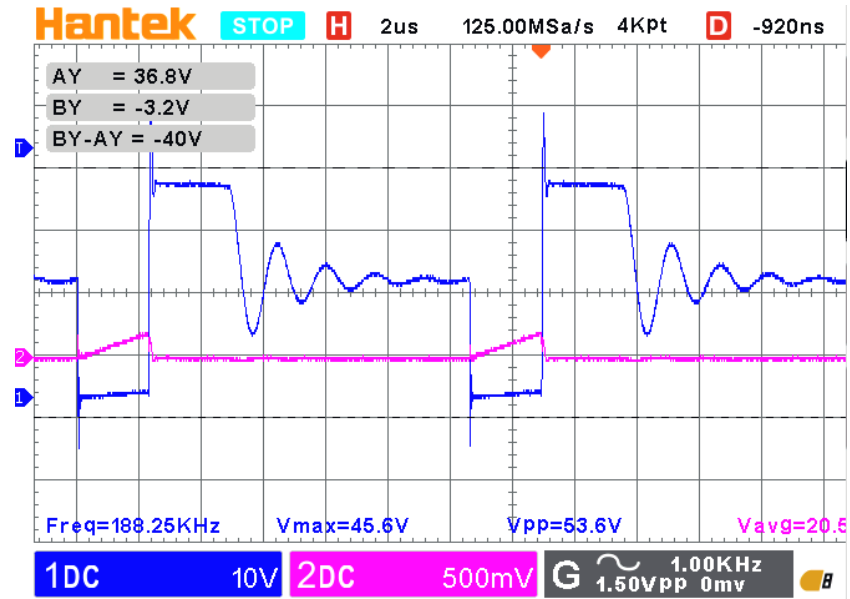


Figure 5.4: Blue: U_{DS} across the MSOFET and Pink: U_{CS} across the shunt resistors

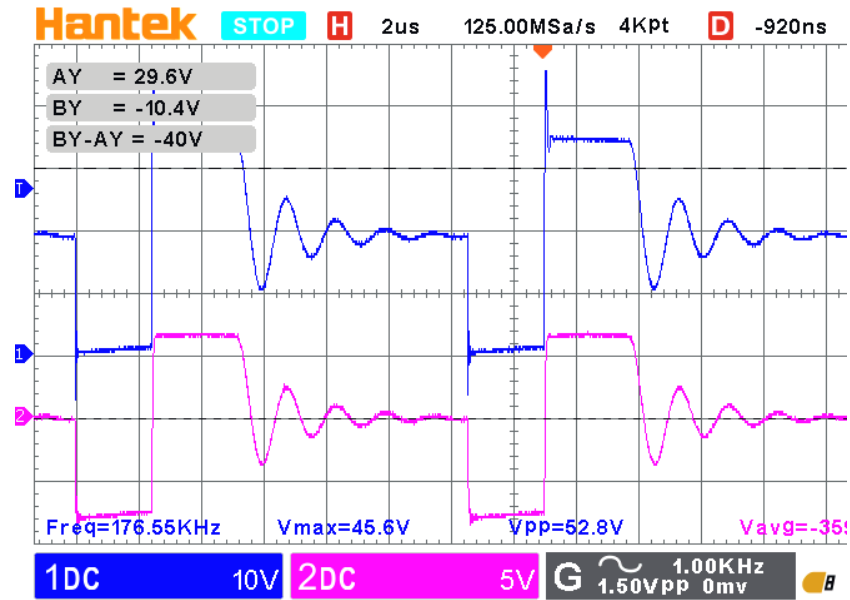


Figure 5.5: Blue: U_{DS} across the MSOFET and Pink: U_2 on the 6V secondary winding

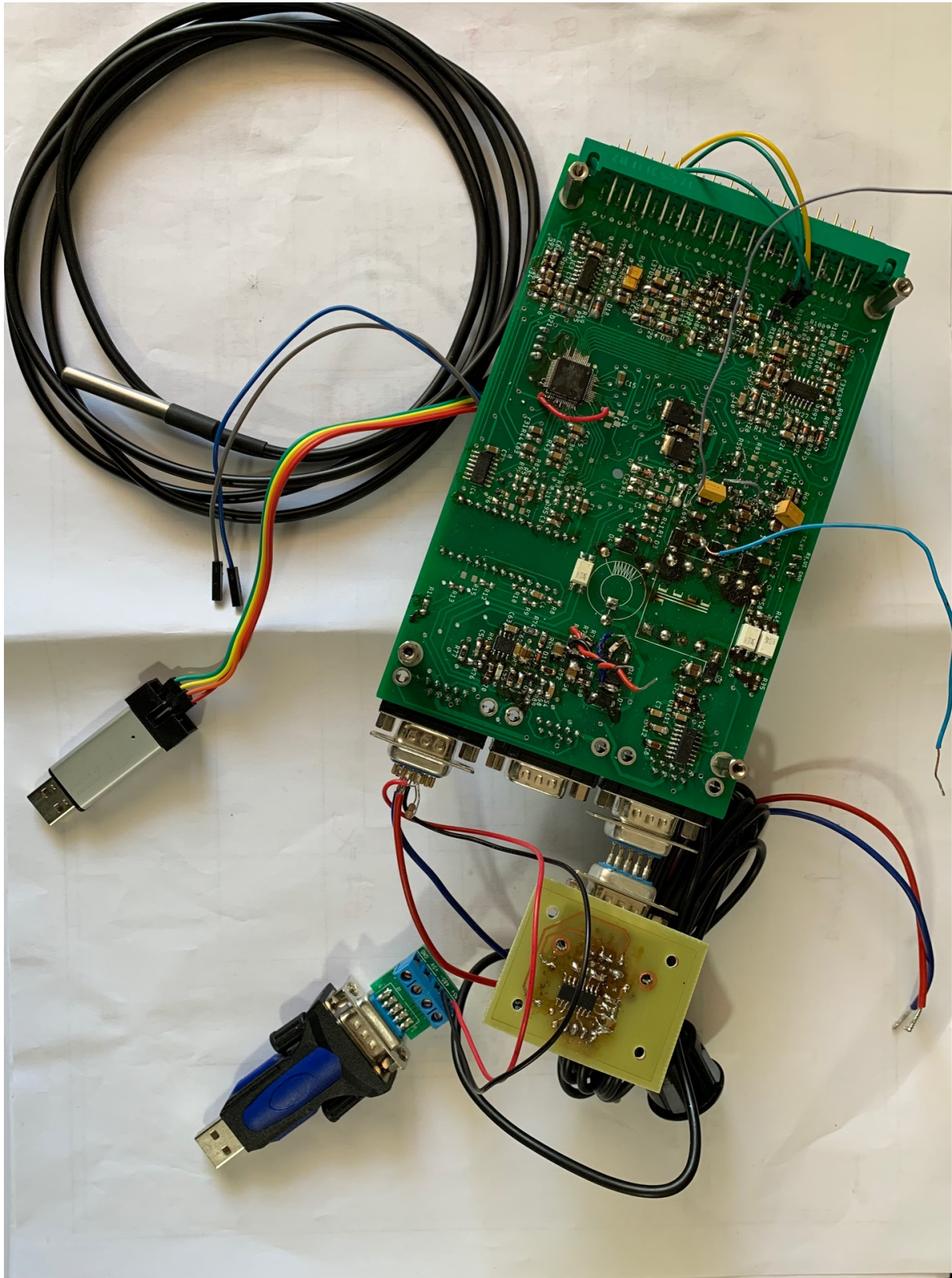


Figure 5.6: Bottom side of final main board

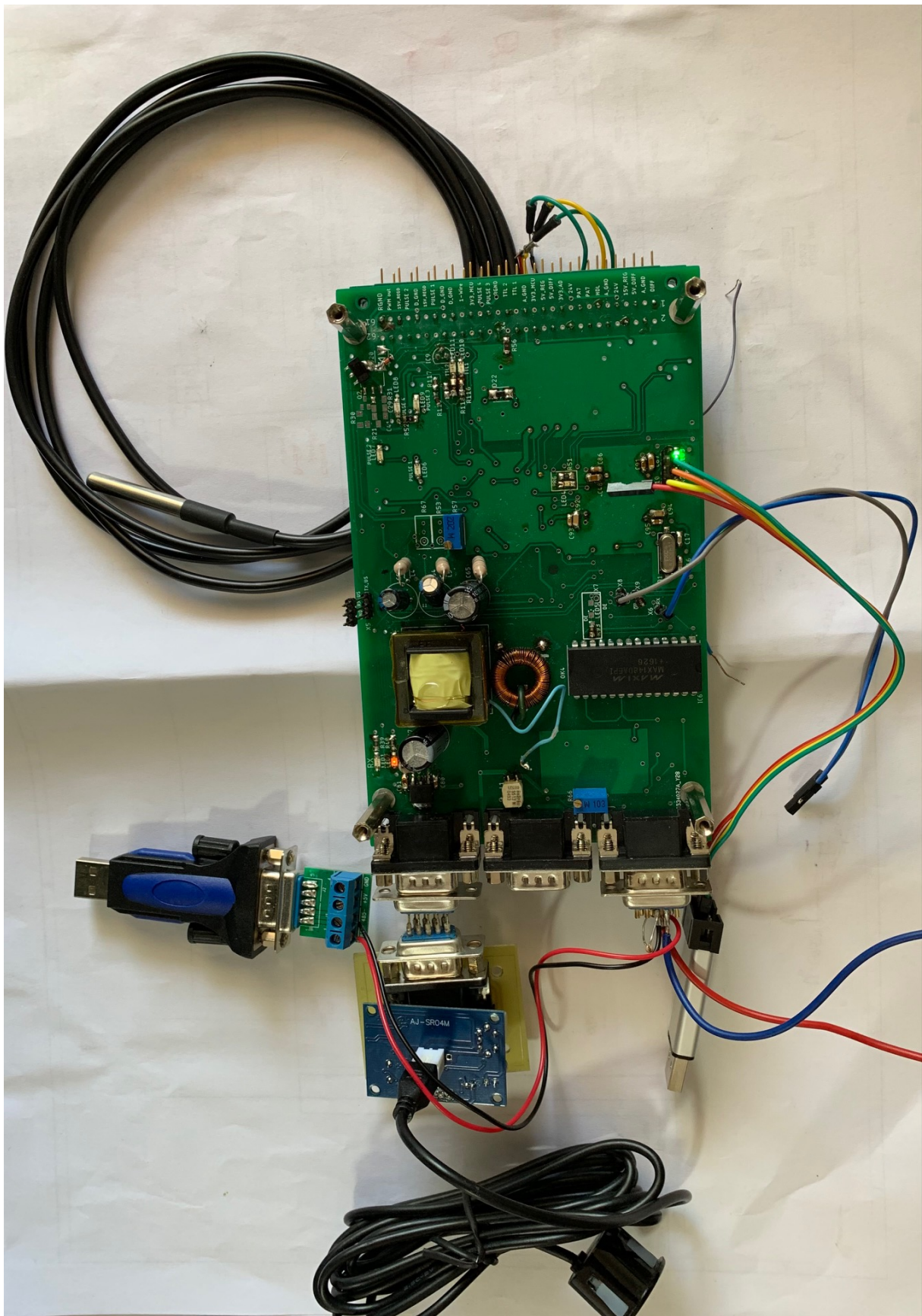


Figure 5.7: Top side of final main board

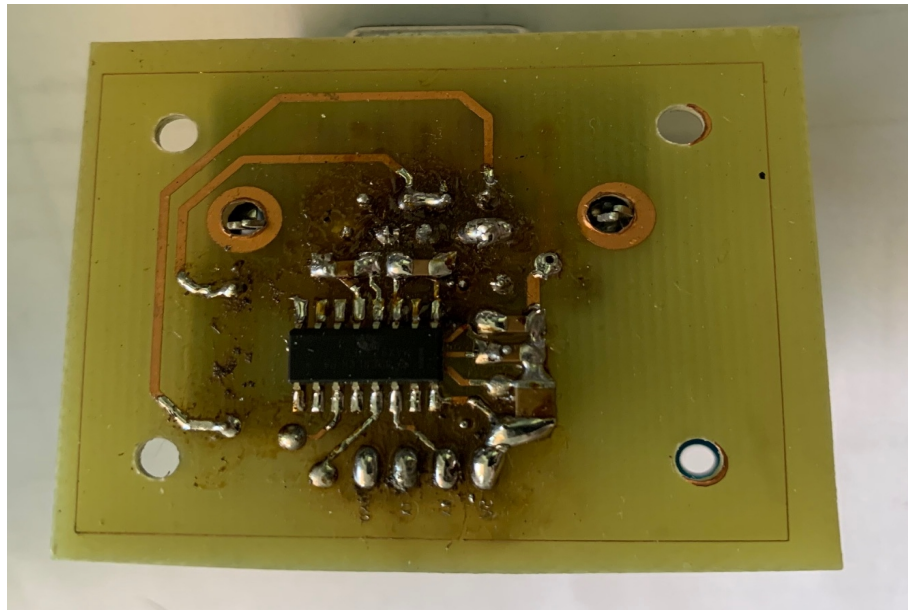


Figure 5.8: Bottom side of the ultrasound module

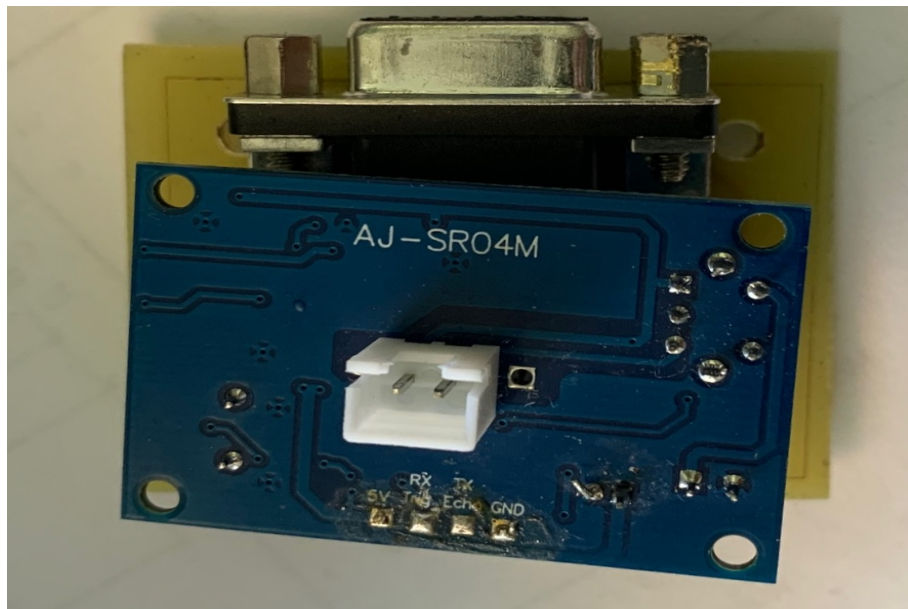


Figure 5.9: Top side of the ultrasound module

6 Software implementation and testing

The software was developed in the STM32CubeIDE and for memory monitoring a Cube-Programmer application was used. In the following sections are figures of the programming workflow, tested inputs of the sensors, and the RS485 communication.

6.1 IAP implementation and testing

The idea of the IAP presented in the software design section was developed on the Nucleo-F303RE board with the organization of memory in pages. This code was then changed to fit the MCU STM32F446RET6 memory organization into sectors. An example of IAP SW programming is displayed in figure 6.3. For facilitating the file transfer, a custom GUI was created for creating packets from the SW binary file. To suit the needs of programming the software with DMA peripheral on the MCU a custom file transfer protocol was designed. The file transfer protocol is based on the XMODEM protocol with a lot of exceptions and adjustments to work with the DMA peripheral. The serial line on the UART4 has a DMA receive circular buffer configuration. When a byte arrives a callback function of the transfer complete flag is raised and writes the byte to the buffer, when a buffer (after every packet of 240 bytes) is filled or more data is not coming (last packet has equal or fewer data than the rest packets) a full buffer is written to the flash memory. When the last packet reaches an IAP structure in the flash memory is modified and the last packet is flashed. Last, the software reset is initiated and the bootloader chooses the new application. Figure 6.3 shows the exchange between the old and new application and jumping to the new app in the memory. The programs and all code used in the software development is in the attached file *ExportedProjects+GUI.zip*.

6.2 RS485 communication

To test the RS485 a function for handling the DMA transfer, enabling the DE pin for data transfer is needed. The example shows working RS485 communication to a terminal of a computer. Sprintf() function loads the measured data to the buffers with the measured values and the profibus_send_string() function sends the data over the RS485 line. The algorithm 6.2 shows the pseudocode of the transmission. The transmission function is given along with the thesis specifications and then adjusted for particular MCU. Figure 6.2 shows the temperature and distance data acquisition from the filter clogging module (RS232 communication) over RS485 serial communication to the computer. The figure 6.1 shows how the data are transmitted to the computer.

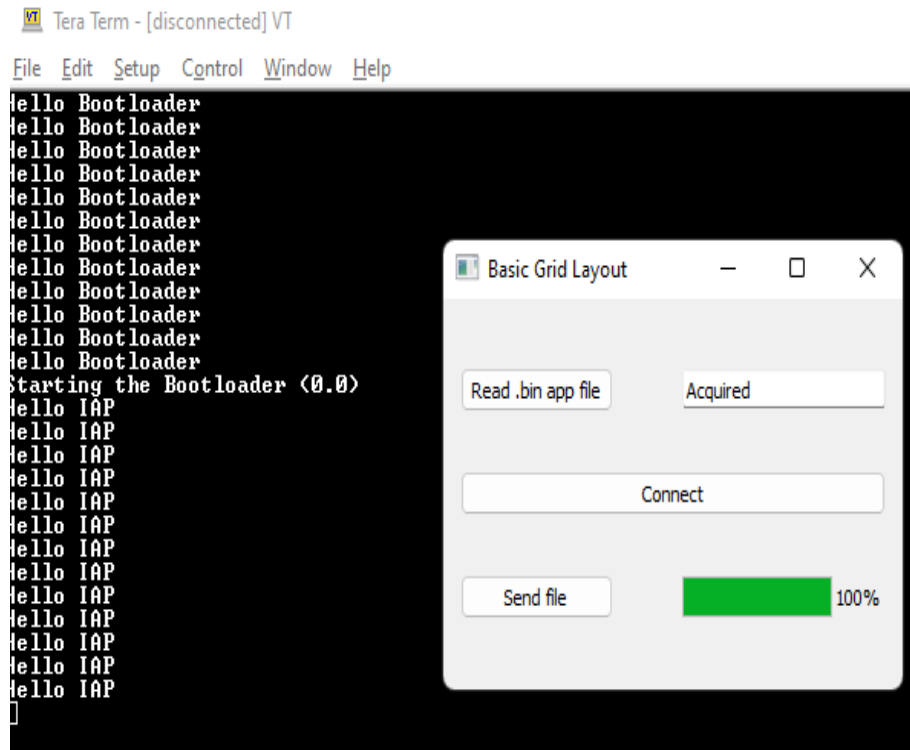


Figure 6.1: Example of the flashing environment

Data: Address, FC, string, dataLength

Result: void

```

if not transmission on going then
    | setDMAmemmoryAddress(string);
    | setDMAdataLength();
    | PB_DE_SET();
    | EnableStream();
else
end

```

Algorithm 2: profibus_send_string() pseudocode

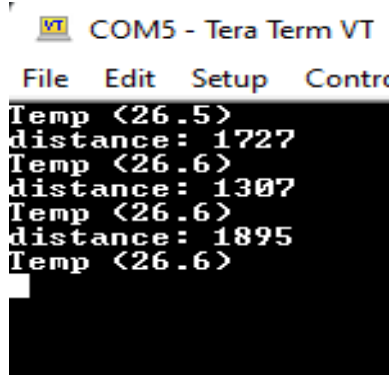


Figure 6.2: Data received in the terminal through the RS485-USB adapter

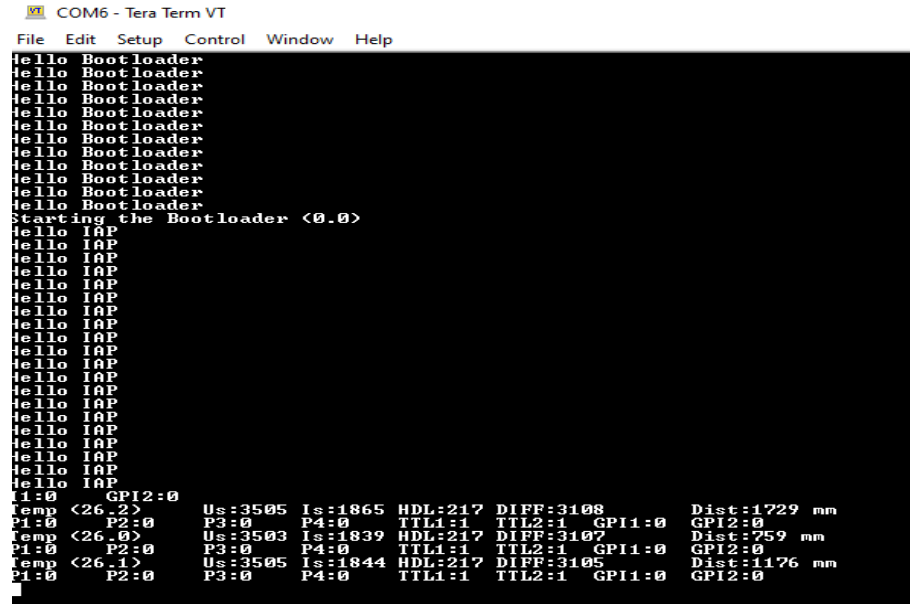


Figure 6.3: Testing the Bootloader + IAP + updating new software while the old application is running and jumping to the new application

Listing 6.1: Code example for the data transmission over RS485

```
sprintf(strbuff1 , "distance: %ld\n\r",val);
profibus_send_string(1, 0, strbuff1, 16);

Presence = DS18B20_Start ();
HAL_Delay (1);
DS18B20_Write (0xCC); // skip ROM
DS18B20_Write (0x44); // convert t
HAL_Delay (800);

Presence = DS18B20_Start ();
HAL_Delay(1);
DS18B20_Write (0xCC); // skip ROM
DS18B20_Write (0xBE); // Read Scratch-pad

Temp_byte1 = read();
Temp_byte2 = read();
TEMP = (Temp_byte2<<8) | Temp_byte1;

sprintf(strbuff2, "Temp (%d.%d)\n\r",TEMP/16, TEMP%16);
profibus_send_string(1, 0, strbuff2, 14);
HAL_Delay(2000u);
\label{fig:5.8}
```

6.3 Sensor input testing

The following figures 6.4 and 6.5 show the test of the inputs of the main board. Figures show a temperature measured with the DS18B20 sensor, a sensed secondary voltage, and a primary current from the peak detector. The numbers for Us, Is, HDL and DIFF are analog values of the 12-bit analog-to-digital converter resolution. The Is and Us input is permanent and always present. The DIFF and HDL input depends on the output of the sensors. TTL1 and TTL2 represent TTL signal lines and figure 6.5 show the TTL input and GPI input. Figure 6.4 shows the test of the P1-P4 inputs. P1-P2 is for the pulse input sensors, and P3-P4 is for the end switch. The distance of the filter clogging sensor also works.

Temp <26.1>	Us:3507	Is:1586	HDL:212	DIFF:2043	Dist:348 mm
P1:0 P2:0	P3:0 P4:0	TTL1:1 TTL2:1	GPI1:0	GPI2:0	
Temp <26.1>	Us:3508	Is:1622	HDL:212	DIFF:2042	Dist:861 mm
P1:0 P2:0	P3:0 P4:1	TTL1:1 TTL2:1	GPI1:0	GPI2:0	
Temp <26.1>	Us:3509	Is:1610	HDL:213	DIFF:2042	Dist:856 mm
P1:0 P2:0	P3:0 P4:1	TTL1:1 TTL2:1	GPI1:0	GPI2:0	
Temp <26.2>	Us:3508	Is:1570	HDL:212	DIFF:2041	Dist:869 mm
P1:0 P2:0	P3:0 P4:0	TTL1:1 TTL2:1	GPI1:0	GPI2:0	
Temp <26.1>	Us:3507	Is:1608	HDL:212	DIFF:2041	Dist:873 mm
P1:0 P2:0	P3:1 P4:0	TTL1:1 TTL2:1	GPI1:0	GPI2:0	
Temp <26.2>	Us:3507	Is:1632	HDL:212	DIFF:2041	Dist:876 mm
P1:0 P2:0	P3:1 P4:0	TTL1:1 TTL2:1	GPI1:0	GPI2:0	
Temp <26.1>	Us:3507	Is:1604	HDL:212	DIFF:2040	Dist:888 mm
P1:0 P2:0	P3:0 P4:0	TTL1:1 TTL2:1	GPI1:0	GPI2:0	
Temp <26.2>	Us:3507	Is:1635	HDL:212	DIFF:2040	Dist:792 mm
P1:1 P2:0	P3:0 P4:0	TTL1:1 TTL2:1	GPI1:0	GPI2:0	
Temp <26.2>	Us:3508	Is:1664	HDL:212	DIFF:2039	Dist:788 mm
P1:1 P2:0	P3:0 P4:0	TTL1:1 TTL2:1	GPI1:0	GPI2:0	
Temp <26.1>	Us:3506	Is:1612	HDL:212	DIFF:2039	Dist:882 mm
P1:0 P2:0	P3:0 P4:0	TTL1:1 TTL2:1	GPI1:0	GPI2:0	
Temp <26.2>	Us:3508	Is:1582	HDL:212	DIFF:2038	Dist:304 mm
P1:0 P2:0	P3:0 P4:0	TTL1:1 TTL2:1	GPI1:0	GPI2:0	
Temp <26.2>	Us:3507	Is:1596	HDL:212	DIFF:2039	Dist:304 mm
P1:0 P2:1	P3:0 P4:0	TTL1:1 TTL2:1	GPI1:0	GPI2:0	
Temp <26.1>	Us:3507	Is:1571	HDL:212	DIFF:2039	Dist:304 mm

Figure 6.4: Sensor input image - 1

T1:0	T2:0	T3:0	T4:0	TTL1:1	TTL2:1	GPI1:0	GPI2:0
Temp <26.0>		Us:3508	Is:1585	HDL:212	DIFF:2022		Dist:857 mm
P1:0	P2:0	P3:0	P4:0	TTL1:1	TTL2:1	GPI1:0	GPI2:0
Temp <26.0>		Us:3505	Is:1562	HDL:212	DIFF:2022		Dist:839 mm
P1:0	P2:0	P3:0	P4:0	TTL1:0	TTL2:0	GPI1:0	GPI2:0
Temp <26.1>		Us:3505	Is:1590	HDL:212	DIFF:2021		Dist:848 mm
P1:0	P2:0	P3:0	P4:0	TTL1:1	TTL2:1	GPI1:0	GPI2:0
Temp <26.0>		Us:3507	Is:1538	HDL:211	DIFF:2021		Dist:848 mm
P1:0	P2:0	P3:0	P4:0	TTL1:1	TTL2:1	GPI1:0	GPI2:0
Temp <26.0>		Us:3507	Is:1574	HDL:212	DIFF:2020		Dist:22608 mm
P1:0	P2:0	P3:0	P4:0	TTL1:1	TTL2:1	GPI1:0	GPI2:0
Temp <26.1>		Us:3507	Is:1584	HDL:212	DIFF:2020		Dist:771 mm
P1:0	P2:0	P3:0	P4:0	TTL1:1	TTL2:1	GPI1:0	GPI2:0
Temp <26.1>		Us:3506	Is:1578	HDL:212	DIFF:2018		Dist:771 mm
P1:0	P2:0	P3:0	P4:0	TTL1:1	TTL2:1	GPI1:1	GPI2:1
Temp <26.0>		Us:3504	Is:1568	HDL:212	DIFF:2019		Dist:771 mm
P1:0	P2:0	P3:0	P4:0	TTL1:1	TTL2:1	GPI1:1	GPI2:1
Temp <26.1>		Us:3506	Is:1588	HDL:211	DIFF:2016		Dist:865 mm
P1:0	P2:0	P3:0	P4:0	TTL1:1	TTL2:1	GPI1:0	GPI2:0
Temp <26.1>		Us:3507	Is:1573	HDL:210	DIFF:2015		Dist:852 mm
P1:0	P2:0	P3:0	P4:0	TTL1:1	TTL2:1	GPI1:0	GPI2:0

Figure 6.5: Sensor input image - 2

7 Conclusion

This thesis deals with the design of the signal acquisition unit for rainwater status monitoring and diagnostics. The board specifications and design process were described in the design process and the software development. Firstly a prototype PSU board was created to adjust several components, and then the main PCB and complementary ultrasound module were fabricated. The goals given in the assignment were completed and tested. The PSU efficiency is about 8 per cent higher than expected. Its final efficiency is 88% instead of 80%. Communication over RS485 with the computer was tested. Designed firmware was developed for to STM32 lineup. First, IAP functionality developed firmware for the F3 lineup with memory organization into pages. Then a rework for chosen MCU that has memory organization into sectors.

Different sensors were revived during the development process for different outputs: voltage, current loops, pulse type outputs, RS232, 1-wire bus, and end stop switches. Aside from the input handling, an internal diagnostics of the board is present. There is a current and voltage monitoring possibility and an adjustment of the offset voltage for signal conditioning circuits using DAC. In that regard, RS485 communication was revived and successfully implemented in the software. In that regard, a more comfortable way of updating the SW was developed with the IAP approach. This firmware allows the user to complete remote upload of the new application while the old one is still working. The main advantage is the update through an internet interface. An implementation for false upload protection. With the hard reset of the DPS, a new wrong upload will not be executed, but the old version will. A step-down converter circuit is prepared for further addition.

List of Abbreviations

PCB Printed Circuit Board

DB Database

UPS Uninterruptible Power Supply

IC Integrated circuit

MCU Microcontroller unit

PSU Power supply

SMPS Switch mode power supply

CMOS Complementary metal-oxide semiconductor

ICSP In Circuit System Programming

IAP In application programming

DMA Direct memory access

ADC Analog to digital converter

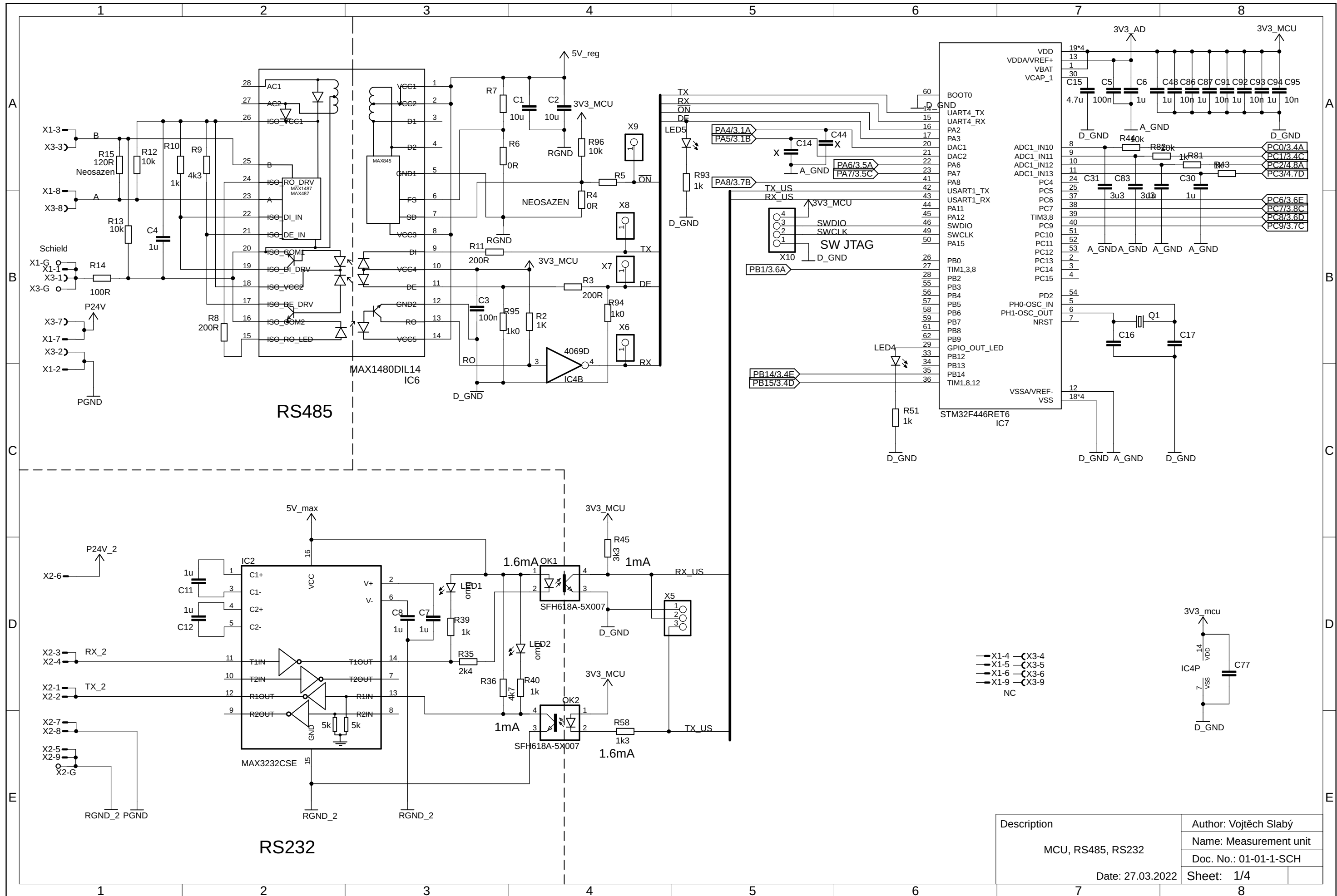
DAC Digital to analog converter

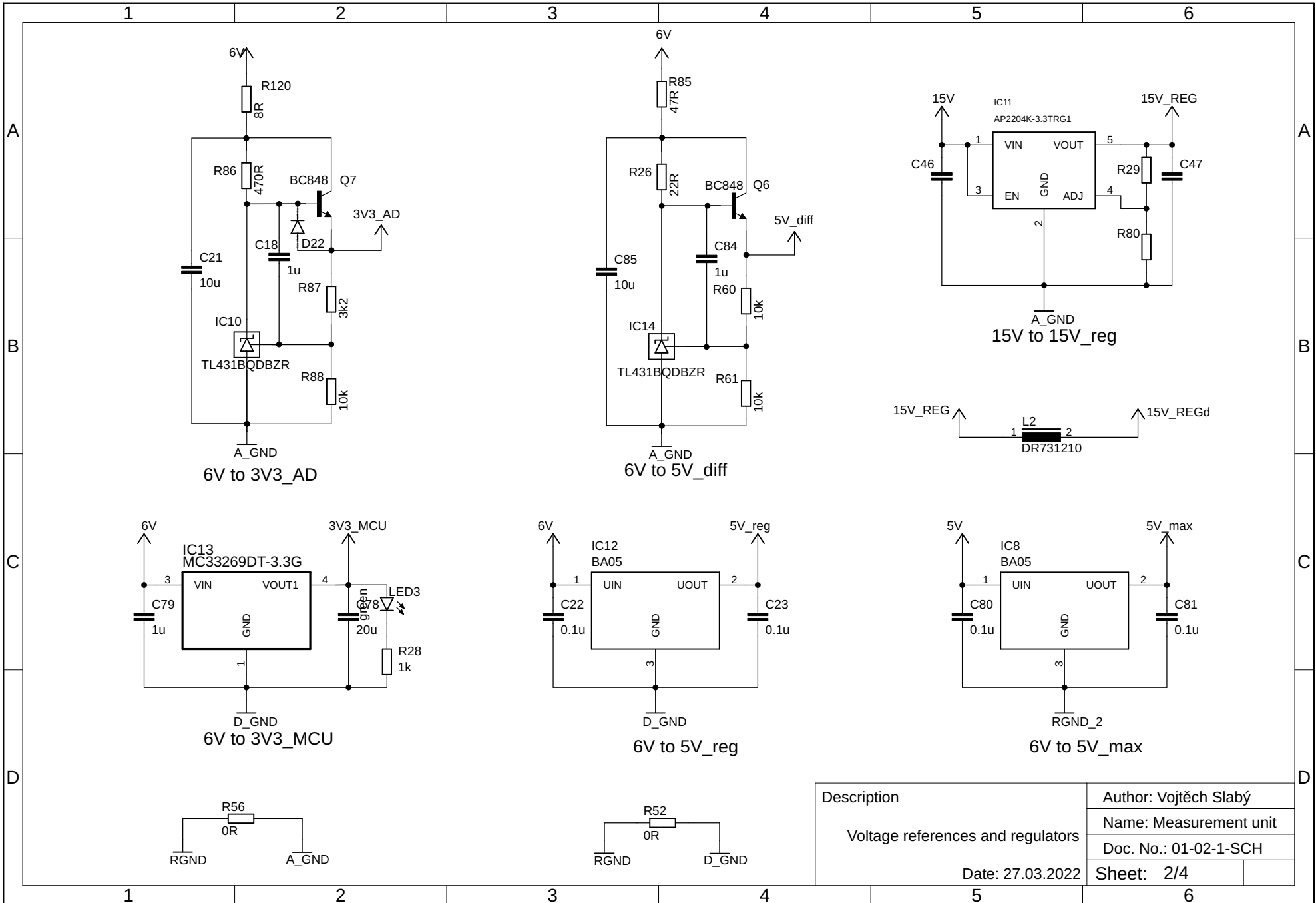
RTOS Real time operating system

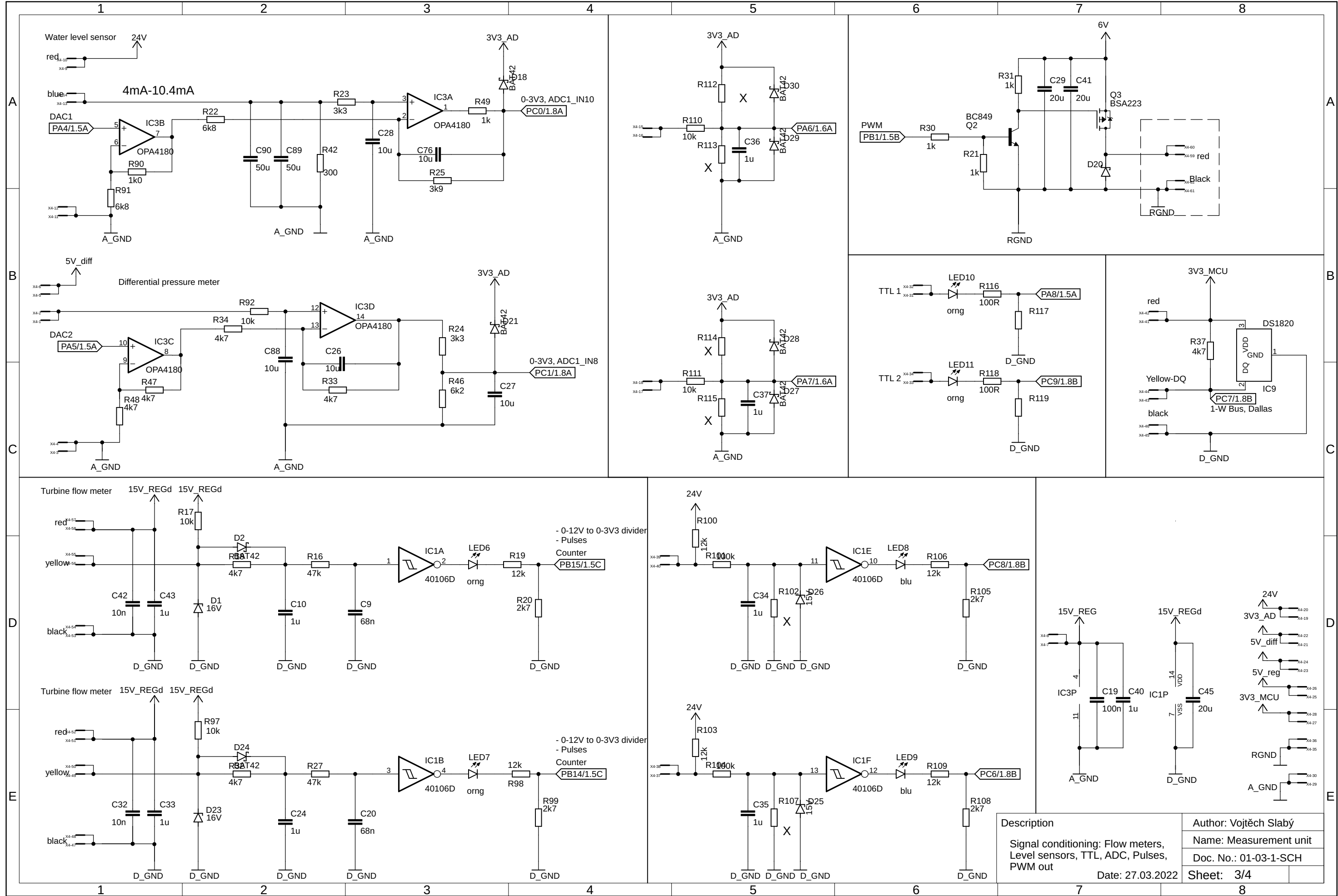
Bibliography

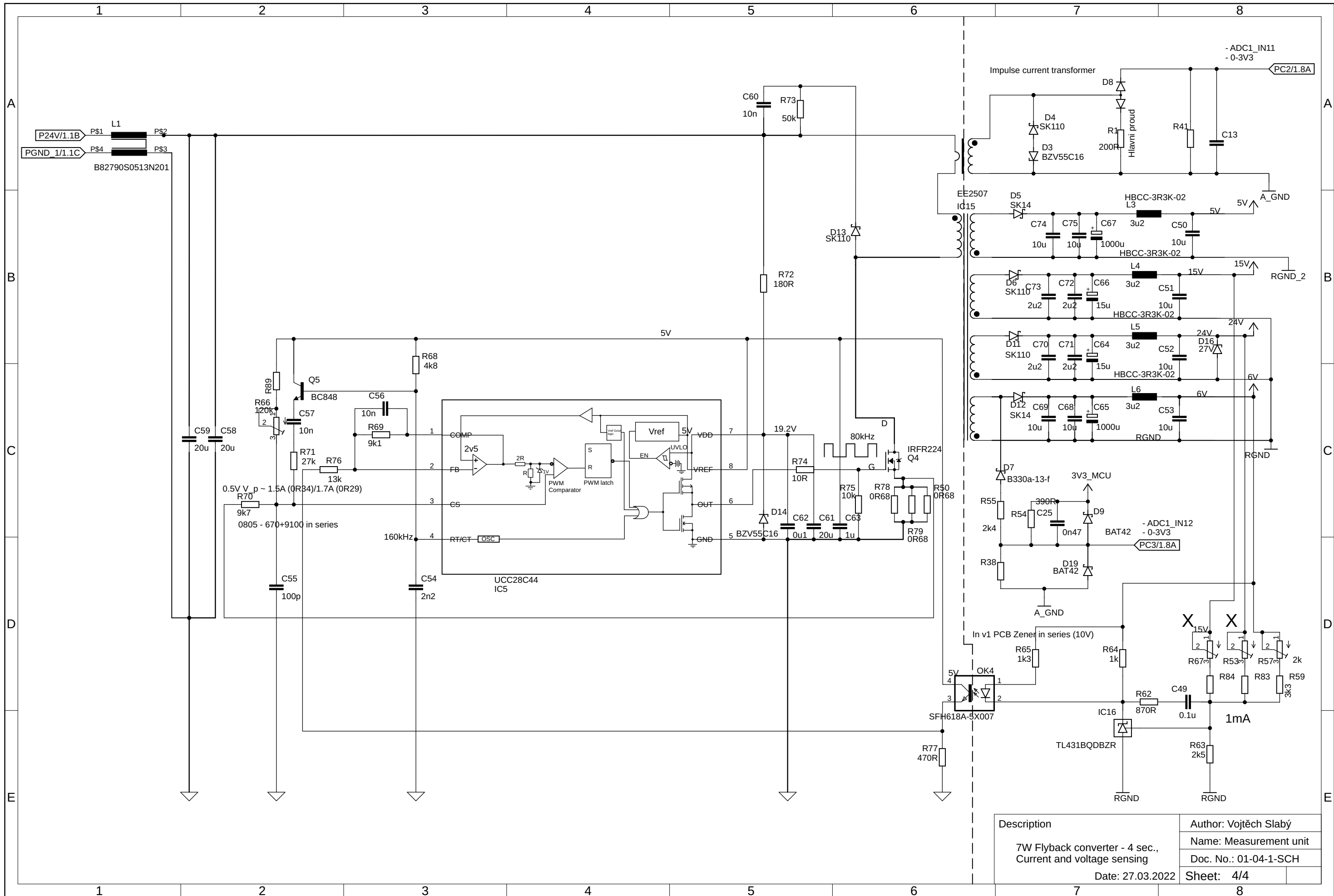
- [1] ĎAĎO, Stanislav a Marcel KREIDL. *Senzory a měřící obvody*. Praha: ČVUT, 1996, 315 s. ISBN 80-01-01500-9.
- [2] VRBA, Kamil a Pavel HANÁK. *Konstrukce elektronických zařízení*. VUTIUM. ISBN 978-80-214-5957-1. Dostupné z: doi:10.13164/book.construction.electronic.devices
- [3] PATOČKA, Miroslav. *Magnetické jevy a obvody ve výkonové elektronice, měřicí technice a silnoproudé elektrotechnice*. V Brně: VUTIUM, 2011, 564 s. : il. ISBN 978-80-214-4003-6.
- [4] HOROWITZ, Paul a Winfield HILL. *The art of electronics*. Third edition. New York: Cambridge University Press, 2015, xxxi, 1192 stran : illustration ; 26 cm. ISBN 978-0-521-80926-9
- [5] STMicroelectronics: *STM32F446 [online]* [Online; visited 8.5.2022] URL <https://www.st.com/resource/en/datasheet/stm32f446re.pdf>
- [6] Maxim integrated: *DS18B20 [online]* [Online; visited 8.5.2022] URL <https://datasheets.maximintegrated.com/en/ds/DS18B20.pdf>
- [7] *XGZP6899A [online]* [Online; visited 8.5.2022] URL <https://www.aliexpress.com/item/1005003023748561.html>
- [8] *FS400A [online]* [Online; visited 8.5.2022] URL <https://www.aliexpress.com/item/32423667920.html>
- [9] *AJ-SR04M [online]* [Online; visited 8.5.2022] URL <https://www.aliexpress.com/item/33002362860.html>
- [10] *Trojúhelníkový měrný přeliv s otevřenou hladinou*. 2021. Pars aqua s.r.o. [online]. Praha: -. Available at: https://pars-aqua.cz/img/carousel/volna_hladina/trojuhelnikovy_merny_preliv_otevrena_hladina.jpg
- [11] MAJERLE, Tilen. 2022. *STM32 UART DMA RX and TX*. Github [online]. -: Github. Available at: <https://github.com/Majerle/stm32-usart-uart-dma-rx-tx>
- [12] VLACH, Radek. *Tepelné procesy v mechatronických soustavách*. Brno: Akademické nakladatelství CERM, 2009, 94 stran : ilustrace. ISBN 978-80-214-3976-4
- [13] *UART Interface Waveform*. Realtek. Realtek [online]. -: Realtek. Available at: <http://www.amebaiot.com/wp-content/uploads/2017/05/u1.png>

- [14] *3.0V to 5.5V, Low-Power, Up to 1Mbps, True RS-232 Transceivers.* 2019. Maxim Integrated [online]. -: Maxim Integrated Products. Available at: <https://datasheets.maximintegrated.com/en/ds/MAX3222-MAX3241.pdf>
- [15] *Complete, Isolated RS-485/RS-422 Data Interface.* 2019. Maxim Integrated [online]. -: Maxim Integrated Products. Available at: <https://datasheets.maximintegrated.com/en/ds/MAX1480A-MAX1490B.pdf>
- [16] *PM0059 Programming manual.* 2020. STMicroelectronics [online]. -: STMicroelectronics. Available at: https://www.st.com/resource/en/programming_manual/pm0059-stm32f205215-stm32f207217-flash-programming-manual-stmicroelectronics.pdf
- [17] *AN4657 STM32 in-application programming (IAP) using the USART.* 2020. STMicroelectronics [online]. -: STMicroelectronics. Available at: https://www.st.com/resource/en/application_note/an4657-stm32-inapplication-programming-iap-using-the-usart-stmicroelectronics.pdf
- [18] CHRISTENSEN, Ward. 192AD. *Xmodem Protocol Overview.* Packetizer [online]. Chicago: Packetizer. Available at: <https://techheap.packetizer.com/communication/modems/xmodem.html>
- [19] *RM0390 Reference manual.* 2020. STMicroelectronics [online]. -: STMicroelectronics. Available at: https://www.st.com/resource/en/reference_manual/rm0390-stm32f446xx-advanced-armbased-32bit-mcus-stmicroelectronics.pdf
- [20] *LJ E 2507.* Semic Trade, s.r.o [online]. -: Semic Trade, s.r.o. Available at: https://semic.cz/!old/files/pdf_www/Lj_138E2507_CF.pdf
- [21] *IRFR224.* 2013. Vishay Intertechnology, Inc. [online]. -: Vishay Intertechnology, Inc.. Available at: <https://www.micro-semiconductor.com/datasheet/ed-IRFR224PBF.pdf>
- [22] *UCCx8C4x BiCMOS Low-Power Current-Mode PWM Controller.* 2022. Texas Instruments. [online]. -: Texas Instruments. Available at: <https://www.ti.com/lit/ds/symlink/ucc28c42.pdf>
- [23] RIDLEY, Ray. 2005. *Flyback converter with Snubber design* [online]. -: Switching Power Magazine. Available at: https://ridleyengineering.com/images/phoca/download/12%20flyback_snubber_design.pdf
- [24] *LJ T 1606.* Semic Trade, s.r.o [online]. -: Semic Trade, s.r.o. Available at: https://semic.cz/!old/files/pdf_www/Lj_T1606_CF.pdf
- [25] NEMETH, Ferenc. 2020. *stm32-bootloader.* Github [online]. -: Github. Available at: <https://github.com/ferenc-nemeth/stm32-bootloader>



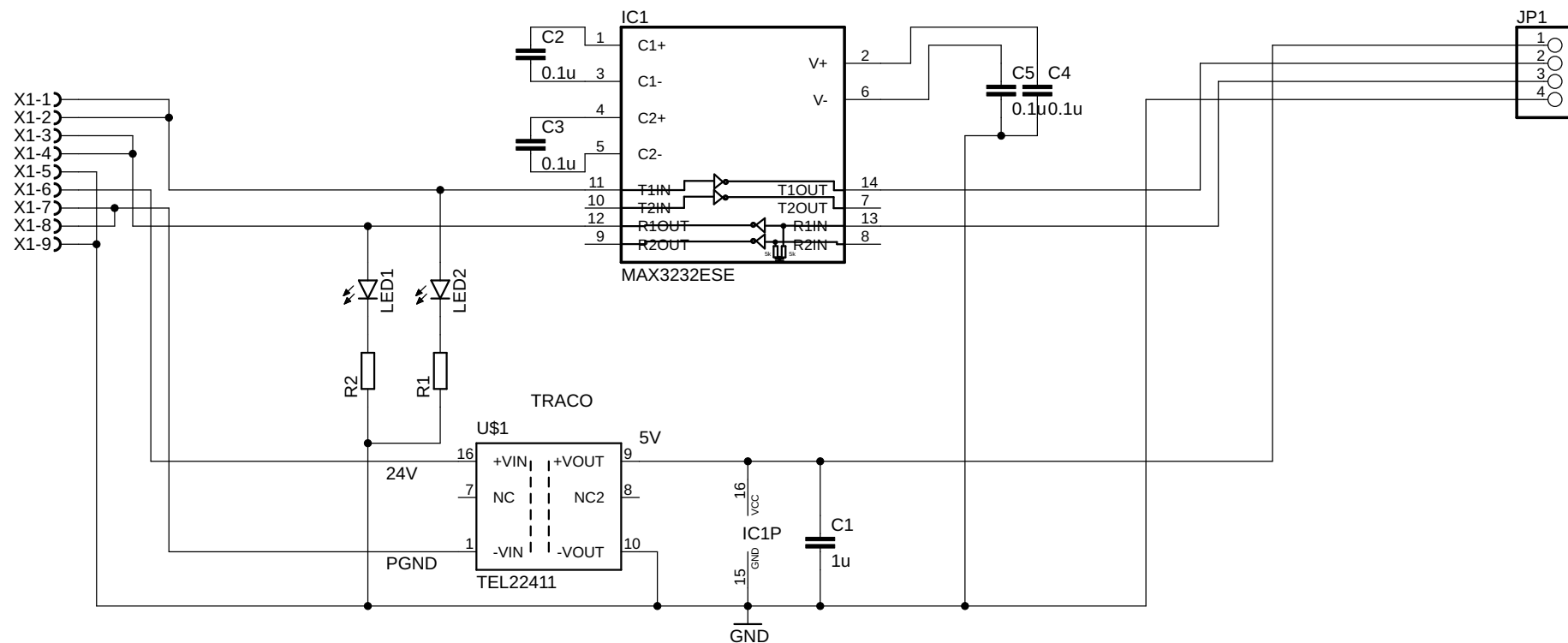






A

A



B

B

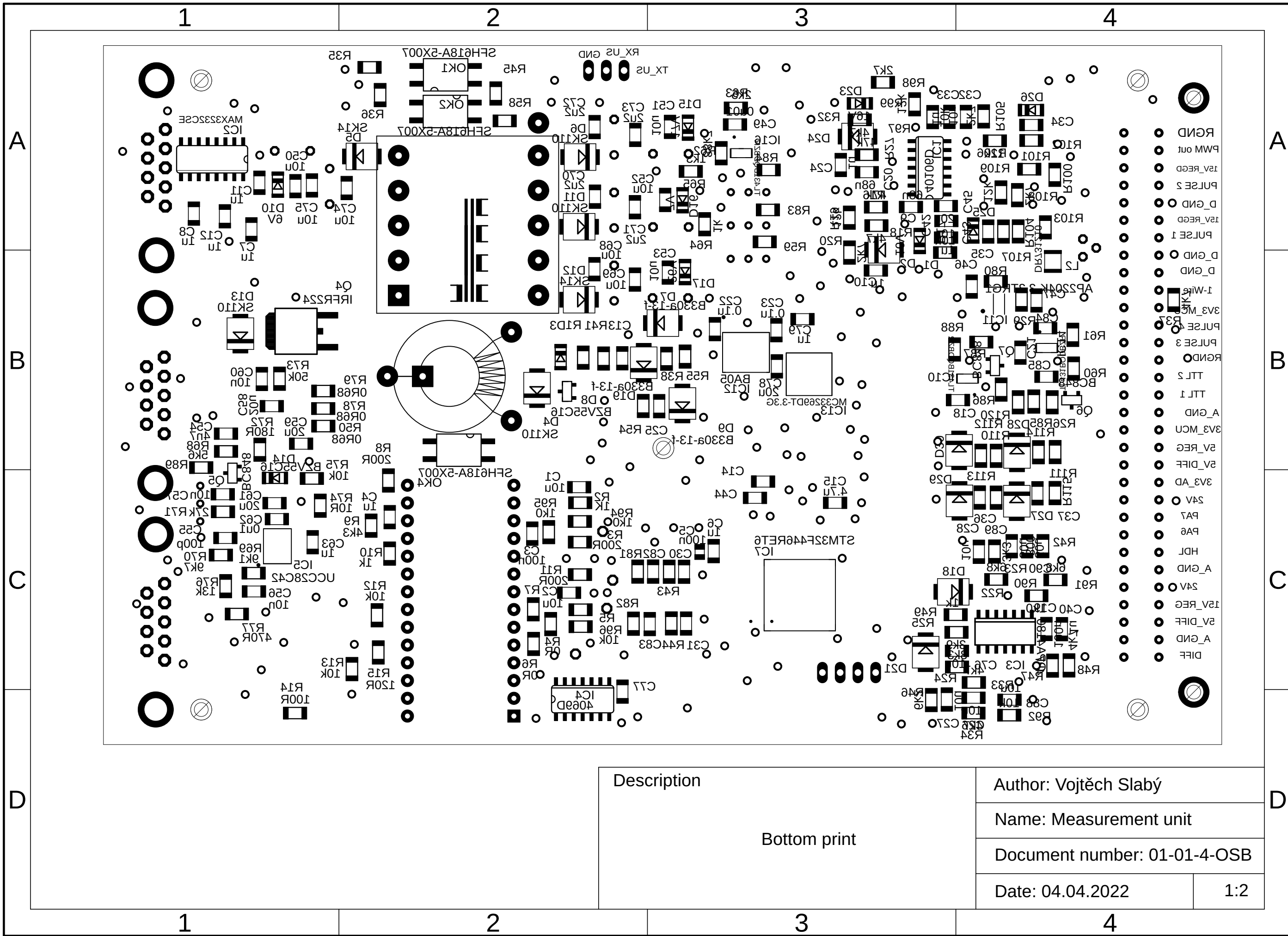
C

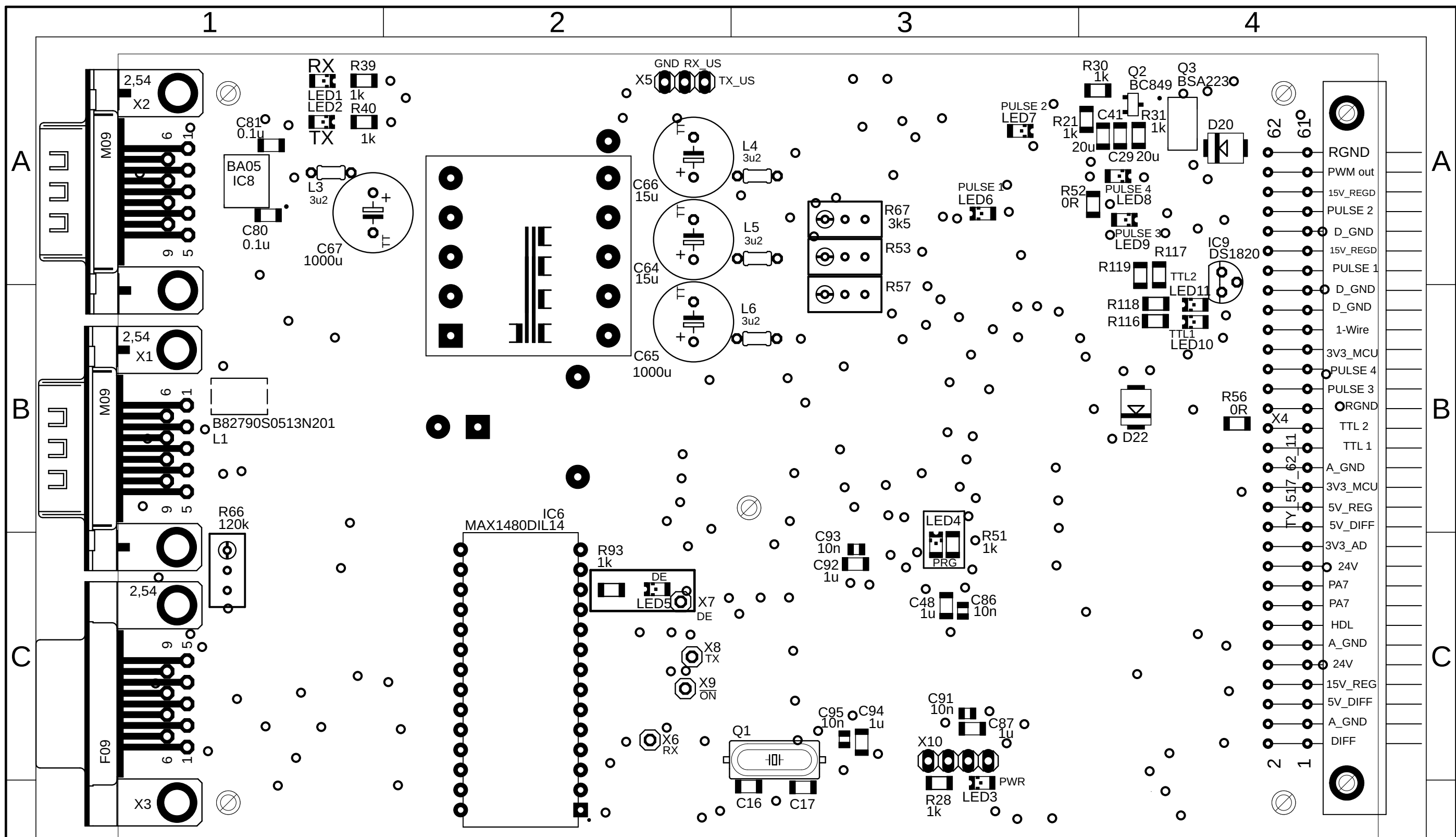
C

D

D

Description	Author: Vojtěch Slabý
TRACO, MAX232	Name: sensor's module
	Doc. No.: 02-01-1-SCH
Date: 27.03.2022	Sheet:





Description

Top print

Author: Vojtěch Slabý

Name: Measurement unit

Document number: 01-01-3-OST

Date: 04.04.2022

1:2

A

A

B

B

C

C

D

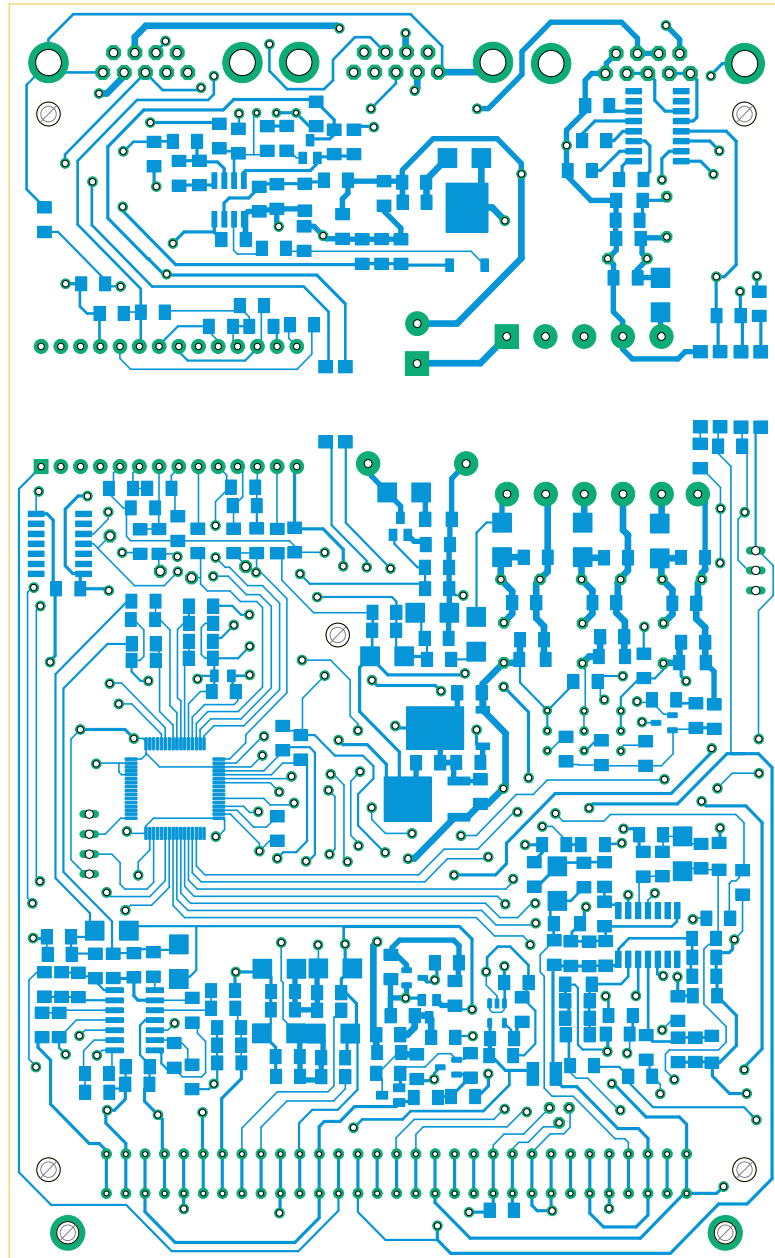
D

E

E

F

F



Description:

Bottom, Dimensions, Pads, Vias

Author: Vojtěch Slabý

Name: Measurement unit

Document number: 01-01-2

Date: 26.03.2022

1:1

1 2 3 4

A

A

B

B

C

C

D

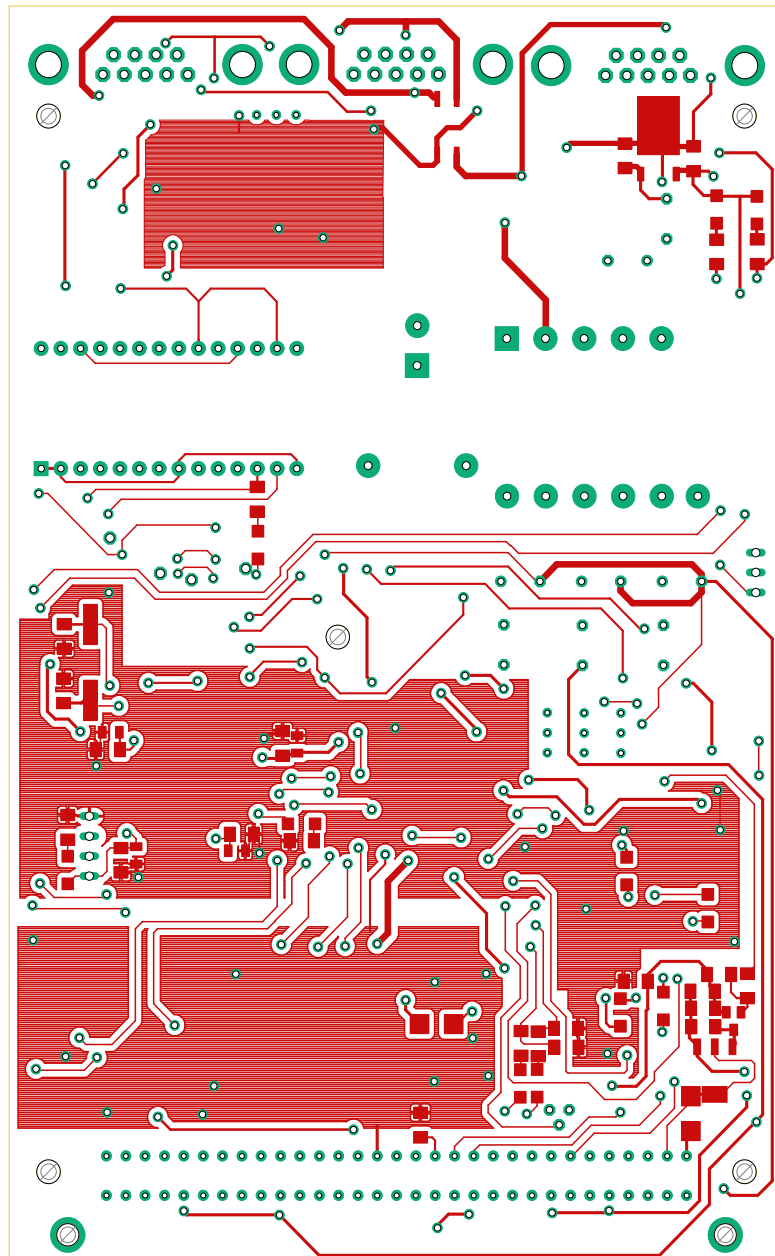
D

E

E

F

F



Description:

Top, Dimensions, Pads, Vias

Author: Vojtěch Slabý

Name: Measurement unit

Document number: 01-01-1

Date: 26.03.2022

1:1

1 2 3 4

1

2

3

4

A

B

C

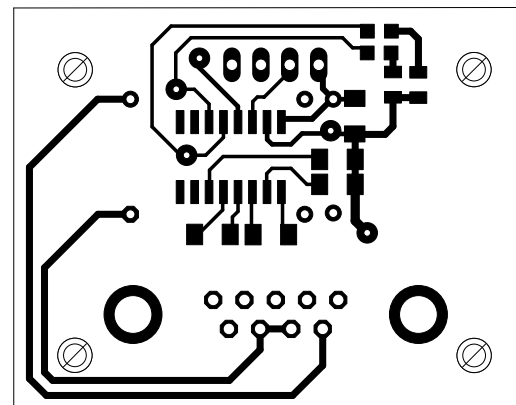
D

A

B

C

D



Description

Board

Author: Vojtěch Slabý

Name: Ultrasound module

Document number: 01-01-1

Date: 04.04.2022

1:1

1

2

3

4

1

2

3

4

A

B

C

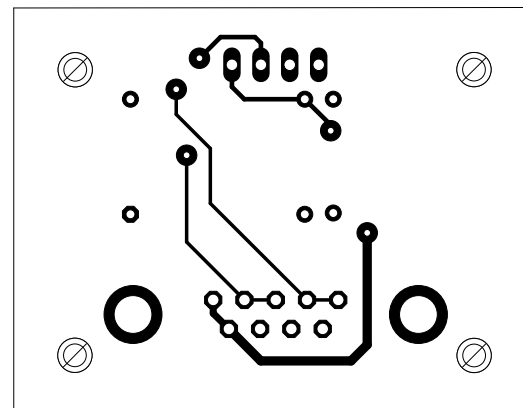
D

A

B

C

D



Description

Board

Author: Vojtěch Slabý

Name: Ultrasound module

Document number: 01-01-1

Date: 04.04.2022

1:1

1

2

3

4

D List of capacitors

Part	Value	Package
C1	10u	C1206
C2	10u	C1206
C3	100n	C1206
C4	1u	C1206
C5	100n	C0805
C6	1u	C1206
C7	1u	C1206
C8	1u	C1206
C9	68n	C1206
C10	1u	C1206
C11	1u	C1206
C12	1u	C1206
C13	1u	C1206
C15	4.7u	C1206
C16	15p	C1206
C17	15p	C1206
C18	1u	C1206
C19	100n	C1206
C20	68n	C1206
C21	10u	C1206
C22	0.1u	C1206
C23	0.1u	C1206
C24	1u	C1206
C25	0n47	C1206
C26	10u	C1206
C27	10u	C1206
C28	10u	C1206
C29	20u	C1206
C30	1u	C1206
C31	3u3	C1206
C32	10n	C1206
C33	1u	C1206
C34	1u	C1206

Table 7.1: List of capacitors - part 1

Part	Value	Package
C35	1u	C1206
C36	1u	C1206
C37	1u	C1206
C40	1u	C1206
C41	20u	C1206
C42	10n	C1206
C43	1u	C1206
C45	20u	C1206
C46	1u	C1206
C47	1u	C1206
C48	1u	C1206
C49	0.1u	C1206
C50	10u	C1206
C51	10u	C1206
C52	10u	C1206
C53	10u	C1206
C54	2n2	C1206
C55	100p	C1206
C56	10n	C1206
C57	10n	C1206
C58	20u	C1206
C59	20u	C1206
C60	10n	C1206
C61	20u	C1206
C62	0u1	C1206
C63	1u	C1206
C64	15u	TT5D10
C65	1000u	TT5D10
C66	15u	TT5D10
C67	1000u	TT5D10
C68	10u	C1206
C69	10u	C1206

Table 7.2: List of capacitors - part 2

D LIST OF CAPACITORS

Part	Value	Package
C70	2u2	C1206
C71	2u2	C1206
C72	2u2	C1206
C73	2u2	C1206
C74	10u	C1206
C75	10u	C1206
C76	10u	C1206
C77	1u	C1206
C78	20u	C1206
C79	1u	C1206
C80	0.1u	C1206
C81	0.1u	C1206
C82	1u	C1206
C83	3u3	C1206
C84	1u	C1206
C85	10u	C1206
C86	10n	C0805
C87	1u	C1206

Table 7.3: List of capacitors - part 3

Part	Value	Package
C88	10u	C1206
C89	50u	C1206
C90	50u	C1206
C91	10n	C0805
C92	1u	C1206
C93	10n	C0805
C94	1u	C1206
C95	10n	C0805

Table 7.4: List of capacitors - part 4

E List of diodes

Part	Value	Package
D1	16V	SOD80C
D2	BAT42	SMB
D3	BZV55C16	SOD80C
D4	SK110	SMB
D5	SK14	SMB
D6	SK110	SMB
D7	B330a-13-f	SMB
D8		SOT23
D9	BAT42	SMB
D11	SK110	SMB
D12	SK14	SMB
D13	SK110	SMB
D14	BZV55C16	SOD80C
D16	27V	SOD80C
D18	BAT42	SMB
D19	BAT42	SMB
D20	BAT42	SMB
D21	BAT42	SMB
D22	BAT42	SMB
D23	16V	SOD80C
D24	BAT42	SMB
D25	15V	SOD80C
D26	15V	SOD80C
D27	BAT42	SMB
D28	BAT42	SMB
D29	BAT42	SMB
D30	BAT42	SMB

Table 7.5: List of diodes

F List of LEDs

Part	Value	Package
led1	orng	CHIPLED_1206
led2	orng	CHIPLED_1206
led3	green	CHIPLED_1206
led4	orng	CHIPLED_1206
led5	orng	CHIPLED_1206
led6	orng	CHIPLED_1206
led7	orng	CHIPLED_1206
led8	blu	CHIPLED_1206
led9	blu	CHIPLED_1206
led10	orng	CHIPLED_1206
led11	orng	CHIPLED_1206

Table 7.6: List of LEDs

G List of Integrated circuits

Part	Value	Package
IC1	40106D	SO14
IC2	MAX3232CSE	SO16
IC3	OPA4180	SO14
IC4	4069D	SO14
IC5	UCC28C44	SOIC127P568X175-8N
IC6	MAX1480DIL14	DIP1524W46P254L3734H508Q28
IC7	STM32F446RET6	QFP50P1200X1200X160-64N
IC8	BA05	TO230P950X230-3N
IC9	DS1820	TO-92
IC10	TL431BQDBZR	SOT95P237X112-3N
IC11	AP2204K-3.3TRG1	SOT95P280X145-5N
IC12	BA05	TO230P950X230-3N
IC13	MC33269DT-3.3G	TO229P990X238-4N
IC14	TL431BQDBZR	SOT95P237X112-3N
IC15	EE2507	EE16-10P
IC16	TL431BQDBZR	SOT95P237X112-3N
IC17	CS-TRAFO	CS-TRAFO

Table 7.7: List of ICs

H List of transistors

Part	Value	Package
Q1	8MHz	SM49
Q2	BC849	SOT23-BEC
Q3	BSA223	SOT230P700X180-4N
Q4	IRFR224	TO252
Q5	BC848	SOT23
Q6	BC848	SOT23
Q7	BC848	SOT23

Table 7.8: List of transistors

I List of connectors and optocouplers

Part	Value	Package
OK1	SFH618A-5X007	SMD4-7
OK2	SFH618A-5X007	SMD4-7
OK4	SFH618A-5X007	SMD4-7

Table 7.9: List of optocouplers

Part	Value	Package
X1		M09HP
X2		M09HP
X3		F09HP
X4		TY_517_62_11
X5		1X03
X6		1X01
X7		1X01
X8		1X01
X9		1X01
X10		1X04

Table 7.10: List of connectors

J List of resistors

Part	Value	Package
R1	200R	R1206
R2	1K	R1206
R3	200R	R1206
R4	0R	R1206
R5	0R	R1206
R6	0R	R1206
R8	200R	R1206
R9	4k3	R1206
R10	1k	R1206
R11	200R	R1206
R12	10k	R1206
R13	10k	R1206
R14	100R	R1206
R15	120R	R1206
R16	47k	R1206
R17	10k	R1206
R18	4k7	R1206
R19	12k	R1206
R20	2k7	R1206
R21	1k	R1206
R22	6k8	R1206
R23	3k3	R1206
R24	3k3	R1206
R25	3k9	R1206
R26	22R	R1206
R27	47k	R1206
R28	1k	R1206
R29	120k	R1206
R30	1k	R1206
R31	1k	R1206
R32	4k7	R1206
R33	4k7	R1206
R34	4k7	R1206

Table 7.11: List of resistor parts - 1

J LIST OF RESISTORS

Part	Value	Package
R35	2k4	R1206
R36	4k7	R1206
R37	4k7	R1206
R39	1k	R1206
R40	1k	R1206
R41	10k	R1206
R42	300	R1206
R43	1k	R1206
R44	10k	R1206
R45	3k3	R1206
R46	6k2	R1206
R47	4k7	R1206
R48	4k7	R1206
R49	1k	R1206
R50	0R68	R1206
R51	1k	R1206
R52	0R	R1206
R54	390R	R1206
R55	2k4	R1206
R56	0R	R1206
R57	2k	RTRIM3296W
R58	1k3	R1206
R59	3k3	R1206
R60	10k	R1206
R61	10k	R1206
R62	870R	R1206
R63	2k5	R1206
R64	1k	R1206
R65	1k3	R1206
R66	120k	RTRIM3296W
R68	4k8	R1206
R69	9k1	R1206
R70	9k7	R1206
R71	27k	R1206
R72	180R	R1206
R73	50k	R1206
R74	10R	R1206

Table 7.12: List of resistor parts - 2

J LIST OF RESISTORS

Part	Value	Package
R75	10k	R1206
R76	13k	R1206
R77	470R	R1206
R78	0R68	R1206
R79	0R68	R1206
R80	10k	R1206
R81	1k	R1206
R82	10k	R1206
R85	47R	R1206
R86	470R	R1206
R87	3k2	R1206
R88	10k	R1206
R89	5k	R1206
R90	1k0	R1206
R91	6k8	R1206
R92	10k	R1206
R93	1k	R1206
R94	1k0	R1206
R95	1k0	R1206
R96	10k	R1206
R97	10k	R1206
R98	12k	R1206
R99	2k7	R1206
R100	12k	R1206

Table 7.13: List of resistor parts - 3

Part	Value	Package
R101	100k	R1206
R103	12k	R1206
R104	100k	R1206
R105	2k7	R1206
R106	12k	R1206
R108	2k7	R1206
R109	12k	R1206
R110	10k	R1206
R111	10k	R1206
R116	100R	R1206
R118	100R	R1206
R120	8R	R1206

Table 7.14: List of resistor parts - 4

K List of parts for ulrasound module

Part	Value	Package
C1	1u	C1206
C2	0.1u	C1206
C3	0.1u	C1206
C4	0.1u	C1206
C5	0.1u	C1206
IC1	MAX3232ESE	SO16
JP1		1X04
led1	orng	CHIPLED_0805
led2	orng	CHIPLED_0805
R1		R0805
R2		R0805
Q1	TEL22411	TRACOPOWER2W
X1		F09HP

Table 7.15: Ultrasound sensor module parts list